The role of PARAXIS as a mediator of epithelial-mesenchymal transitions during the development of the vertebrate musculoskeletal system.

by

Megan Rowton

A Dissertation Presented in Partial Fulfillment
of the Requirements for the Degree
Doctor of Philosophy

Approved November 2013 by the
Graduate Supervisory Committee:

J. Alan Rawls, Chair
N. Jeanne Wilson-Rawls
Kenro Kusumi
Jürgen Gadau

ARIZONA STATE UNIVERSITY

December 2013

ABSTRACT

The development of the vertebrate musculoskeletal system is a highly dynamic process, requiring tight control of the specification and patterning of myogenic, chondrogenic and tenogenic cell types. Development of the diverse musculoskeletal lineages from a common embryonic origin in the paraxial mesoderm indicates the presence of a regulatory network of transcription factors that direct lineage decisions. The basic helix-loop-helix transcription factor, PARAXIS, is expressed in the paraxial mesoderm during vertebrate somitogenesis, where it has been shown to play a critical role in the mesenchymal-to-epithelial transition associated with somitogenesis, and the development of the hypaxial skeletal musculature and axial skeleton. In an effort to elucidate the underlying genetic mechanism by which PARAXIS regulates the musculoskeletal system, I performed a microarray-based, genome-wide analysis comparing transcription levels in the somites of *Paraxis*$^{-/-}$ and *Paraxis*$^{+/+}$ embryos. This study revealed targets of PARAXIS involved in multiple aspects of mesenchymal-to-epithelial transition, including *Fap* and *Dmrt2*, which modulate cell-extracellular matrix adhesion. Additionally, in the epaxial dermomyotome, PARAXIS activates the expression of the integrin subunits α4 and α6, which bind fibronectin and laminin, respectively, and help organize the patterning of trunk skeletal muscle. Finally, PARAXIS activates the expression of genes required for the epithelial-to-mesenchymal transition and migration of hypaxial myoblasts into the limb, including *Lbx1* and *Met*. Together, these data point to a role for PARAXIS in the morphogenetic control of musculoskeletal patterning.

DEDICATION

Many thanks to my friends Josh Gibson, Ben Katchman, Martin Helmkampf, Kevin Haight, Rajani George, Doug Anderson, Brian Beres, Jeremy Marcott, Sarah Kessans, Minnie Fonte, Veronica Gutierrez, and Tucker Johnston for all the good times we've shared along the way.

I'm also grateful to my entire family for their encouragement in this endeavor, especially my mom and dad, Heather and Pete Rowton, for their emotional, financial and nutritional support.

Most of all, I'd like to thank my partner, Elizabeth Johnson, for her incredible spirit and invaluable support throughout the last four years. You have been there when I needed help, brought more compassion and empathy into my life, shared my love of science and nature, you climbed and hiked with me, taught me to love gently and started a family with me. It was you who made this long journey possible, so it is to you that I dedicate this work.

ACKNOWLEDGMENTS

I would like to acknowledge my committee members Alan Rawls, Jeanne Wilson-Rawls, Kenro Kusumi and Jürgen Gadau for their helpful suggestions and critiques. I would also like to thank my labmates Brian Beres, Doug Anderson, Rajani George, Amanda Mulia, Erik Rogers, John Cornelius and many undergraduate students for their assistance and suggestions. Finally, I would like to thank those who allowed me to use their lab's equipment to complete my experiments, including Kenro Kusumi, Jeanne Wilson-Rawls, Miles Orchinik, Page Baluch, Scott Bingham and Heather Cunliffe.

TABLE OF CONTENTS

LIST OF TABLES

Chapter 2

Table Page

LIST OF FIGURES

Chapter 1

Chapter 2

Chapter 3

Chapter 4

Figure Page

Chapter 1

Introduction

The development of the vertebrate musculoskeletal system is an intricate and highly dynamic process, resulting in the proper organization and function of the bone, cartilage, tendon and skeletal muscle of which it is composed (Watkins, 2009). However, due to the enormous complexity inherent in the development of a system comprised of multiple tissue types, it is no surprise that even the slightest disruption can result in devastating congenital defects. The muscle degeneration characteristic of Duchenne Muscular Dystrophy, or the vertebral fusions present in patients with spondylocostal dysostosis, can be caused by the mutation of individual genes that are expressed in the progenitor tissue of muscle and bone (Bulman et al., 2000; Dickson et al., 1992; Ervasti and Campbell, 1993; Hoffman et al., 1987). While the determinants of a few disorders of the musculoskeletal system have been identified, our knowledge of the genetic pathways involved in the specification, differentiation and localization of its diverse cell types is far from complete. The activation or repression of the genes critical for these processes is often modulated by DNA-binding transcription factor proteins. Transcription factors control multiple aspects of embryonic development, and can function as "master regulators" of developmental programs. The study of transcription factor activity, within the context of the developing vertebrate embryo, is therefore critical to the pursuit of a complete understanding of the development and diseases of the musculoskeletal system. The focus of the work presented here is the characterization of the role of the basic-helix-loop helix (bHLH) transcription factor PARAXIS (TCF15) in the development of the tissues of the musculoskeletal system. An appreciation of the origins of these tissues is

necessary for an informed examination of the role of PARAXIS during embryonic development.

The formation of the somites

One of the defining characteristics of the vertebrate body plan is a metamerically-arranged axial skeleton encasing the central nervous system (Smith et al., 2013). This is reflected in muscles associated with the ribs and vertebrae, including the erector spinae, serratus, and intercostal muscles (H. Shinohara, 1999). The axial skeleton, skeletal muscle and tendon comprising the musculoskeletal system derive from a common origin in the vertebrate embryo, the paraxial mesoderm, and the metamery displayed by these tissues is the result of a transient restructuring of the paraxial mesoderm within the embryo to produce the somites (Meier, 1984). Somites are paired, epithelial spheres of cells situated on either side of the neural tube, the midline structure that will eventually form the spinal cord (Figure 1). Christ and Ordahl (1995) proposed a somite staging system to standardize the comparisons made between different age embryos, such that the somites are enumerated in a posterior-anterior direction with roman numerals. The formation of the somites imposes a segmental organization not only on somite-derived tissues, but also on the developing nervous system and vasculature (Bronner-Fraser and Stern, 1991; Kalcheim and Teillet, 1989; Keynes and Stern, 1984; Stern and Keynes, 1987; Teillet et al., 1987). The segmentation of the somites within the paraxial mesoderm, a heavily studied process termed somitogenesis, begins at the anterior end of the embryo and moves towards the posterior end, repeating at regular, species-specific intervals (Gomez et al., 2008).

Somitogenesis is dependent upon three distinct, yet interrelated, processes required to (1) determine the timing of boundary formation, (2) establish the site of

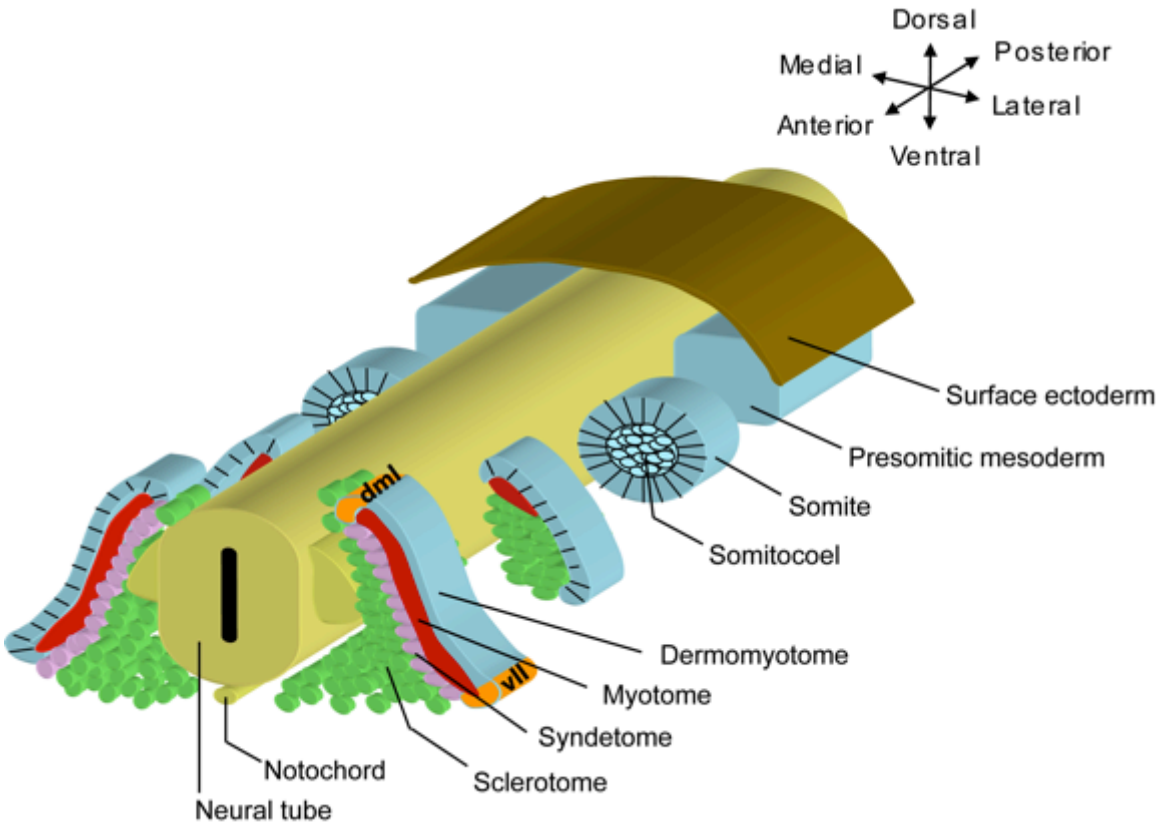

Figure 1. The tissues of the musculoskeletal system are derived from a common embryonic origin. Beginning at the anterior end of the embryo, the presomitic mesoderm is periodically segmented and epithelialized in a mesenchymal-to-epithelial transition to form the somites. The epithelialization of the somites is critical to the pattering of its derivatives. Maturing somites then undergo multiple rounds of epithelial-to-mesenchymal transition to form the tissue-specific somitic compartments. The sclerotome will give rise to the axial cartilage and bone and the syndetome will give rise to tendon. The dermomyotome will give rise to the myotome, which will form skeletal muscle. The remaining dermomyotome will give rise to the dermis, adipocytes and endothelial cells.

boundary formation and (3) undergo a morphological change from a mesenchyme to an epithelium. These processes are regulated by distinct tissues, signaling factors and genetic pathways (recently reviewed in Dequéant and Pourquié, 2008; Maroto et al., 2012; Saga, 2012). A model to explain the mechanism underlying the first two processes was first proposed in the 1970s as the "clock and wavefront model" (Cooke and Zeeman, 1976). The "clock" refers to the segmentation clock, or the oscillating gene expression that controls the length of the interval between the segmentation events of adjacent somites, which was initially described in the avian embryo (Palmeirim et al., 1997) and subsequently observed in mouse (Forsberg et al., 1998), zebrafish (Holley et al.) and *Xenopus* (Li et al., 2003) embryos, as well. Cells in the posterior presomitic mesoderm (PSM) of the mouse embryo synchronously activate the expression of Notch pathway genes, including the *Drosophila* Delta-homologue *Dll1* (Maruhashi et al., 2005), the hairy and enhancer of split genes *Hes1, Hes5, Hes7* (Bessho et al., 2001; Dunwoodie et al., 2002; Jouve et al., 2000), *lunatic fringe* (*Lfng*) (Forsberg et al., 1998), and the intracellular domain of the NOTCH receptor, itself (Morimoto et al., 2005). The expression of these genes in posterior cells leads to their activation in neighboring cells to the anterior, such that the expression is propagated autonomously from the posterior PSM towards the site of somite formation near the anterior end of the PSM (Palmeirim et al., 1997). At the same time, the posterior cells repress the expression of the Notch pathway genes through a negative feedback loop involving *Hes7* and *Lfng*, producing a wave of gene expression that cycles with rhythmic periodicity (Bessho, 2003; Dale et al., 2003; Morimoto et al., 2005). Recently, genes in additional signaling pathways have been implicated in the segmentation clock and are also expressed in a cyclical pattern, including *Axin2* and *Dkk1* in the Wnt pathway (Aulehla et al., 2003; Dequeant et al., 2006), as well as the fibroblast growth factor (FGF) signaling components *Spry2* and

Dusp6 (Dequeant et al., 2006). The mechanisms by which these pathways interact with each other to generate a "pacemaker" that regulates the initiation and timing of oscillatory gene expression have not yet been fully characterized (Dequéant and Pourquié, 2008). It was recently discovered that the pace of oscillating expression in the PSM is species-specific, and that it is more rapid in organisms that must form a large number of segments (Gomez et al., 2008).

The "wavefront" is a positional cue that directs cells within the anterior PSM to segment at a distinct axial level, called the determination front (Dubrulle et al., 2001). The determination front is defined by the confluence of an anterior-posterior gradient of retinoic acid (RA) activity originating at the anterior end of the paraxial mesoderm, and a posterior-anterior gradient of both FGF8 and nuclear localized β-CATENIN that originates in the posterior PSM (Aulehla et al., 2003; Diez del Corral et al., 2003; Dubrulle et al., 2001). Cells that pass through the determination front are thought to be competent to begin segmentation with each pulse of the segmentation clock (Dubrulle et al., 2001). Experimental manipulation of the FGF8 gradient alters the location of the determination front and therefore the number of cells that have passed through it, leading to the formation of somites of irregular size (Dubrulle et al., 2001; Sawada et al., 2001).

The final events required for the formation of a somite are the morphological transitions that accompany the segmentation and epithelialization of cells at the anterior border of the PSM. In addition to the segmentation clock, the physical separation of the newly forming somite is also regulated by the oscillating activation of Notch (Saga et al., 1997). When high levels of Notch intracellular domain (NICD) reach the anterior PSM, NICD and TBX6 combine to activate the expression of the transcription factor MESP2 (Oginuma et al., 2008; Yasuhiko, 2006). *Mesp2* is expressed in a one-somite wide stripe

just anterior to the determination front (Saga et al., 1997), and is thought to induce segmentation through the regulation of the cell adhesion and repulsion receptor EPHA4 (Nakajima, 2006; Watanabe et al., 2009). *EphA4* which is expressed in the anterior half of somite S-1 binds to its receptor, *ephrinB2*, expressed on the neighboring cells in the posterior half of somite S0, activating a bi-directional signaling cascade that leads to the repulsion of the neighboring cells and the separation of somite S0 from somite S-1 within the anterior PSM (Watanabe et al., 2009).

Mesenchymal-epithelial transitions in somitogenesis

Concurrently, the cells around the exterior of the newly forming somite undergo a morphological transition from a loose mesenchyme to a compact, epithelial sphere. This transition is characterized by increased cell-cell adhesion and cell-extraceullar matrix (ECM) interaction, the decreased motility of individual cells, and the establishment of an epithelium with apicobasal polarity that surrounds a persistent mesenchymal core, the somitocoel (Bellairs, 1979; Duband et al., 1987). The somitic mesenchymal-to epithelial transition (MET) is the least-well studied aspect of vertebrate somitogenesis, yet it is critical to the survival of the organism. Indeed, mouse embryos that do not undergo somitic MET die shortly after birth, due to a severe disorganization of the somite-derived adult tissues of the musculoskeletal system (Burgess et al., 1996).

The initial stages of somitic MET require cytoskeletal rearrangements that direct the localization and formation of tight and adherens junctions on the lateral and apical surfaces of cells that will form the somitic epithelium (Duband et al., 1987; Glazier et al., 2008; Kimura et al., 1995; Linask et al., 1998). Cytoskeletal reorganizations also control the formation of focal adhesions between the somite epithelium and the extracellular matrix (ECM) surrounding the PSM, such that the cells can adhere to, and modify the

organization of, the ECM (Jacob et al., 1991; Lash, 1985; Lash et al., 1984). This interaction of somites with the ECM is critical to the maintenance of an epithelial state in zebrafish and mouse embryos ((Girós et al., 2011; Julich et al., 2009; Koshida et al., 2005).

MET in mouse paraxial mesoderm is initiated by changes in gene expression within the PSM that are induced by signaling molecules from the surface ectoderm overlying it (Correia and Conlon, 2000; Rifes et al., 2007; Šošić et al., 1997). Indeed, when the surface ectoderm dorsal to the PSM is removed, epithelial somites fail to form (Correia and Conlon, 2000). This induction of MET in the PSM requires the bHLH transcription factor, PARAXIS (Burgess et al., 1996; Linker, 2005). The mechanisms by which PARAXIS controls somitic MET, however, have not yet been elucidated. Somite epithelialization, and the role of PARAXIS in this mesenchymal-to-epithelial transition will be discussed in further detail in Chapter 2.

Maturation of the somites

The epithelial somite will mature into four recognized compartments: the dermomyotome, the myotome, the sclerotome and the syndetome that will are the anlagen for the dermis, skeletal muscle, bone/cartilage, and tendons, respectively (reviewed in Brand-Saberi et al., 1996b; Brent, 2002; Christ and Ordahl, 1995). The morphological formation of these compartments occurs through sequential EMT in response to signals from the surrounding tissues. Disruption of this process leads to altered metameric organization of the axial musculoskeletal system and the associated peripheral nerves and vasculature.

The sclerotome is the first somitic compartment to form in response to Sonic Hedgehog (Shh) and Noggin expressed in the notochord and the floor plate of the neural

tube (Christ and Wilting, 1992; Christ et al., 2000; Christ et al., 1978). Cells in the ventro-medial portion of the epithelial S-III somite begin to express *Pax1* and undergo an EMT to migrate towards the notochord (Brand-Saberi et al., 1993a; Ebensperger et al., 1995; Fan and Tessier-Lavigne, 1994; McMahon et al., 1998). The medially positioned sclerotome cells from one somite meet the medially positioned sclerotome cells from the contralateral somite and surround the notochord to form the anlagen of the vertebral bodies (Christ and Wilting, 1992). The lateral sclerotome cells migrate dorsally and laterally to ultimately form the neural arches, pedicles and proximal ribs (Christ and Wilting, 1992).

At somite stage SXVI, the most dorso-lateral cells of the sclerotome differentiate into a more recently described compartment: the syndetome (Brent et al., 2003). The syndetome is comprised of cells that will give rise to tendons, and it forms in the space between the future cartilage and muscle with which it will eventually connect. FGF and TGFβ signaling are required to specify and maintain cells in the syndetome lineage. This includes promoting expression of the bHLH transcription factor *Scleraxis* (*Scx*) and tendon-specific differentiation markers including *Fibromodulin (Fmod), Tenomodulin (Tmod)* and *Mohawk (Mkx)* (Brent et al., 2003; Ito et al., 2010; Shukunami et al., 2006; Svensson, 1999).

During the EMT of the sclerotome, the dermomyotome, a sheet of cells from the dorso-lateral aspect of the somite, remains epithelialized in response to Wnt signaling from the surface ectoderm and neural tube and its cells express the paired-box transcription factor PAX3 (Brent, 2002; Scaal and Christ, 2004). The dermomyotome is a population of self-renewing cells that are the source of the progenitor cells for a wide variety of tissues, including skeletal muscle, satellite cells, the dermis of the back, interscapular brown fat, scapular cartilage and blood vessels of the body wall, limbs and

aorta (Atit et al., 2006; Christ et al., 1983; Gros et al., 2005; Huang et al., 2000; Kardon et al., 2002; Kassar-Duchossoy, 2005; Mauger, 1972; Pardanaud et al., 1996; Relaix et al., 2005; Venters and Ordahl, 2002; Wilting et al., 1995). The first cells to exit the dermomyotome form the myotome, which is the source of all of the skeletal muscle in the vertebrate embryo (Huang and Christ, 2000; Ordahl and Le Douarin, 1992).

Development of the skeletal muscle of the trunk and limb

The myotome is formed from cells that exit the dermomyotome to occupy the space between the dermomyotome and the newly mesenchymal sclerotome compartment (Buckingham, 2006; Hollway and Currie, 2005; Scaal and Christ, 2004). The myotome abuts the apical surface of the dermomyotome epithelium, and is separated from the sclerotome by a basement membrane (Anderson et al., 2009; Thorsteinsdóttir et al., 2011). Cells entering the myotome from the dors0-medial lip (DML) of the dermomyotome will give rise to the deep, epaxial skeletal muscles of the back, while cells entering the myotome from the ventro-lateral lip (VLL) will give rise to the hypaxial muscles of the ventral body wall, neck and appendages (Gros et al., 2004).

Many studies have addressed the formation of the myotome in both chick and mouse embryos, and the results have led to the development of multiple models describing the morphogenesis of the primary myotome (Cinnamon et al., 1999; Denetclaw et al., 1997; Hollway and Currie, 2005; Kahane et al., 1998; Scaal and Christ, 2004). A more recently proposed, unifying model suggests that pioneer myoblasts delaminate from the DML, migrate subjacently to enter the myotome and elongate bidirectionally towards the anterior and posterior ends of the dermomyotome (Gros et al., 2004). In the mouse embryo, these cells are induced to migrate out of the dermomyotome by a combination of signaling from the notochord, the dorsal neural

tube and the lateral plate mesoderm (LPM). An asymmetric cell division, in which one daughter cell sequesters the Notch-inhibitory protein Numb and enters the myotome, and the other daughter cell remains within the dermomyotome, is thought to be the mechanism by which the delamination is initiated (Holowacz et al., 2006; Venters and Ordahl, 2005). Migrating myoblasts bind laminin in the ECM and organize it into a basal lamina, restricting the migration of subsequently delaminating cells to the myotome compartment (Bajanca, 2006).

According to the Gros et al. (2004) model, the pioneer myoblasts within the myotome are soon joined by myoblasts delaminating from all four edges of the dermomyotome. Cells entering from the VLL elongate bidirectionally towards the anterior and posterior ends of the myotome (Gros et al., 2004). Myoblasts that enter from either the anterior or posterior ends elongate unidirectionally to meet the opposite end (Gros et al., 2004). In mouse embryos lacking PARAXIS, elongation of myoblasts towards the anterior and posterior borders of the dermomyotome is severely disrupted, and can be visualized with a transgene labeling cells that express the muscle differentiation transcription factor MYOGENIN (Wilson-Rawls et al., 1999). The expression of *Myogenin* and other muscle-specific transcription factors at this stage of myotome formation initiates the process of myogenic differentiation and is required for myoblast survival, the activation of muscle structural genes and the fusion of myoblasts into myotubes (Hasty et al., 1993; Nabeshima et al., 1993; Sassoon et al., 1989).

The second phase of myotome development is characterized by its growth due to the addition of myoblasts from the VLL and from regions other than the dermomyotome lips (Hollway and Currie, 2005). Dermomyotomes at inter-limb axial levels expand ventrally from the VLL into the somatopleure to generate the hypaxial muscle masses of the ventral body wall, such as the intercostal muscles (Cinnamon et al., 1999). Under the

control of PAX3, myoblasts entering the myotome from the VLL begin to express the muscle regulatory factor MYOD, which correlates with the expression of muscle structural genes such as embryonic Myosin Heavy Chain (Borycki et al., 1999; Brunelli et al., 2007; Hu et al., 2008; Sassoon et al., 1989; Tajbakhsh et al., 1997). In embryos lacking PARAXIS, the expression of *MyoD* in the hypaxial myotome is delayed, and *Pax3* expression is reduced, indicating that PARAXIS expression is required for the specification of these myocytes (Wilson-Rawls et al., 1999). The central dermomyotome, which contains cells that express both *Pax3* and *Pax7*, undergoes an EMT, with some of the cells contributing to the myotome and others adopting dermal or angiogenic fates, while the DML and VLL remain epithelial (Tajbakhsh and Buckingham, 2000; Venters and Ordahl, 2002). Cells of the central dermomyotome undergo an asymmetric cell division in which the cell adhesion protein N-CADHERIN is segregated into only those cells that will contribute to the myotome (Ben-Yair, 2005). Myoblasts continue to express N-CADHERIN within the myotome, where it helps to maintain the integrity of the compartment (Cinnamon, 2006; Delfini et al., 2009; Deries et al., 2010; Inuzuka et al., 1991). Finally, the persistently epithelial DML and VLL undergo EMT and the dermomyotome disperses, due to an inhibition of surface ectoderm-derived Wnt signaling (Geetha-Loganathan, 2006).

Prior to the ventral extension of the hypaxial myotome, myogenic progenitor cells (MPCs) in the VLL delaminate from the dermomyotome and begin distinct, long-range migrations (reviewed in Bothe et al., 2007; Buckingham, 2006; Evans et al., 2006). MPCs from the most anterior (occipital) somites will give rise to cells that migrate ventrally and anterior to the developing heart, forming a stream of cells called the hypoglossal chord which contains the progenitors of the laryngeal, neck and diaphragm muscles (Bladt et al., 1995; Evans et al., 2006; Huang et al., 1999; Noden, 1983). MPCs

from dermomyotomes at the level of the forelimb or hindlimb, responding to signaling factors from the adjacent limb bud mesenchyme, migrate instead into the limb through modifications to cell-ECM interactions (Brand-Saberi et al., 1996a; Heymann et al., 1996). After progenitor cells have colonized the limb, they proliferate and enter into the myogenic differentiation program to form the ventral and dorsal muscle masses of the limb that will differentiate into the flexor and extensor muscles of the appendages, respectively (Delfini et al., 2000; Duprez et al., 1998; Marcelle et al., 1995; Tajbakhsh and Buckingham, 1994). The onset of this differentiation program in the limb is delayed in mouse embryos lacking PARAXIS (Wilson-Rawls et al., 1999). However, *Paraxis*$^{-/-}$ neonates are born with normal forelimb muscles, suggesting that there is a mechanism by which the embryo compensates for a lack of the transcription factor (Wilson-Rawls et al., 1999).

bHLH transcription factor regulation of muscle development in vertebrates

Much of what we know about the genetic pathways involved in skeletal muscle development comes from studies involving the myogenic regulatory factors (MRFs). The MRFs include MYF5, MYOD, MRF4 and MYOGENIN, which form the MyoD family of basic helix-loop-helix (bHLH) transcription factors (Olson, 1990). The myogenic bHLH transcription factors share ~80% amino acid identity within their bHLH domains, which are required for DNA binding and dimerization (Olson, 1990). These transcription factor bind hexanucleotide sequences (consensus sequence CANNTG) called E boxes (Atchley and Fitch, 1997). The MRFs bind to E boxes found within the promoters and enhancers of muscle-specific genes, including their own, that are important for determination or differentiation to activate or repress their transcription (Olson and

Klein, 1994). BHLH transcription factors utilize the helix-loop-helix domain to dimerize with other bHLH proteins prior to DNA binding (Atchley and Fitch, 1997). The MRFs often heterodimerize with E proteins, such as the *E2A* encoded E12 and E47, which are ubiquitously expressed, in order to spatially regulate the activation the muscle differentiation program (Murre et al., 1989).

While the MRFs can all induce skeletal muscle development when introduced into mesodermal cells in culture (Olson and Klein, 1994), they have overlapping but distinct functions in the vertebrate embryo. In mouse embryos, MYF5 and MYOD are required for the specification of cells that give rise to the epaxial and hypaxial muscles, respectively (Lassar et al., 1989; Ott et al., 1991; Sassoon et al., 1989). *Mrf4* is expressed in post-mitotic mononuclear myotubes and adult skeletal muscles, rather than in myoblasts (Hinterberger et al., 1991), and appears to play a bigger role in regulating satellite cell activity in adult muscle than muscle development (Zhang et al., 1995). Finally, *Myogenin* is expressed in elongating myocytes in the myotome and is essential for muscle differentiation (Hasty et al., 1993; Nabeshima et al., 1993). The discovery that MYOGENIN can both activate, and be activated by, the myocyte-specific enhancer-binding factor MEF2 suggests that the MRFs do not act alone to initiate and maintain the muscle differentiate program, but instead that they participate in a complex regulatory network involving positive and negative feedback loops (Cheng et al., 1993; Cserjesi and Olson, 1991; Edmondson et al., 1992).

PARAXIS and the development of the musculoskeletal system

Studies to date have identified additional bHLH transcription factors that direct the differentiation of individual tissues of the musculoskeletal system. While bHLH transcription factors were known to play a central role in promoting (MYF5, MYOD,

MYOGENIN, MRF4) or inhibiting (TWIST, MYOR, OUT, HES, AND EPICARDIN) muscle development, attempts to identify new bHLH family members that regulate the specification of somitic cells to the myogenic lineage led to the discovery of two closely related bHLH transcription factors, PARAXIS and SCLERAXIS (Burgess et al., 1995; Cserjesi et al., 1995; E E Quertermous, 1994). Phylogenetically, PARAXIS and SCLERAXIS are most closely related to TWIST1 and TWIST2, which are known to regulate myogenesis, osteogenesis and immune system development. In early mouse and chick embryos, these genes have complementary, non-overlapping expression patterns in the paraxial mesoderm. PARAXIS transcripts are detected in the presomitic mesoderm and epithelial somite, before becoming restricted to the dermomyotome (Barnes et al., 1997; Burgess et al., 1995). In contrast, SCLERAXIS is transiently expressed in the sclerotome before becoming restricted to the syndetome (Cserjesi et al., 1995; Schweitzer et al., 2001). Similar patterns of expression have been observed in the somites of other vertebrates, such as *Xenopus* and zebrafish (Carpio et al., 2004; Shanmugalingam and Wilson, 1998; Tseng and Jamrich, 2004). As will be described below, PARAXIS appears to be critical for the regulation of the morphological events associated with somite MET, muscle differentiation and patterning of the axial skeleton. This uniquely positions PARAXIS as a morphogenetic regulator of musculoskeletal system in vertebrates.

Targeted null mutations were used to examine the function of PARAXIS during somitogenesis in the mouse embryo. Segmentation occurred at the normal developmental timepoint in the absence of *Paraxis,* however, the cells maintained the loose mesenchymal phenotype of the presomitic mesoderm instead of the canonical epithelium of the somite (Burgess et al., 1996). Genetic markers for the sclerotome, myotome, syndetome, and dermomyotome cell lineages were present and expressed at

the appropriate time, predicting that the process of specification was not altered in mutant embryos. Postnatally, *Paraxis*-deficient mice displayed radical deficiencies in the axial skeleton, including caudal agenesis fusion and underossification of the vertebrate and ribs (Burgess et al., 1996). Further studies revealed a loss of the anterior-posterior somite polarity required for segmentation of the vertebrate and ribs, illuminating a cause for the bone phenotype observed in neonates lacking PARAXIS (Johnson et al., 2001; Takahashi et al., 2007).

Paraxis is highly expressed in premyogenic cells that populate the DML and VLL of the dermomyotome, raising the possibility that the gene contributes to the proliferation or differentiation of skeletal muscle. This hypothesis was supported by the absence of the transverse abdominal muscles and hypotrophic intercostals muscles in *Paraxis*$^{-/-}$ neonatal mice (Burgess et al., 1996). In mice deficient for both *Myf-5* and *Paraxis*, there is a profound loss of axial hypaxial muscles and a reduction in appendicular limb muscles. This demonstrates a role for PARAXIS in the development of the hypaxial muscles that is partially compensated by a MYF-5-dependent myogenic lineage (Wilson-Rawls et al., 1999).

Regulation of* Paraxis *Transcription

Transcription of *Paraxis* is initiated and maintained by signals from the surface ectoderm, dorsal neural tube and tailbud. Removal of the surface ectoderm from the caudal PSM results in a loss of *Paraxis* transcription and a failure of somite epithelialization (Correia and Conlon, 2000; Šošić et al., 1997). Maintenance of *Paraxis* expression requires the activation of canonical Wnt signaling, as *Wnt6* expression in the surface ectoderm induces and maintains somitic MET and *Paraxis* transcription, and ectopic *Wnt6* expression is able to substitute for a lack of surface ectoderm in a

mechanism that is β-CATENIN dependent (Linker, 2005; Schmidt et al., 2004). Furthermore, forced expression of *Paraxis* is able to rescue somite epithelialization in the absence of Wnt signaling (Linker, 2005). These results suggest that PARAXIS functions downstream of the Wnt signaling pathway, and that the target genes of PARAXIS are necessary to induce MET in presomitic mesoderm.

Downstream Targets of PARAXIS

Understanding the function of PARAXIS is ultimately linked to identifying its transcriptional targets during somitogenesis and myogenesis. These targets have remained largely elusive. Several genes important for musculoskeletal development, including the paired-box transcription factors PAX1 and PAX3 and the homeobox transcription factor MKX, are downregulated in the absence of PARAXIS (Anderson et al., 2006; Takahashi et al., 2007; Wilson-Rawls, 2004). However, the direct activation of these genes by PARAXIS, has not yet been demonstrated. The results of a recent study suggest that PARAXIS functions to prime its target genes for transcriptional activation by binding to enhancer elements and activating transcription immediately upon the repression of inhibitory proteins (Davies et al., 2013). Like all bHLH transcription factors, PARAXIS can bind directly to consensus E Box sequences (CANNTG) as homodimers or heterodimers with members of the E12 subfamily (Wilson-Rawls, 2004). PARAXIS can bind to, and activate transcription from, a multimerized Ebox found within the *Scleraxis* promoter (Wilson-Rawls, 2004). The significance of this interaction remains to be determined as there is little overlap in *Paraxis* and *Scleraxis* transcription in the embryo (Burgess et al., 1996). Due to the importance of PARAXIS for somitogenesis and muscle development, the identification of its direct targets and the

genetic pathways in which it functions is critical to our understanding of these processes and the prevention of musculoskeletal defects.

For my dissertation project, I have taken a systematic approach to identifying the downstream targets of PARAXIS in the anterior PSM and the first four somites in the mouse embryo at E9.5. This represents a tissue that is undergoing MET and thus should provide novel insight into the genes critical for the regulation of this process during somitogenesis. As the transition between a mesenchymal and epithelial phenotype plays a role in both normal development and malignancies such as metastatic carcinoma, this work may also open new avenues for cancer therapies. I will extend my findings regarding PARAXIS targets to address PARAXIS' function in the establishment of the myotome and the migration of MPCs into the limbs. This will help us to understand how morphological regulators, such as those associated with MET, may also participate in cell migration and organization during myogenesis.

Chapter 2

Regulation of mesenchymal-to-epithelial transition by PARAXIS during somitogenesis

Introduction

The morphological transition of cells between a mesenchymal and epithelial state plays an essential role in the development of complex tissues during embryogenesis, and is also associated with the progression of diseases such as cancer and renal fibrosis (reviewed in Nieto; Thiery and Sleeman, 2006; Yang and Weinberg, 2008). A notable example of mesenchymal-to-epithelial transition (MET) occurs during somite formation in vertebrate embryos. Somitogenesis establishes the metameric patterning of the axial musculoskeletal system, in addition to influencing the migration of endothelial and neural crest cells that give rise to the vasculature and peripheral nervous system, respectively (Burgess et al., 1996; Johnson et al., 2001; Wilson-Rawls et al., 1999). While the confluence of signaling pathways that direct the segmentation of somites from the anterior presomitic mesoderm (PSM) has been extensively studied, the genetic pathways that regulate the concomitant MET have not been well characterized (reviewed in Maroto et al., 2012; Saga, 2012). However, somite epithelialization has been shown to require the activity of the bHLH transcription factor, PARAXIS (Burgess et al., 1996). Identification of genes downstream of PARAXIS has been limited to somite compartment makers in the mouse embryo (Takahashi et al., 2007; Wilson-Rawls, 2004; Wilson-Rawls et al., 1999), and *meox2* in *Xenopus* (Gaspera et al., 2012). The role of PARAXIS in regulating the transcription of genes associated with the archetypal cell processes of MET during early somitogenesis remains to be determined.

Morphologically, MET is initiated by the formation of a two-dimensional sheet of cells through the acquisition of primordial cadherin-mediated adherens junctions at the

apicolateral borders of adjacent cells (Baum and Georgiou, 2011) (Figure 1). In parallel, reorganization of the microtubule cytoskeleton establishes a distinct cell polarity and directs the assembly of tight junctions on the apical cell surface of the epithelium (Radice et al., 1997; Rhee et al., 2003). Cytoskeletal reorganizations also control the formation of focal adhesions between the somite epithelium and the extracellular matrix (ECM) surrounding the PSM, such that the cells can adhere to, and modify the organization of, the ECM (Jacob et al., 1991; Lash, 1985; Lash et al., 1984). The interaction of somites with the ECM is critical to the maintenance of an epithelial state in zebrafish and mouse embryos. For example, somitic MET requires the condensation of fibronectin surrounding the somite epithelium, which is organized by cell surface proteins on the basal surface of the somite epithelium, such as integrin α5 (Girós et al., 2011; Julich et al., 2009; Koshida et al., 2005).

Members of the Rho family of small GTPases (RHOA, RAC1 and CDC42) have been shown to be critical for the integration of signals from cell adhesion receptors, including cadherins, integrins and Eph receptors, that leads to the reorganization of the cytoskeleton required for the formation of adherens/tight junctions and focal adhesions during MET (reviewed in Van Aelst, 2002). Studies performed in chick embryos demonstrate that RHOA, RAC1 and CDC42 play a role in MET in the somites (Nakaya et al., 2004; Takahashi et al., 2005). Nakaya et al. (2004) show that activated CDC42 promotes a mesenchymal state in the paraxial mesoderm, while activated RAC1 promotes an epithelial state and is required for PARAXIS-directed epithelialization of the somites. These studies predict that PARAXIS participates in a regulatory pathway that links canonical Wnt signaling to Rho GTPase activity and the regulation of the morphogenetic changes associated with somitic MET. However, this simple pathway

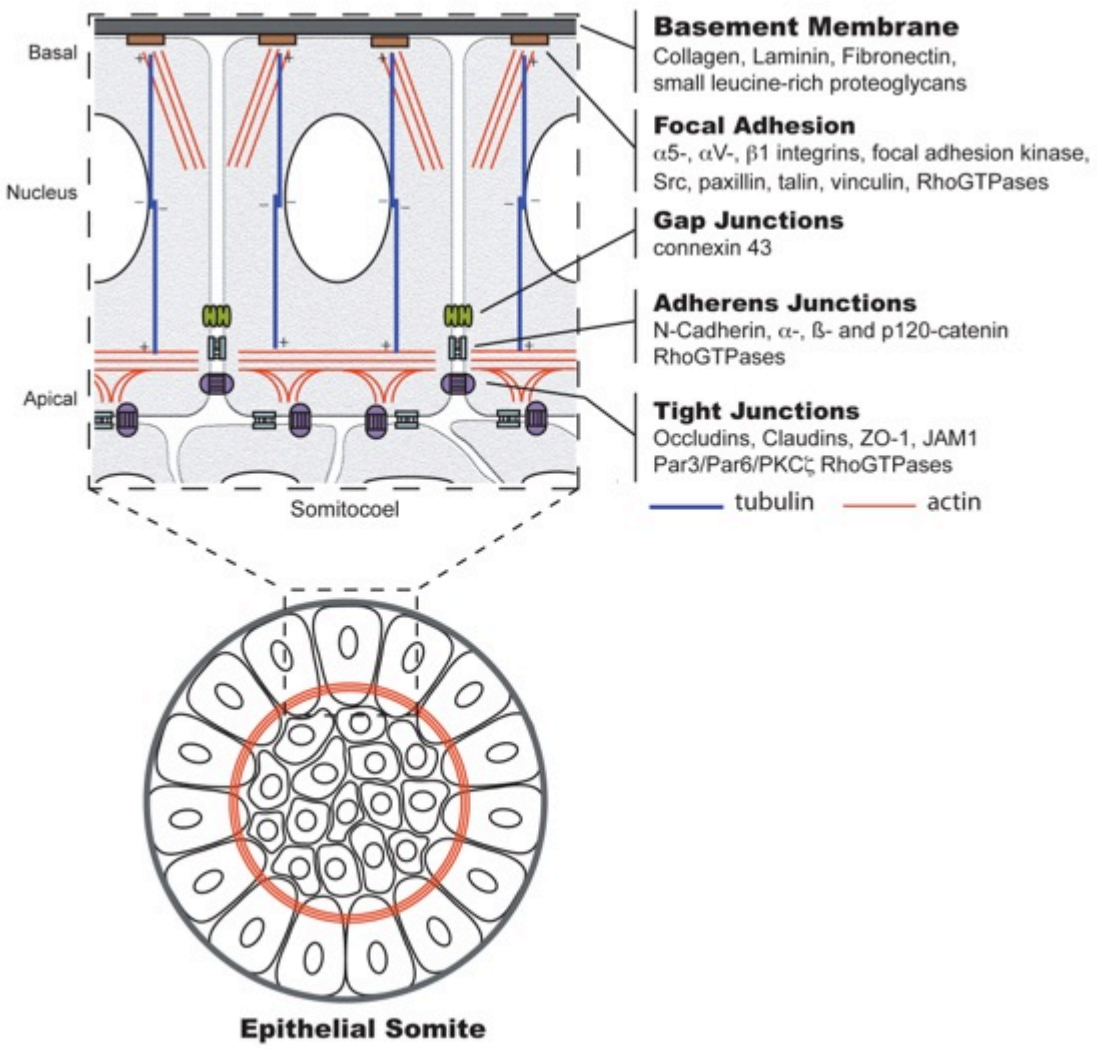

Figure 1. Cell-cell and cell-ECM interactions in the epithelial somite. A schematic of the organization of cellular and ECM adhesive junctions which are organized during somite epithelialization, and the proteins known to be associated with each interaction.

does not describe the mechanisms by which PARAXIS regulates its downstream target genes to affect Rho GTPase activity and MET in the paraxial mesoderm.

Here, we use a combination of confocal microscopy and microarray analysis to examine somite cell morphology and gene expression in E9.5 *Paraxis*$^{-/-}$ embryos, as compared to wild type embryos. In the absence of PARAXIS, the cells of the forming somite failed to generate the ECM organization associated with MET. The loss of PARAXIS led to the deregulation of modifiers of Rho GTPase activity, but did not alter the mRNA levels of RAC1 or other members of the Rho GTPase family directly. Our data also revealed a novel role for PARAXIS in regulating genes that are not associated with the canonical GTPase signaling pathway, but are implicated in MET or EMT, including those involved in ECM production and stability, cytoskeletal rearrangements via focal adhesion and adherens/tight junction assembly, and the non-canonical Wnt pathway.

Materials and Methods

Animals

Mice carrying a null allele for the gene *Paraxis* (Burgess et al., 1996) were maintained as heterozygotes (*Paraxis*$^{+/-}$) according to Institutional Animal Care and Use Committee guidelines. Embryos were genotyped by duplex PCR on embryo yolk sacs using the primers ParaxisWTF: GTCTGGCGTCCAGCTACATC, ParaxisNeoF: TGCTCCTGCCGAGAAAGTAT, ParaxisWT/NeoR: GAGCATCAGGCAAGAGGAAG. All embryos used in this study were at day 9.5 of gestation.

Microarray Analysis

Tissue from the anterior presomitic mesoderm plus somites I-IV was dissected from fifteen *Paraxis*$^{+/+}$ and fifteen *Paraxis*$^{-/-}$ embryos in cold PBS, individually flash

frozen and stored at -80 °C until genotyping was completed. The tissue was pooled into three samples of five embryos per genotype, disrupted by sonication using the Covaris S-2 system (Covaris; Woburn, MA), and total RNA was extracted with an RNeasy Micro kit (Qiagen; Valencia, CA). RNA purity, quantity and integrity were assessed using a Nanodrop ND-1000 spectrophotometer (Nanodrop; Wilmington, DE) and an Agilent 2100 Bioanalyzer (Agilent Technologies, Palo Alto, CA). 250ng of RNA, with a minimum RNA Integrity Number of 7.9 or higher (Bioanalyzer), was used to prepare fluorescent cRNA probes using labeling kits and protocols recommended by Agilent. A dye swap was performed on each of the three sample groups for both genotypes to account for Cy3- or Cy5-conjugated nucleotide incorporation bias. Labeled probes from a reference wild type sample and a *Paraxis*$^{-/-}$ sample were combined and hybridized to dual color 4x44k Mouse Gene Expression Microarrays (Agilent, Design ID 014868), according to manufacturer's protocols. Array slides were washed and scanned at 5uM using an Agilent Microarray Scanner (model G2505B) in an ozone controlled environment, and data were extracted, processed and normalized using Agilent Feature Extraction software (v10.5). Genespring GX 10.0 (Agilent) was then used to assign absent, marginal, and present annotations. If multiple array probes for a single gene showed consistent deregulation, the probe with the highest fold change was used for further analysis. To compare expression levels between samples, we used quantile normalization in Genespring to minimize technical variation. The microarray data discussed in this publication have been deposited at the Gene Expression Omnibus (Edgar et al., 2002) at the National Center for Biotechnology Information (NCBI) under GEO Series accession number GSE47905 (http://www.ncbi.nlm.nih.gov/geo/query/acc.cgi?acc=GSE47905).

Quantitation of Transcription in Embryos

Quantitative RT-PCR (qRT-PCR) was used to confirm the altered expression levels of selected genes from each category within Tables 2 and 3. PSM and somite tissue was microdissected from *Paraxis*$^{+/+}$ and *Paraxis*$^{-/-}$ embryos, frozen, stored and pooled, as stated above. Total RNA was extracted with Trizol reagent (Invitrogen), and converted to cDNA with Superscript III (Invitrogen). QRT-PCR was performed on selected genes using the ABI Prism 7900HT Sequence Detection System (Applied Biosystems). Cycling conditions were 95 °C for 10 minutes, followed by 45 cycles of 95 °C for 15s, 60 °C for 30s and 72 °C for 30s. Selected genes assayed were normalized to *Gapdh* expression levels. Statistical analysis on expression data was carried out using a nonparametric Mann-Whitney test with a *p*-value of ≤ 0.05. Statistically significant differences in gene expression were found for most of the genes tested from Tables 2 and 3, but not for all, including *Numa1*, *Pard3* and *Dnm3os*.

Whole Mount In Situ Hybridization

Embryos were fixed in 4% PFA overnight, washed in PBSw (0.01% Tween-20 in PBS), and dehydrated in a methanol series for storage at -20 °C until use. To generate antisense digoxygenin-labeled RNA probes, selected genes were amplified by RT-PCR from E9.5 mouse whole embryo cDNA. Gene-specific primers for genes from Tables 2 and 3 which are known to be expressed in the somites were designed using Primer3 (Rozen and Skaletsky, 1999) and then modified by adding the T7 RNA polymerase binding site sequence (5'-CTAATACGACTCACTATAGGGAGA-3') to the 5' end of the downstream primer. Generation of digoxigenin-labeled antisense RNA probes and *in situ* hybridization was carried out as described in Johnson et al. (2001). *In situ* hybridization was performed using an automated InsituPro (Intavis, LLC, San Marcos, CA), as described previously (Belo et al., 1997). Embryos were photographed using a

SMZ1000 stereodissecting microscope (Nikon) with a Retiga CCD digital camera (Q-Imaging).

Indirect Immunofluorescence

For whole mount immunofluorescence, E9.5 embryos were harvested and fixed in 4% PFA overnight at 4°C, washed in PBSw, and permeabilized for 2 to 3 days in 1% Triton X-100 in PBS (PBST) at 4 °C. For section immunofluorescence, fixed embryos were embedded, frozen and sectioned as described previously (Anderson et al., 2006). Rabbit primary antibodies specific for laminin (Sigma L9393-.2ML, 1:400 dilution), EphA7 (Santa Cruz Biotechnologies sc-1015, 1:100 dilution), or FAPα (Santa Cruz Biotechnologies sc-135069, 1:100 dilution) proteins were used with anti-rabbit Alexa Fluor 488-IgG (Molecular Probes, Life Technologies A21206, 1:1000 dilution) as a secondary antibody. Whole mount immunofluorescence was imaged with a Leica SP2 scanning confocal microscope, using 40x and 63x objectives. Z stacks were viewed as average or maximum projections. Section immunofluorescence was imaged with a 40x objective on a Nikon Eclipse TE2000-U inverted microscope.

Luciferase Reporter Assay

Six copies of the Ebox (CATCTG) located within the first exon -5bp from the *Fap* translational start site were PCR amplified and sublconed into the XhoI/Kpn1 sites of pGL3Promoter plasmid (Promega, Madison, WI). The PARAXIS and E47 coding sequences were subcloned into the XhoI/XbaI sites of the CS2-HA plasmid to create the fusion proteins HA-PARAXIS and HA-E47. All clones were sequenced for verification. NIH3T3 mouse fibroblast cells were seeded at $4x10^4$ cells/well in complete media [DMEM supplemented with 10% Newborn Calf Serum] in 24-well tissue-culture dishes.

Each well was transfected with a total of 400 ng of plasmid DNA using 1 µl of Lipofectamine (Invitrogen, Carlsbad, CA) and 4 µl of PLUS reagent (Invitrogen, Carlsbad, CA), according to manufacture's protocol. Transfected cells were lysed 24 hours post-transfection in 100 µl/well Luciferase Cell Culture Lysis Buffer (Promega, Madison, WI) and subjected to a single freeze-thaw cycle at -80°C. Luciferase activity was measured for each well by reacting 20 µl of cell lysate with 100 µl of Luciferase Assay Buffer (Promega, Madison, WI) in white 96-well plates, using an FLx800 microplate reader (BioTek Instruments, Inc., Winooski, VT). The experiment was performed in triplicate, and fold-change was calculated relative to luciferase activity levels derived from the 6xDmrt2 Ebox-pGL3P vector co-transfected with expression vectors encoding only the Ha peptide.

Results And Discussion

The phenotype of the *Paraxis*$^{-/-}$ neonate, which results in lethality shortly after birth, is dominated by defects in the patterning of somite derivatives, suggesting that the primary role of PARAXIS is to maintain the spatial order of the compartments of the somite through the incipient epithelialization of the somites, and the maintenance of an epithelialized dermomyotome. Since PARAXIS activity is required for the induction of MET, identifying the genetic factors downstream of PARAXIS regulation in the newly formed somite and dermomyotome is a critical step in the characterization of the morphogenetic processes that occur during MET and EMT.

ECM components Are Mislocalized in Paraxis$^{-/-}$ *Somites*

The proper organization of the extracellular matrix components laminin and fibronectin is critical to the maintenance of an epithelial morphology in the somites (Danker et al.,

1992; Girós et al., 2011; Koshida et al., 2005). To assess the degree of ECM organization surrounding cells in newly formed somites in E9.5 *Paraxis*$^{-/-}$ embryos, we examined the distribution of laminin using indirect immunofluorescence. An increased aggregation of laminin between adjacent somites is evident in wild type embryos (Figure 2A). The equivalent region of the *Paraxis*$^{-/-}$ embryo stained positive for laminin in disorganized patches, but it did not display the same condensation at the intersomitic clefts (Figure 2B). We also examined the distribution of fibronectin within the *Paraxis*$^{-/-}$ somite. In wild type somites, a fibronectin matrix surrounded the entire somite epithelium and was also concentrated within the mesenchymal somitocoel (Figure 2C). Fibronectin is less organized at the dorsal surface of *Paraxis*$^{-/-}$ somites and does not form continuous boundaries between somites in the mutant embryos (Figure 2D). Fibronectin normally condensed within the somitocoel was dispersed and was also observed to span somite boundaries in the absence of PARAXIS. These observations are consistent with a requirement for PARAXIS in the establishment of a proper ECM structure surrounding the somite during the initial stages of MET.

Microarray Analysis of Somite MET in Paraxis$^{-/-}$ *Mice Reveals Deregulated Genes Involved in Multiple MET Processes*

To identify genes whose expression is impacted downstream of *Paraxis* during somite formation, we performed gene expression microarray analyses on pooled total RNA isolated from the anterior PSM and the four newest somites of E9.5 *Paraxis*$^{-/-}$ and *Paraxis*$^{+/+}$ embryos. This represents an embryonic time period when there is robust *Paraxis* expression in the anterior PSM and early somites. Tissue from five embryos with the same number of somites was pooled to create a sample, and three samples were collected for each genotype, as biological replicates. Genes displaying deregulation across

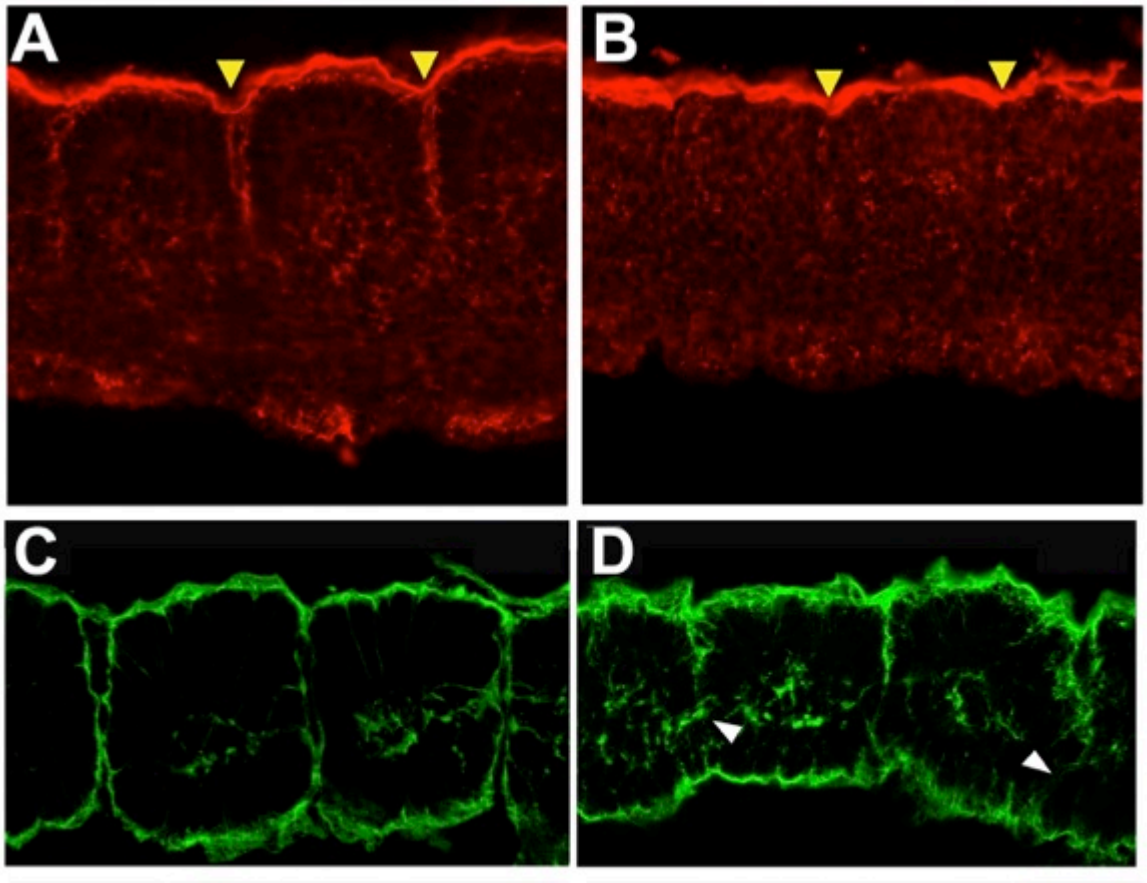

Figure 2. The ECM constituents laminin and fibronectin are mislocalized in the *Paraxis*$^{-/-}$ embryo. Laminin protein labeled by indirect immunofluorescence in the posterior somites of E9.5 wild type (A) and *Paraxis*$^{-/-}$ embryos (B). Laminin is enriched at the intersomitic boundaries of wild type somites (arrowheads in A), but is lacking between *Paraxis*$^{-/-}$ somites (arrowheads in B). Indirect immunofluorescence in somite sections also reveals disorganized localization of fibronectin at the intersomitic boundaries of *Paraxis*$^{-/-}$ somites (white arrowheads in D), along the basal surface of the dorsal epithelium and in the region of the somitocoel, as compared to wild type embryos. Images display somites I-III, and are presented with anterior to the left and dorsal at the top. Image magnification is 400x.

all biological replicates were analyzed with Agilent Genespring GX software in order to identify those genes with expression level differences of at least 1.5-fold between *Paraxis*$^{+/+}$ and *Paraxis*$^{-/-}$ embryonic tissue (Figure 3).

Our microarray analysis identified 795 genes whose expression was at least 1.5-fold up- or down-regulated in *Paraxis*$^{-/-}$ tissue, relative to wild type tissue. PARAXIS is predicted to function as a transcriptional activator (Wilson-Rawls, 2004), and consistent with this, genes with the most significant changes in mRNA levels were downregulated in the absence of PARAXIS. However, this approach alone cannot distinguish between direct and indirect transcription regulation. Deregulated genes closely correlated ($p < 0.01$) with a limited number of gene ontology (GO) term classifications associated with embryonic development processes, the extracellular matrix and the cell surface (Table 1), which is consistent with PARAXIS being required for the transcription of genes participating in cell-cell and cell-ECM adhesion. A more relaxed threshold ($p<0.05$) included GO terms associated with cell signaling pathways and transcription factor activity (Table 1), indicating that PARAXIS may control the transcription of MET-associated genes through the activation of additional regulators. Based on either demonstrated or predicted function, we identified those genes that are associated with ECM organization, cytoskeleton organization, cell adhesion/repulsion, or cell signaling/transcription regulation from among the 795 deregulated genes (Tables 2 and 3). A change in expression level in the absence of PARAXIS was validated by qRT-PCR (Figure 5) for a select subset of these genes representing each table category, and for selected genes known to be expressed in the somites by whole-mount *in situ* hybridization (Figures 4 and 6). The diversity of the deregulated genes identified in our study suggests that PARAXIS is responsible for promoting several distinct morphological events associated with somite epithelialization.

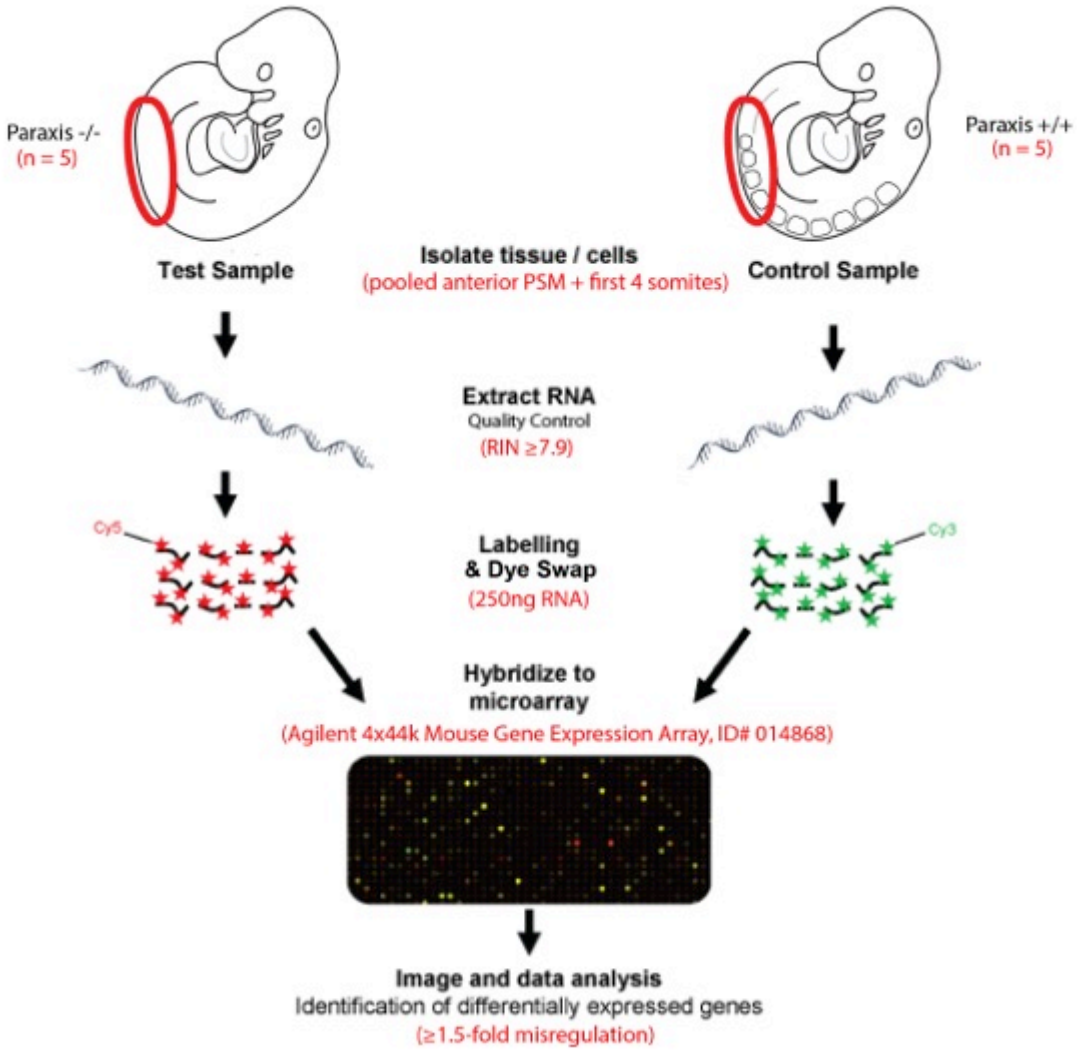

Figure 3. Experimental design of our microarray-based gene expression analysis of *Paraxis*$^{-/-}$ embryos. Total RNA was extracted from PSM/early somite tissue samples from E9.5 wild type and *Paraxis*$^{-/-}$ embryos. RNA was pooled from 5 embryos for each of three biological replicates of each genotype, and used to create cRNA probes labeled with Cy3 and Cy5 dyes. Probes were combined and hybridized to an Agilent two color gene expression microarray, and fluorescence intensities were measured to identify genes misexpressed in the *Paraxis*$^{-/-}$ embryo by at least 1.5-fold, relative to wild type samples.

Table 1. Microarray analysis reveals potential direct PARAXIS targets and associated Gene Ontology terms.

GO Term	# of genes	P value
Cellular development process	153	p<0.01
Extracellular region	134	p<0.01
Anatomical structure morphogenesis	112	p<0.01
Regulation of cell communication	79	p<0.05
Sequence-specific DNA binding transcription factor activity	62	p<0.05
Cell surface	45	p<0.01
Embryonic morphogenesis	41	p<0.01
Pattern specification process	39	p<0.05
Skeletal system development	37	p<0.01

Table 2. Selected genes involved in MET/EMT, cell migration and/or cell adhesion that are upregulated at least 1.5-fold in *Paraxis*$^{-/-}$ vs *Paraxis*$^{+/+}$ embryo PSM and somitic tissues.

Gene Symbol	Fold Change	Gene Name	Accession No.	Known or Inferred Function
Extracellular matrix organization				
S100a4	2.8	S100 calcium binding protein A4	NM_011311	Positive regulation of MMP expression, cell migration
A2m	2.5	alpha-2-macroglobulin	NM_175628	Protease inhibitor
Olfml2a	2.0	olfactomedin-like 2A	AK037205	Bind proteoglycans in the ECM*
Mmp9	1.9	matrix metallopeptidase 9	NM_013599	Metalloendopeptidase activity
Clu	1.5	clusterin	NM_013492	MMP chaperone in ECM
Mfap5	1.5	microfibrillar associated protein 5	NM_015776	Positive regulation of elastic fiber macroassembly
Cell adhesion / repulsion				
Sdc4	4.1	syndecan 4	NM_011521	Positive regulation of focal adhesion assembly
Cldn11	2.3	claudin 11	NM_008770	Tight junction assembly
Dsc2	1.7	desmocollin 2	NM_013505	Desmosome assembly
Ctnna2	1.6	catenin, alpha 2	NM_009819	Links adherens junctions to the cytoskeleton
Itga11	1.6	integrin alpha 11	NM_176922	Receptor for collagen
Nebl	1.6	nebulette	NM_028757	Positive regulation of focal adhesions
Cytoskeleton organization				
Mid1	1.9	midline 1	AY540038	Negative regulation of microtubule depolymerization
S100a6	1.8	S100 calcium binding protein A6 (calcyclin)	NM_011313	Interacts with tropomyosin to modulate actin dynamics*
Scin	1.7	scinderin	NM_009132	Actin filament capping and severing*
Krtap13	1.7	keratin associated protein 13	NM_010671	Intermediate filament structural protein*
Add2	1.7	adducin 2 (beta)	NM_013458	Actin-spectrin network assembly
Cobl	1.7	cordon-bleu	NM_172496	Complexes with syndapin to regulate actin nucleation
Tmod1	1.6	tropomodulin 1	NM_021883	Regulates actin filament lengths
Krt23	1.5	keratin 23	NM_033373	Intermediate filament structural protein
Krtap2	1.5	keratin associated	NM_001191	Intermediate filament

2-2		protein 22-2	018	structural protein *
Rhoh	1.5	ras homolog gene family, member H	NM_00108 1105	Negative regulation of actin filament assembly
Anxa8	1.5	annexin A8	NM_013473	Regulation of actin dynamics
Cell signaling / transcription regulation				
Afap1l 2	2.2	actin filament associated protein 1-like 2	NM_146102	Positive regulation of EGFR signaling *
Lhx2	1.8	LIM homeobox protein 2	NM_010710	Transcription factor activity, mesoderm development
Cer1	1.8	cerberus 1	NM_00988 7	BMP antagonist
Errfi1	1.7	ERBB receptor feedback inhibitor 1	NM_133753	Inhibitor of EGFR signaling,
Arhgef 6	1.6	Rac/Cdc42 guanine nucleotide exchange factor (GEF) 6	NM_152801	Regulation of Rac1 signal transduction
Rasgrf 1	1.5	RAS protein-specific guanine nucleotide-releasing factor 1	NM_00103 9655	Negative regulation of Cdc42 activation

* Function inferred from sequence orthology or indirect assay.

Table 3. Selected genes involved in MET/EMT, cell migration and/or cell adhesion that are downregulated at least 1.5-fold in *Paraxis*$^{-/-}$ vs *Paraxis*$^{+/+}$ embryo PSM and somitic tissues.

Gene Symbol	Fold Change	Gene Name	Accession No.	Known or Inferred Function
Extracellular matrix organization				
Fap	16.2	fibroblast activation protein	NM_007986	Serine protease, regulation of EMT/MET
Itih5	3.7	inter-alpha (globulin) inhibitor H5	NM_172471	Serine-type endopeptidase inhibitor activity*
Abi3bp	3.0	ABI gene family, member 3 (NESH) binding protein	NM_001014423	Collagen binding, positive regulation of cell-substrate adhesion
Plod1	1.9	procollagen-lysine, 2-oxoglutarate 5-dioxygenase 1	NM_011122	Collagen assembly
Pcolce	1.7	procollagen C-endopeptidase enhancer protein	NM_008788	Stimulation of procollagen processing
Cell adhesion / repulsion				
Adam18	11.0	a disintegrin and metallopeptidase domain 18	NM_010084	Metalloprotease / disintegin activity *
Adamtsl3	2.2	ADAMTS-like 3	NM_001190374	Regulation of cell-ECM interaction, assembly of ECM
Wisp2	2.1	WNT1 inducible signaling pathway protein 2	NM_016873	Inhibition of fibrinogen-integrin binding
Epha7	2.0	Eph receptor A7	NM_001122889	Eph-ephrin bi-directional signaling
Lin7a	1.9	lin-7 homolog A	NM_001039354	Regulation of tight junction assembly
Vcam1	1.9	vascular cell adhesion molecule 1	NM_011693	Interacts with α4β1 integrins to mediate cell-cell adhesion
Ntn1	1.8	netrin 1	NM_008744	Binds receptor to mediate cell-cell and cell-ECM interactions
Lnx1	1.8	ligand of numb-protein X 1	BC040367	Facilitates the redistribution of JAM4 to newly forming tight junctions
Nlgn1	1.8	neuroligin 1	AK083116	Forms intercellular junctions by binding beta-neurexins
Pcdhga12	1.7	protocadherin gamma subfamily A, 12	BC066851	Mediates calcium-dependent cell-cell adhesion*
Pcdhb16	1.6	protocadherin beta 16	NM_053141	Mediates calcium-dependent cell-cell adhesion*
Ntm	1.6	neurotrimin	AK018085	Cell adhesion molecule*
Epha3	1.6	Eph receptor A3	NM_010140	Eph-ephrin bi-directional signaling
Sdk2	1.6	Sidekick homolog 2	AK052040	Transmembrane protein mediating homophilic cell adhesion

Tgfb3	1.6	transforming growth factor, beta 3	NM_009368	Activates repressors of cadherin-based adhesion, initiates EMT
Itgav	1.5	integrin alpha V	AK080357	Heterodimeric receptor for ECM-mediated focal adhesion assembly
Frmd4a	1.5	FERM domain containing 4A	AK029073	Scaffolding protein mediating Arf6 activation at adherens junctions
Utrn	1.5	utrophin	NM_011682	Member of a complex which links the cytoskeleton to the ECM
Cytoskeleton organization				
Dnm3	5.4	dynamin 3	NM_001038619	Microtubule bundle assembly, vesicle endocytosis
Krt79	2.0	keratin 79	NM_146063	Intermediate filament structural protein *
Daam2	2.0	dishevelled associated activator of morphogenesis 2	NM_001008231	Regulation of cell polarity, binds Rho GTPase and cytoskeleton
Cttnbp2	1.8	cortactin binding protein 2	NM_080285	Regulation of cortactin-dependent actin dynamics
Numa1	1.8	nuclear mitotic apparatus protein 1	NM_133947	Positive regulation of microtubule assembly
Mapre1	1.7	microtubule-associated protein, RP/EB family, member 1	NM_007896	Positive regulation of microtubule assembly
Dst	1.6	dystonin	NM_134448	Integration of cytoskeletal elements
Dock2	1.6	dedicator of cyto-kinesis 2	NM_033374	Regulation of actin polymerization, Rac GTPase activator activity
Nav1	1.6	neuron navigator 1	NM_173437	Positive regulation of microtubule assembly
Cald1	1.6	caldesmon 1	NM_145575	Stabilization of actin filaments
Pard3	1.6	par-3 (partitioning defective 3) homolog (C. elegans)	NM_033620	Regulation of cell polarity, formation of tight junctions
Zfp185	1.6	zinc finger protein 185	NM_009549	Modulation of actin filament dynamics *
Akap2	1.5	A kinase (PRKA) anchor protein 2	NM_001035533	Modulation of actin filament dynamics*
Capn6	1.5	calpain 6	AK048028	Positive regulation of microtubule stability, modulation of Rac GTPase
Cell signaling / transcription regulation				
Meox2	3.1	Mesenchyme homeobox 2	NM_008584	Transcription factor activity, mesoderm specification
Dmrt2	3.0	doublesex and mab-3 related	NM_145831	Transcription factor activity

		transcription factor 2		
Heyl	2.3	hairy/enhancer-of-split related with YRPW motif-like	NM_013905	Transcription factor activity, Notch signaling
Wnt2	2.0	wingless-related MMTV integration site 2	NM_023653	Binds frizzled receptor and induces EMT by activating β-catenin
Twist1	1.7	twist homolog 1	NM_011658	Transcription factor activity, positive regulation of EMT
Twist2	1.7	twist homolog 2	NM_007855	Transcription factor activity
Onecut 1	1.6	one cut domain, family member 1	NM_008262	Transcription factor activity, regulation of cell-matrix adhesion
Ets1	1.6	E26 avian leukemia oncogene 1, 5' domain	NM_011808	Transcription factor activity, cell migration, activates MMPs
Rnd2	1.6	Rho family GTPase 2	NM_009708	GTPase mediated signal transduction, modulation of cell migration
Met	1.6	met proto-oncogene	NM_008591	Positive regulation of EMT
Tead1	1.5	TEA domain family member 1	NM_009346	Transcription factor activity, paraxial mesoderm specification

* Function inferred from sequence orthology or indirect assay.

PARAXIS Regulates Genes Associated with Extracellular Matrix Stabilization and Remodeling

The most striking changes in gene expression in *Paraxis*$^{-/-}$ somites and PSM were found among cell surface proteins that modify ECM organization (Tables 2 and 3). Many of these genes were not previously predicted to participate in somite MET. Notable among these was *fibroblast activation protein alpha* (*Fap*) (16.2-fold down-regulated; Table 3), a gene encoding a transmembrane protein that possesses dipeptidyl peptidase and gelatinase/collagenase activities, and that increases the level of fibronectin and collagen fiber organization in ECM (Aertgeerts, 2005; Lee et al., 2011; Levy et al., 1999). FAP, through association with integrins and urokinase plasminogen activator receptor (UPAR) within focal adhesions, regulates the integrin-dependent cell migration of tumor cells (Artym, 2002; Lee et al., 2011; Mueller, 1999). We confirmed that *Fap* transcripts are reduced in *Paraxis*$^{-/-}$ somites by qRT-PCR (Figure 5B) and *in situ* hybridization (Figure 4A & B). In E9.5 wild type mouse embryos, FAP was localized to both the apical and basal cell surfaces of the epithelial cells in the somite (Figure 4C), suggesting that FAP is important for the interaction of the epithelium with the ECM, perhaps controlling the establishment and maintenance of the separation of the epithelium from its surrounding tissues. Consistent with this, the organization of the fibronectin matrix surrounding *Paraxis*$^{-/-}$ somites is disturbed (Figure 2). Given the dramatic downregulation of *Fap* in *Paraxis*$^{-/-}$ somites, we examined whether *Fap* was a direct target of PARAXIS. When forming a dimer with E47, PARAXIS was able to modestly activate transcription from a highly conserved Ebox located within the *Fap* promoter. These results suggest that PARAXIS can directly activate *Fap* in newly forming somites, and that this activation is essential for proper somite ECM organization.

Among the genes that were upregulated in the absence of *Paraxis* were those that

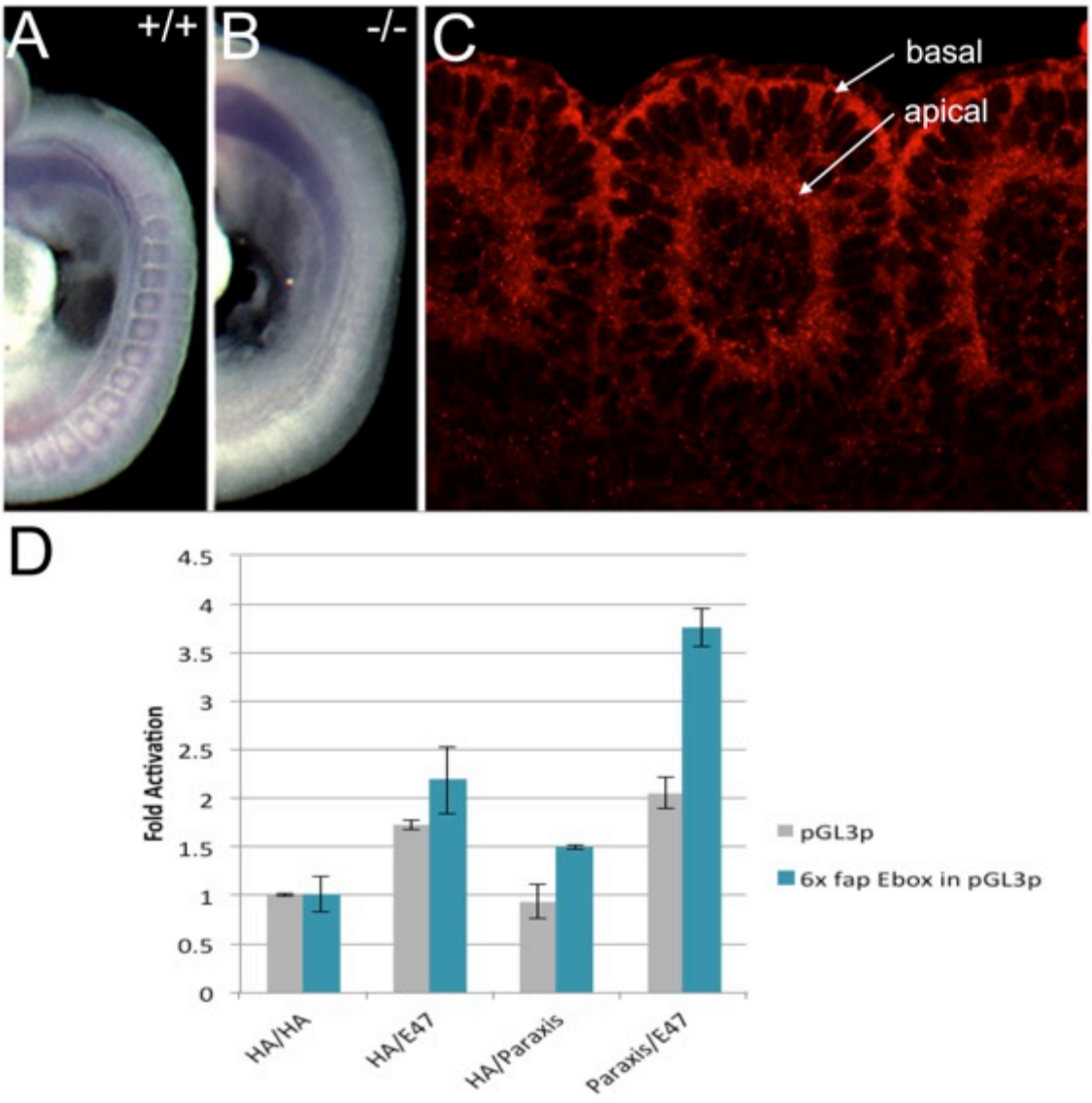

Figure 4. Expression of Fibroblast Activating Protein in the Somite Epithelium is localized to the apical and basal epithelial surfaces, and is activated by PARAXIS. Whole-mount *in situ* hybridization for *Fap* in E9.5 wild type (A) and *Paraxis*$^{-/-}$ (B) somites and PSM reveals strong downregulation in the absence of *Paraxis*. (C) The distribution of FAP in somite IV of the E9.5 wild type embryo was visualized by indirect immunofluorescence using an antibody specific for FAP-α. FAP was localized to both the apical and basal aspects of the somite epithelium. Luciferase-based reporter assays (D) demonstrate that PARAXIS, in combination with E47, is able to activate transcription more than 3.5-fold from a multimerized Ebox found within the first exon of *Fap*. Somite images are presented with anterior to the left and dorsal at the top, and image magnification in C is 200x.

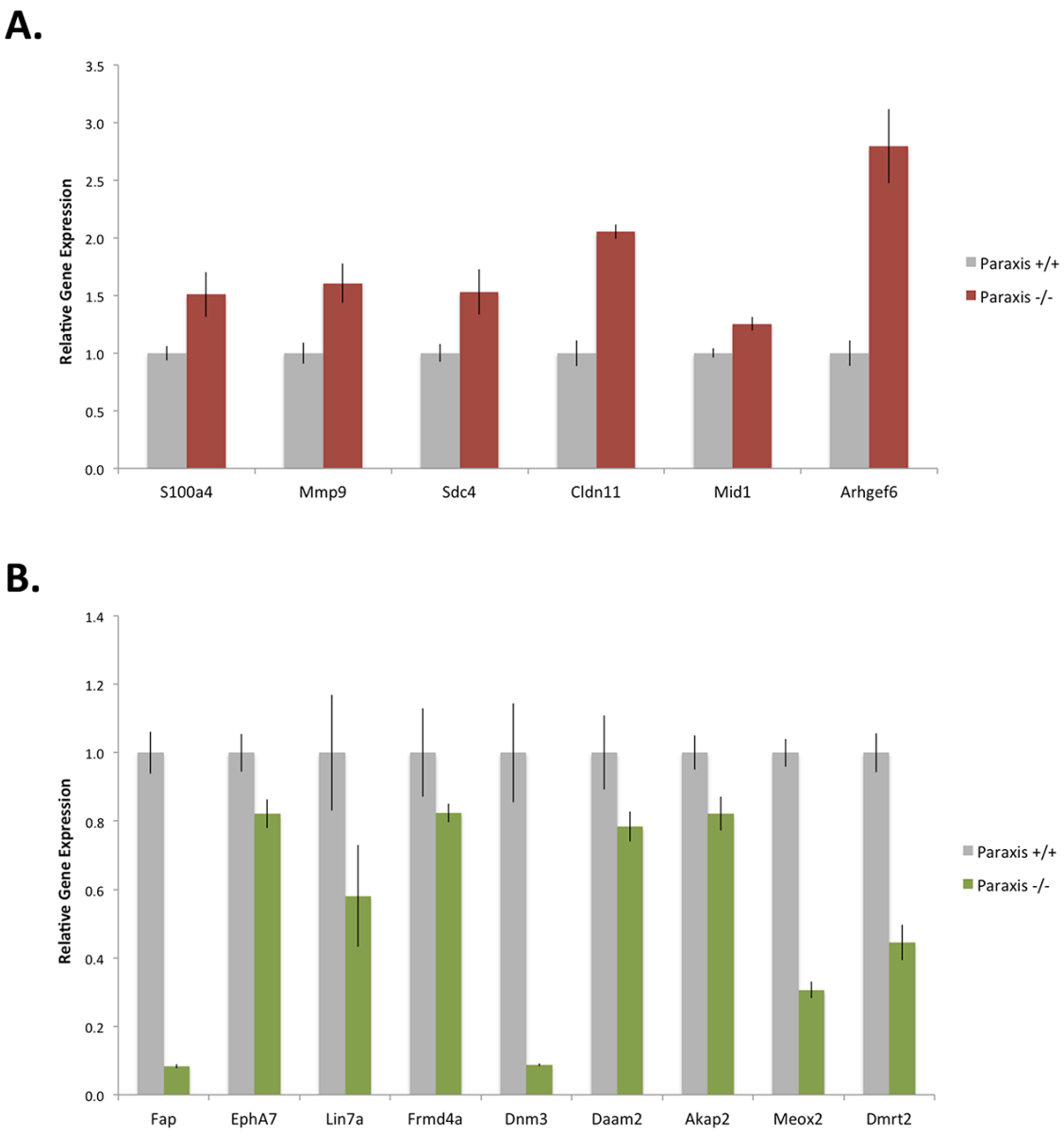

Figure 5. Genes involved in MET processes are deregulated in the *Paraxis*$^{-/-}$ PSM and somite tissue. Relative gene expression, as measured by qRT-PCR, of selected upregulated (A) and downregulated (B) genes known to be involved in ECM organization, cell-cell and cell-ECM adhesion, cytoskeletal rearrangements and MET-related cell signaling and transcriptional regulation. QRT-PCR was performed in triplicate, with duplicate samples for each genotype. Error bars represent +/- one standard deviation. Expression level differences for each gene shown were analyzed using a non-parametric Mann-Whitney test, and found to be statistically significant at a *p*-value of 0.05.

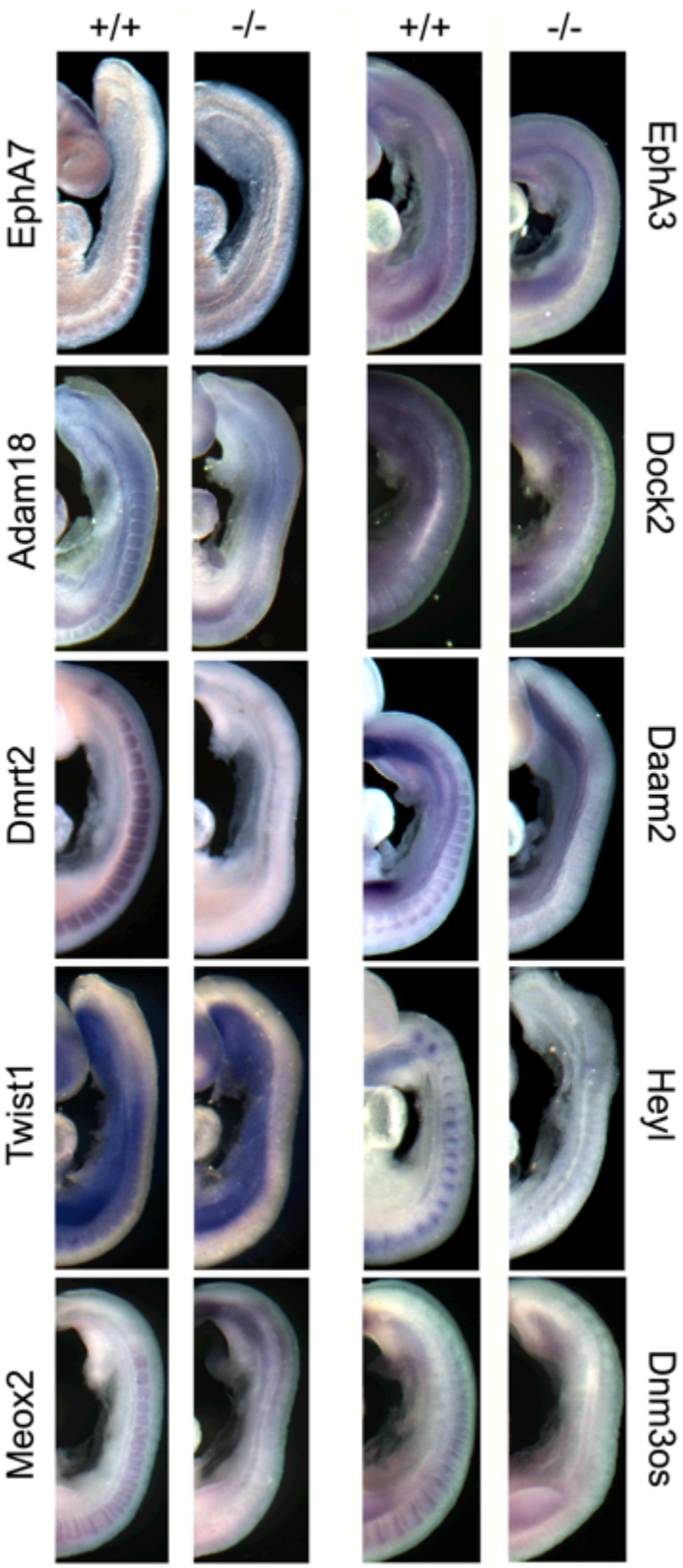
+/+
-/-
+/+
-/-
EphA7
Adam18
Dmrt2
Twist1
Meox2
EphA3
Dock2
Daam2
Heyl
Dnm3os

Figure 6. PARAXIS positively regulates the expression of genes that are involved in MET. *In situ* hybridization of selected downregulated MET genes in wild type and *Paraxis* $^{-/-}$ E9.5 embryos. Expression levels of *EphA7*, *EphA3*, *Adam18*, *Dmrt2, Daam2, Twist1, Heyl, Meox2, Dnm3os and Dock2* were either dramatically reduced, or entirely lost, in the posterior somites and presomitic mesoderm of *Paraxis* $^{-/-}$ embryos. Faint expression of *EphA7*, *Daam2* and *Dock2* remained in the anterior somites, and a weak stripe of *EphA3*, *Dmrt2*, *Heyl, and Meox2* expression persisted in the presomitic mesoderm of mutant embryos. Expression domains and intensities of these genes outside of the paraxial mesoderm were unaffected.

promote cell migration through ECM breakdown. Included in these were *S100a4*, encoding an EF-hand calcium-binding protein associated with metastatic tumors (reviewed in Helfman et al., 2005; Schneider et al., 2008) and the matrix metalloproteinase, MMP9 (Table 2, Figure 5A). Interestingly, S100A4-dependent invasion of tumor cells is dependent on promoting MMP transcription and activity, including MMP9 (Saleem et al., 2006; Schmidt-Hansen, 2004). The metalloproteinase activity of MMP9 promotes EMT in renal tubular cells (Tan et al., 2010). It is possible that PARAXIS represses the same pathway in the paraxial mesoderm in order to abrogate the destruction of the ECM necessary to support the establishment of an epithelium.

PARAXIS Regulates Genes Encoding Cell-ECM and Cell-Cell Adhesion Proteins

Based on the importance of cell-ECM and cell-cell interactions in MET, genes associated with these processes were examined in the *Paraxis*$^{-/-}$ embryos. Genes associated with both interactions were found to be deregulated in the absence of PARAXIS (Table 2 & 3). Notable among them was *Itgav*, encoding an integrin that, along with ITGA5, binds to fibronectin and is essential for the formation of focal adhesions in somites (Yang et al., 1999). It has been previously shown that blocking focal adhesion formation does not inhibit *Paraxis* transcription, suggesting that PARAXIS activity occurs upstream of focal adhesion assembly (Rifes et al., 2007). Interestingly, *syndecan 4* (*Sdc4*), encoding an integrin co-receptor, was upregulated 4.1-fold (Table 2; Figure 5A). The impact of the increase in *Sdc4* on somite morphology in the *Paraxis*$^{-/-}$ embryo is not clear. However, it is possible that this change may cause a disruption of focal adhesions through a stoichiometric imbalance.

The Eph-ephrin bidirectional signaling pathway regulates the reorganization of the

cytoskeleton that can direct either cell-cell adhesion or repulsion (reviewed in Noren and Pasquale, 2004; Poliakov et al., 2004). *EphA3* and *EphA7* receptors were downregulated 1.6- and 2.0-fold, respectively (Table 3). Downregulation of *EphA7* was confirmed by qRT-PCR (Figure 5B), and *in situ* hybridization for both genes in the *Paraxis*$^{-/-}$ embryo (Figure 6). Previously, EPHA3 activity was shown to be required for somite boundary formation in Zebrafish, while EPHA7 was associated with neural crest cell migration (Araujo and Nieto, 1997; Araujo et al.; Lackmann, 1998). This raises the possibility that EPHA3 and EPHA7 are required for adhesive processes during the epithelialization of the somites. *EphA7* is subsequently expressed in the dermomyotome (Araujo and Nieto, 1997), which maintains the epithelialization established during somitogenesis, supporting the idea that this receptor may be required to establish and maintain highly adhesive tissues.

Members of the A Disintegrin and Metalloprotease (ADAM) family, *Adam18* and *Adamtsl3* were downregulated significantly in *Paraxis*$^{-/-}$ embryo PSM and somites (Table 3). The membrane-bound proteins encoded by these genes can participate directly in cell adhesion or inhibit adhesion through ectodomain shedding of type I or type II transmembrane proteins (Weber and Saftig, 2012). ADAM18 is a cell surface protein present on sperm membranes, where it is predicted to increase cell adhesion through interactions with egg integrins (Frayne, 2002; Weber and Saftig, 2012). By *in situ* hybridization, we confirmed that *Adam18* is transcribed in somites and is downregulated in the absence of PARAXIS (Figure 6), raising the possibility that it promotes MET through a PARAXIS-dependent mechanism.

PARAXIS Regulates Cytoskeleton Reorganization During MET

MET is associated with a reorganization of the cytoskeleton that affects cell

morphology, promotes apical/basal polarity, and provides structural support for cell adhesion. Members of the Rho GTPase family (RHOA, RAC1, CDC42) integrate signals from adhesion molecules to direct distinct morphological outcomes that help to stabilize the epithelium (reviewed in Hall, 2005). All three of these GTPases are known to be involved in the regulation of cytoskeletal dynamics during somitogenesis (Nakaya et al., 2004; Takahashi et al., 2005; Watanabe et al., 2007). While actin filaments and RHOA protein are not properly localized in *Paraxis*$^{-/-}$ somites (Rowton et al., 2013), the mRNA levels of *RhoA*, *Rac1* and *Cdc42* themselves were not altered by at least 1.5-fold by microarray. Instead, modifiers of Rac1 and Cdc42 GTPase activity were altered (Tables 2 & 3). The guanine nucleotide exchange factor (GEF), *Dock2* (Fukui et al., 2001), was downregulated 1.6-fold, which was confirmed by *in situ* hybridization in E9.5 *Paraxis*$^{-/-}$ embryos (Figure 6). The Rac1-specific GEF, *Arhgef6* was upregulated in *Paraxis*$^{-/-}$ tissue, 1.6-fold (Table 2, Figure 5A). Further, *Capn6* (1.5-fold down, Table 3), coding for a microtubule-stabilizing protein, is expressed in the somites of mouse embryos (Dear and Boehm, 1999) and can promote RAC1 activity by binding ARHGEF2 (Tonami et al.). The deregulation of genes encoding modifiers of RAC1 activity predicts that regulation of Rho GTPase activity by PARAXIS occurs indirectly during somitogenesis.

PARAXIS Controls Developmental Regulatory Genes Associated with Somitogenesis

Activation of the canonical Wnt signaling pathway has been implicated in both segmentation and MET during somitogenesis. WNT6, acting through a β-CATENIN-dependent pathway, is required to maintain *Paraxis* transcription and somite MET in the chick embryo (Linker, 2005). In our microarray analysis of *Paraxis*$^{-/-}$ somites, the transcription of components of the canonical Wnt signaling pathway, including *Wnt2*, *Wisp2*, and *Daam2*, were downregulated (Table 3). The transcript level reduction of

Daam2, the product of which stabilizes the DVL3/AXIN2 complex and modulates the activity of Rho GTPases (Lee and Deneen, 2012), was confirmed by both qRT-PCR and *in situ* hybridization (Figure 5B and 6). *Dvl3* is also expressed in the somites of mouse embryos (Tsang et al., 1996) and is required for normal somite formation in zebrafish embryos (Gray et al., 2009). These findings reveal a potential positive feedback loop between PARAXIS and Wnt signaling, as well as a possible mechanism by which PARAXIS may regulate Rho GTPases.

Several transcription factors associated with specification and differentiation of paraxial mesoderm are downregulated in the absence of PARAXIS. Of particular interest was *Dmrt2,* as the somites of *Dmrt2*$^{-/-}$ mutants fail to epithelialize, a phenotype similar to *Paraxis*$^{-/-}$ embryos (Burgess et al., 1996; Seo et al., 2006). *Dmrt2* was downregulated 3.0-fold by microarray analysis and almost 60% by qRT-PCR (Table 3, Figure 5B). Based on *in situ* hybridization, this reduction was specific to the somites (Figure 6). It has been proposed that DMRT2 controls somite MET through induction of laminin expression (Seo et al., 2006). The downregulation of *Dmrt2* is therefore consistent with the reduced and diffuse expression of laminin observed in *Paraxis*$^{-/-}$ embryos (Figure 2). These observations predict that PARAXIS modulates the localization of laminin and other ECM proteins required for epithelialization through the activation of *Dmrt2* in the newly forming somites. Alternatively, the disruption of laminin may be linked to the disruption of fibronectin, which we also observed in *Paraxis*$^{-/-}$ somites (Figure 2).

Additional transcription factors that require PARAXIS for proper somite expression include, MEOX2, TWIST1, TWIST2, and HEYL (Table 3). MEOX2, which regulates somite epithelialization and directs *Paraxis* transcription in combination with MEOX1 (Mankoo, 2003), was downregulated 3.1-fold (Figures 5B & 6). This finding is supported by a recent report that demonstrates that Paraxis cooperates with Mef2d to

direct transcription of *meox2* in the *Xenopus* PSM (Gaspera et al., 2012). Together, these observations indicate that there is a positive feedback loop between MEOX2 and PARAXIS during somitogenesis. Further, PARAXIS is required for proper transcription of *Twist1* and *Twist2* (Table 3), which share strong homology with PARAXIS in their bHLH domains. TWIST1 is essential for specification of paraxial mesoderm and positively regulates the transcription of *Fap* (Mikheeva et al., 2010), *Dynamin3* (*Dnm3*), and *Dnm3os* (Loebel et al., 2005), genes that are also downregulated in our studies (Table 3, Figure 6). *Heyl,* a downstream target of Notch signaling, was also found to be downregulated (2.3-fold) in *Paraxis*$^{-/-}$ somites (Table 3). *Heyl* is dynamically expressed in the presomitic mesoderm as a component of the segmentation clock (Leimeister et al., 2000; Nakagawa et al., 1999), in addition to being statically expressed in the posterior aspect of somites (Figure 6). *HeyL* expression was undetectable in the somites of *Paraxis*$^{-/-}$ embryos, and strongly downregulated in the anterior PSM (Figure 6). In addition to *Meox2*, *Twist1*, *Twist2* and *HeyL*, genes encoding additional transcription factors, such as *Pax1* (36.0-fold downregulated, data not shown), were deregulated in the absence of PARAXIS, indicating that PARAXIS is involved not only in the regulation of various MET processes, but also in cell fate decisions within the paraxial mesoderm.

Our transcriptional analysis of the somites and PSM of *Paraxis*$^{-/-}$ embryos has provided unique insight into the functional role of PARAXIS in somite MET. Instead of participating in a linear regulatory path that promotes the transcription of structural genes necessary for the initiation of an epithelial cell morphology, PARAXIS appears to participate in a more complex regulatory network that acts at the basal surface of the epithelium, through the stabilization of the ECM and regulation of the transcription of genes required for cell-ECM adhesion, and through the organization of cytoskeletal elements by differential modulation of Rho GTPase activity. Previous studies have

demonstrated the importance of ECM composition and adhesion proteins at focal adhesions for proper somitogenesis (George et al., 1993; Jülich et al., 2005; Mostafavi-Pour et al., 2003; Rifes and Thorsteinsdóttir, 2012; Rifes et al., 2007; Wehrle-Haller, 2012; Woods and Couchman, 2001; Yang et al., 1999; Yang et al., 1993). These studies, combined with our expression analyses, suggest that PARAXIS serves as a regulatory node for integrating intra- and extracellular cellular events that are temporally connected during somite MET. Further, this study has identified additional genes that are expressed in the mouse somite and may serve as critical regulators during somitogenesis. Significant among these are *Fap*, *Adam18*, and *EphA7*, encoding proteins that are predicted to participate in ECM reorganization, focal adhesions, and cell migration in other tissues in the embryo (Frayne, 2002; Lee et al., 2011; Mueller, 1999; Niedermeyer et al., 2001; Weber and Saftig, 2012).

Finally, one of the more striking findings of our analysis was the role of PARAXIS in promoting the expression of key developmental regulatory genes. The Wnt and Notch pathways are both critical for patterning, MET, and tissue differentiation during somitogenesis. Through induction of *Daam2* and *Heyl* transcription, PARAXIS can modify the signaling activity of these pathways. Further, MEOX2 and DMRT2 are transcription factors that have been implicated in somite MET based on deletion studies in mouse embryos (Mankoo, 2003; Seo et al., 2006). This makes both genes likely proximate targets of a PARAXIS-directed regulatory cascade. In support of this, *Xenopus* PARAXIS and MEF2C are able to directly activate the *Meox2* promoter (Gaspera et al., 2012). Future studies will be required to determine if *Meox2* and other PARAXIS-dependent genes are direct targets of PARAXIS in mouse somite MET.

Chapter 3

PARAXIS controls epaxial and hypaxial myogenesis through PAX3-dependent pathways

Introduction

In many vertebrates, including mammals and birds, skeletal muscle is derived from myogenic progenitor cells (MPCs) embedded in the epithelial dermomyotome compartment of individual somites. The first evidence of cells specified to the myogenic lineage is associated with their delamination from the dorso-medial lip (DML) of the dermomyotome and subjacent migration to the interface with the sclerotome. As described in Chapter 1, the subsequent growth and organization of the resulting myotome compartment is inextricably linked to the dermomyotome through waves of cell migration, and because the epithelium serves as a scaffold for myocyte elongation. At the limb level, a unique migratory population of MPC's delaminate from the ventro-lateral lip (VLL) of the dermomyotome to form the premuscle masses of the appendicular and limb girdle muscles (reviewed in Brand-Saberi et al., 1996b; Brent, 2002; Christ and Ordahl, 1995). The spatio-temporal regulation of the morphogenesis of the myotome from the dermomyotome is well-studied (Buckingham, 2006; Buckingham et al., 2003; Molkentin and Olson, 1996; Olson and Klein, 1994). However, the factors controlling myotome patterning, and the subsequent migration of the subset of dermomyotomal cells fated to the myogenic lineage into the limbs, is not as well understood.

The epithelial state of the dermomyotome is initially regulated by Wnt signaling directed from the surface ectoderm. WNT6, acting through the canonical Wnt pathway protein, β-CATENIN, maintains dermomyotome epithelialization. WNT-6 and β-CATENIN stimulate *Paraxis* transcription, predicting a mechanism by which the Wnt

pathway directs epithelialization. This is supported by the observation that overexpression of *Paraxis* will rescue the epithelial phenotype of the dermomyotome in the absence of WNT6 (Linker, 2005). WNT11, collaborates with WNT6 to maintain the DML and VLL of the dermomyotome, containing the MPC in an epithelial state (Geetha-Loganathan, 2006). WNT11 is also required for the proper orientation of myoblast elongation in the myotome, suggesting a link between the epithelial state of the dermomyotome and myotome organization (Gros et al., 2008). This is most likely mediated by the extracellular matrix produced along the apical surface of the dermomyotome epithelium and between the myotome and sclerotome. Candidates for mediating this interaction are the integrins expressed on the surface of $MYF5^{+ve}$ myoblasts, which bind fibronectin or laminin. Cells in the region of the DML and the adjacent myotome express α6β1 integrin, which binds laminin in the ECM and organizes it into a basal lamina (Bajanca, 2006). In the medial and ventral region of the myotome, the expression shifts to α4β1 integrin, which binds fibronectin, suggesting a change in affinity (Bajanca et al., 2004).

A second, migratory population of MPCs are derived from the VLL of epithelial dermomyotome (Bothe et al., 2007; Buckingham, 2006; Evans et al., 2006). In the anterior somites that express Tbx3, the migratory cells coalesce to form the hypoglossal chord, which gives rise to integral muscles of the neck and the diaphragm (Huang et al., 1999). At the levels of the forelimb and hindlimb buds MPCs express *Met* and *Lbx1* and migrate laterally into the limb bud mesenchyme (Buckingham et al., 2003). A role for PARAXIS has been predicted in the cells of the VLL. A delay in hypaxial trunk myogenesis is evident in the absence of *Paraxis*, as well as a delay in MPC migration into the limb (Wilson-Rawls et al., 1999). This delay is associated with a lack of expression of the differentiation marker, *MyoD*, in the hypaxial dermomyotome. It has been

hypothesized that compensatory MYF5^{+ve} epaxial myocytes rescue the deficit in myoblast specification and migration after approximately 2 days. Supporting this, *Myf5/Paraxis* double knockout mutants are born missing several epaxial and hypaxial muscles, and display severe hypoplasia of the limb muscles (Wilson-Rawls et al., 1999)

The transcription factor, PAX3, is predicted to play a central role in regulatory networks that control specification, epithelial morphology and migratory behavior of MPCs (Figure 1). *Pax3* is expressed throughout the dermomyotome as it forms, before becoming restricted to the persistently epithelial DML and VLL (Williams and Ordahl, 1994). *Pax3* expression, is dependent upon the combinatorial activity of the homeobox transcription factors, MEOX1 and 2 (Mankoo, 2003).

During the initial formation of the epaxial myotome, PAX3 directly regulates the expression of *Dmrt2* (Sato et al., 2010), which itself controls laminin production in the myotome (Seo et al., 2006). Embryos lacking *Dmrt2* do not form a basement membrane separating the myotome from the sclerotome. This could be due either to a lack of laminin production, or to a lack of *integrin α6β1* activation (Sato et al., 2010).

PAX3-mediated delamination of MPCs from the VLL is dependent on the coordinated action of members of the of SIX and EYA transcription factor families (Figure 1) (Tajbakhsh et al., 1997; Grifone et al., 2007; Grifone et al., 2005). PAX3 activates the expression of the tyrosine kinase receptor MET in MPCs while they are still in the dermomyotome, rendering them competent to delaminate and migrate into the limb in the presence of its ligand, Hepatocyte Growth Factor, also known as scatter factor (HGF/SF), (Brand-Saberi et al., 1996a; Dietrich et al., 1999; Epstein et al., 1996). MPCs fail to migrate into the limb in embryos with mutations in *Pax3*, *Met* or *HGF* (Bladt et al., 1995; Schmidt et al., 1995; Tajbakhsh et al., 1997). After MPCs have delaminated, they migrate towards the dorsal and ventral aspect of the limb bud, where

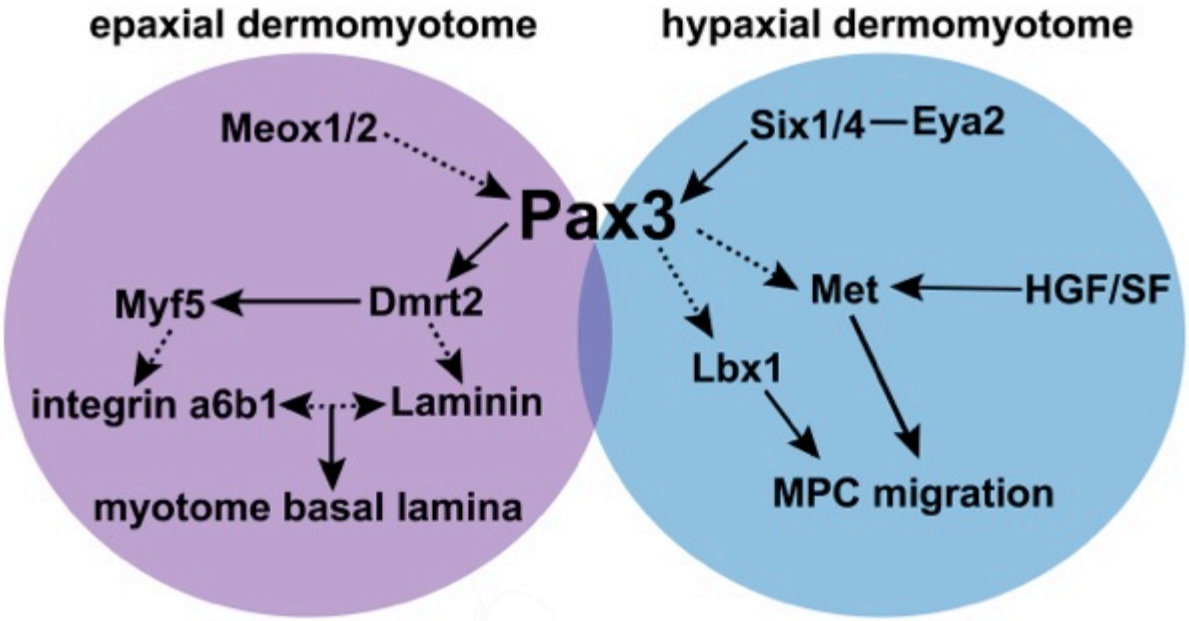

Figure 1. PAX3 regulates epaxial and hypaxial myogenesis. A schematic highlighting PAX3-dependent pathways important for myotome basement membrane formation (purple circle) and limb MPC migration (blue circle). Solid arrows denote direct interactions, while dashed arrows denote interactions for which there is no evidence for direct activation.

they will form the extensor and flexor muscles of the arm and leg (Buckingham et al., 2003). Migrating cells express the ladybird homeobox transcription factor LBX1, which is essential for MPC migration into the limb, and is also targeted by PAX3 transcriptional regulation (Brohmann et al., 2000; Gross et al., 2000; Mennerich et al., 1998; Schafer and Braun, 1999). $LBX1^{+ve}$ cells also express α5β1 and α1β1 integrins, receptors for fibronectin and laminin, respectively (Bajanca and Thorsteinsdóttir, 2002). Both fibronectin and laminin are present in the limb bud during MPC migration (Godfrey and Gradall, 1998; Kosher et al., 1982), and MPCs fail to migrate into the limb when they are inhibited from binding fibronectin (Brand-Saberi et al., 1993b). The results of these studies demonstrate that receptor-ligand interactions are critical to the migration of MPCs into the limb, and that the genetic cascade that controls the expression of these cell-surface receptors are directed by PAX3.

Proliferate and differentiate of MPCs in the limb is dependent on the expression of PAX3, MYF5, MEOX2, and NOTCH (Delfini et al., 2000; Mankoo et al., 1999). Activation of the Notch pathway in myoblasts leads to the stabilization of *Myf5* expression and a downregulation of the differentiation marker *MyoD* (Delfini et al., 2000). *Myf5* expression in the limb is also dependent upon MEOX2, and in the absence of *Meox*2, mouse neonatal limb muscle mass is greatly reduced and several forelimb muscles are absent (Mankoo et al., 1999). The initiation of *MyoD* expression in the limb marks the point at which MPCs stop proliferating and enter into a differentiation program (Kablar et al., 1999). Mouse embryos lacking *MyoD* exhibit a 2.5-day delay in limb myogenesis, while *Pax3* and *Myf5* are normally expressed in these embryos, suggesting that it is *MyoD*, and not genes upstream of it, that is required for the temporal regulation of limb muscle differentiation (Kablar et al., 1997). *MyoD* expression is activated by EYA2 and SIX1, which are expressed in the limb bud at this

time, in addition to regulating *Pax3* expression in the VLL (Heanue et al., 1999). Differentiating limb myoblasts then fuse to form myotubes, while expressing the terminal differentiation markers *Myogenin* and *Mef2* (Edmondson et al., 1994; Sassoon et al., 1989). Finally, tendon precursors migrating from the syndetome express *Scleraxis* and *Mkx*, and migrate between the developing muscle masses and condensing cartilage to connect the components of the appendicular musculoskeletal system (Anderson et al., 2006; Schweitzer et al., 2001).

Paraxis$^{-/-}$ embryos display a dramatic downregulation of *Pax3* in the dermomyotome and the limb buds (Wilson-Rawls et al., 1999), suggesting that the delay in myogenesis observed in *Paraxis*$^{-/-}$ embryos is due to the deregulation of the epaxial and hypaxial PAX3-dependent pathways. The mechanism by which PARAXIS modulates these pathways has not yet been identified. While we know that the differentiation marker, *MyoD*, fails to be properly expressed in the absence of PARAXIS, it is unclear whether this is due to a direct regulation of myogenic differentiation by PARAXIS,. Migratory MPCs in the *Paraxis*$^{-/-}$ somite do not have an epithelial dermomyotome from which to delaminate, raising the possibility that a lack of EMT could lead to aberrant migration or differentiation of these cells. The migration pattern of MPCs and the cell-ECM interactions necessary for migration also have not been characterized in the absence of *Paraxis*. Finally, the proliferation of MPCs in the limb bud prior to differentiation could be affected by a lack of *Paraxis*, leading to the expression of differentiation markers by very few myoblasts in the limb.

Here, we examine the role of PARAXIS in epaxial and hypaxial myogenesis. Using immunofluorescence, qPCR and *in situ* hybridization, we examine the expression levels and distributions of proteins involved in the organization of the early myotome. We find that the basal lamina in *Paraxis*$^{-/-}$ myotomes is not properly formed, leading to

the mislocalization and misalignment of myotomal myocytes. We also demonstrate various defects in neonatal appendicular musculature in the absence of *Paraxis*. We evaluate the potential causes of these defects in the developing embryo, and conclude that the deficits originate from a failure of MPC delamination from a mesenchymal dermomyotome and a lack of MPC migration into the limb. Finally, we demonstrate both direct and indirect regulation of *Pax3* expression by PARAXIS, and we conclude that PARAXIS engages PAX3-dependent pathways to affect the ability of MPCs to interact with their environment.

Materials and Methods

Animals

Mice carrying a null allele for the gene *Paraxis* (Burgess et al., 1996) were maintained as heterozygotes (*Paraxis*$^{+/-}$) according to Institutional Animal Care and Use Committee guidelines. Embryos were genotyped by duplex PCR on embryo yolk sacs using the primers ParaxisWTF: GTCTGGCGTCCAGCTACATC, ParaxisNeoF: TGCTCCTGCCGAGAAAGTAT, ParaxisWT/NeoR: GAGCATCAGGCAAGAGGAAG. For β-galactosidase staining, *Paraxis*$^{+/-}$ mice were crossed to mice carrying the transgene -1565Myogenin-LacZ (Cheng et al., 1992).

β-galactosidase staining

E9.5 or E12.5 wild type *and Paraxis*$^{-/-}$ embryos that carried the -1565Myogenin-LacZ transgene were harvested and fixed in 4% PFA/0.2% Glutaraldehyde in PBS for 30 minutes (E10.5) or 1 hour (E12.5) at room temperature. Embryos were then rinsed in 1x PBS 3 times for 5 minutes, and stained in a solution of 50mM K-Ferrocyanide/50mM K-Ferricyanide/1M MgCl2/20mg/ml X-Gal (Fermentas, #R0401) in PBS overnight with

rotation at room temperature. Embryos were rinsed 3 times for 10 minutes in PBS and fixed in 4% PFA overnight at 4°C. Embryos were photographed using a SMZ1000 stereodissecting microscope (Nikon) with a Retiga CCD digital camera (Q-Imaging). Fixed embryos were embedded, frozen and sectioned as described previously (Anderson et al., 2006), except that 10uM sections were collected. Sections were imaged using 4x and 40x objectives on a Nikon Eclipse TE2000-U inverted microscope. β-galactosidase^{+ve} myocytes from 3 sections each for 3 wild type and 3 *Paraxis*$^{-/-}$ samples were counted using ImageJ (Schneider et al., 2012), and cell counts were compared using a Student's T-test with $p \leq 0.05$.

Immunofluorescence

E10.5 wild type and *Paraxis*$^{-/-}$ embryos were fixed in 4% PFA at 4°C overnight. For whole mount immunofluorescence, embryos were permeabilized in 0.1% Triton-X in PBS (PBS-T) at 4°C for overnight with rotation. Embryos were then blocked in 1%BSA in PBS 2 times for 1 hour and incubated with primary antibody in 0.1%BSA for 3 days at 4°C. Embryos were then rinsed in PBS 5 times for 1 hour and incubated with secondary antibody in 0.1%BSA for 2 days at 4°C. Whole mount immunofluorescence was imaged with a Leica SP2 scanning confocal microscope, using 40x and 63x objectives. Z stacks were viewed as average or maximum projections.

For section immunofluorescence, embryos were embedded, frozen and sectioned as described above for β-galactosidase staining. Sections were permeabilized in 0.1% PBS-T for 20 minutes at room temperature. Antigen retrieval was performed in boiling 10mM sodium citrate buffer, pH 6.0 for 10 minutes when appropriate. Sections were blocked in 10% normal goat serum, 10% normal rabbit serum or 1% BSA in PBS for 1 hour at room temperature, and then incubated with primary antibody overnight at 4°C.

Sections were rinsed with PBS 3 times for 10 minutes and then incubated with secondary antibody for 2 hours at room temperature. Sections were again rinsed 3 times for 10 minutes and incubated with 100 ng/ml 4',6-diamidine-2-phenylidole-dihydrochloride (DAPI) for 10 minutes at room temperature. Sections were rinsed 5 times for 5 minutes with PBS and mounted in a solution of 90% glycerol with p-phenylenediamine (Sigma, #P-6001). Sections were imaged using 10x and 20x objectives on a Nikon Eclipse TE2000-U inverted microscope.

Primary antibodies used were goat anti-DESMIN (Santa Cruz Biotechnologies, #SC-34201, 1:200), mouse anti-PAX7 (Developmental Studies Hybridoma Bank, 1:50), mouse anti-PAX3 (R&D Systems, #MAB2457, 1:50), rabbit anti-LAMININ (Sigma, #L9393-.2ML, 1:400) and rabbit anti-FIBRONECTIN (Sigma, #F3648-.2ML, 1:400). Secondary antibodies used were Alexa Fluor 488 rabbit anti-goat IgG (Life Technologies, #A-11078, 1:1000), Alexa Fluor 488 goat anti-mouse IgG (Life Technologies, #A-11001, 1:1000) and Alexa Fluor 568 goat anti-rabbit IgG (Life Technologies, #A-11011, 1:1000).

Whole mount in situ *hybridization*

E10.5 and 11.5 embryos were fixed in 4% PFA overnight, washed in 0.01% Tween-20 in PBS (PBS-W), and dehydrated in a methanol series for storage at -20 °C until use. To generate antisense digoxygenin-labeled RNA probes, selected genes were amplified by RT-PCR from E10.5 mouse whole embryo cDNA. Gene-specific primers were designed using Primer3 (Rozen and Skaletsky, 1999) and then modified by adding the T7 RNA polymerase binding site sequence (5'-CTAATACGACTCACTATAGGGAGA-3') to the 5' end of the downstream primer. Generation of digoxigenin-labeled antisense RNA probes and *in situ* hybridization was carried out as described in Johnson et al. (2001). *In situ* hybridization was performed using an automated InsituPro (Intavis, LLC, San

Marcos, CA), as described previously (Belo et al., 1997). Embryos were fixed in 4%PFA at 4°C overnight. Embryos were photographed using a SMZ1000 stereodissecting microscope (Nikon) with a Retiga CCD digital camera (Q-Imaging). Some embryos were embedded, frozen and sectioned as described previously (Anderson et al., 2006), and sections were imaged using 10x and 20x objectives on a Nikon Eclipse TE2000-U inverted microscope.

Probes used for WISH spanned the mouse mRNA regions from 588-1,310bp of the *Itga4* transcript, 766-1,467bp of the *Meox2* transcript, 1,421-2,002bp of the *Dmrt2* transcript, 2,973-3,733bp of the *Itga6* transcript, 345-864bp of the *Lbx1* transcript, 2,479-3,098bp of the *Met* transcript, 864-1,463bp of the *Eya2* transcript and 518-1,260bp of the *Six1* transcript.

qPCR

Forelimb-level dermomyotome/myotome tissue from E10.5 embryos, or limb bud tissue from E12.5 embryos, was microdissected from *Paraxis*$^{+/+}$ and *Paraxis*$^{-/-}$ in cold PBS, individually flash frozen and stored at -80 °C until genotyping was completed. Total RNA was extracted with Trizol Reagent (Life Technologies, #15596018), and converted to cDNA with Superscript III (Life Technologies, #18080-044). QRT-PCR was performed on selected genes using Brilliant III Ultra Fast SYBR Green QPCR Master Mix (Agilent, #930882) on the ABI Prism 7900HT Sequence Detection System (Applied Biosystems). Cycling conditions were 95 °C for 3 minutes, followed by 45 cycles of 95 °C for 5s and 60 °C for 15s. Selected genes assayed were normalized to *Gapdh* expression levels. Statistical analysis on expression data was carried out on relative expression levels for 3 wild type and 3 *Paraxis*$^{-/-}$ samples using a nonparametric Mann-Whitney test with $p \leq 0.05$.

Neonate histology

2 wild type and 2 *Paraxis*$^{-/-}$ neonates were collected immediately after birth, euthanized and fixed in 95% ethanol overnight at 4°C. Neonates were dehydrated in an ethanol series and embedded in paraffin for sectioning. 15uM sections were collected along the length of each limb and dried overnight. Select sections representing comparable limb landmarks were subjected to hematoxylin and eosin staining. Representative images of all four limbs were obtained using 4x and 10x objectives on a Nikon Eclipse TE2000-U inverted microscope. Limb structures were identified using the Mouse Limb Anatomy Atlas (April DeLaurier, 2008).

Luciferase Reporter Assay

An 816bp promoter region encompassing the -18kb *Pax3* hypaxial enhancer (Brown et al., 2005) was PCR amplified and sublconed into the XhoI/Kpn1 sites of pGL3Promoter plasmid (Promega, Madison, WI). The PARAXIS coding sequence was subcloned into the XhoI/XbaI sites of the CS2-MT plasmid to create the fusion proteins MT-PARAXIS. The eGFP coding sequence was subcloned into the BamHI/StuI sites of CS2, and E12 was subcloned into the EMSV vector. All clones were sequenced for verification. C2C12 myoblasts/CD1 mouse satellite cells were seeded at $6x10^4$ cells/well in complete media [DMEM/Ham's F-10 supplemented with 10% Newborn Calf Serum/20% Fetal Bovine Serum] in 24-well tissue-culture dishes. After 18 hours, each well was transfected with a total of 500 ng of plasmid DNA using 0.5 µl of X-tremeGENE HP DNA Transfection Reagent (Roche, #06366244001), for a 1:1 DNA:transfection reagent ratio. Transfected cells were lysed 48 hours post-transfection in 100 µl/well Luciferase Cell Culture Lysis Buffer (Promega, Madison, WI) and subjected to a single

freeze-thaw cycle at -80°C. Luciferase activity was measured for each well by reacting 20 µl of cell lysate with 100 µl of Luciferase Assay Buffer (Promega, Madison, WI) in white 96-well plates, using an FLx800 microplate reader (BioTek Instruments, Inc., Winooski, VT). The experiment was performed in triplicate, and fold-change was calculated relative to luciferase activity levels derived from the *Pax3* Hypaxial Enhancer-pGL3P vector co-transfected with expression vectors encoding only the myc peptide.

Results

The localization of myocytes and muscle structural proteins is disrupted in the Paraxis$^{-/-}$ myotome.

The -1565 Myogenin-LacZ transgene was bred into the *Paraxis*$^{+/-}$ mouse line, which allows us to visualize differentiating myocytes in the absence of PARAXIS (Cheng et al., 1992). The forelimb-level myotomes of E9.5 *Paraxis*$^{-/-}$ mice stained for β-galactosidase activity appeared disorganized and compact (Figure 2B) compared to wild type (Figure 2A). Sagittal sections revealed that most of the individual myocytes are centrally located and do not extend to the anterior and posterior borders of the myotome. In some cases, myocytes appear to span the borders between adjacent myotomes (arrowheads in Figure 2D). The myotome was broader along the medial-lateral axis in the *Paraxis*$^{-/-}$ embryos when compared to the wild type myotome (Figure 2E and F), suggesting that the myocytes are not tightly associated with the dermomyotome. These results suggest that the correct localization and orientation of differentiating myocytes depends upon the activity of PARAXIS.

We next examined the distribution of the intermediate filament protein, DESMIN, in the anterior myotome of *Paraxis*$^{-/-}$ embryos by indirect immunofluorescence. DESMIN is concentrated at the tips of elongating myocytes, where it is thought to promote binding

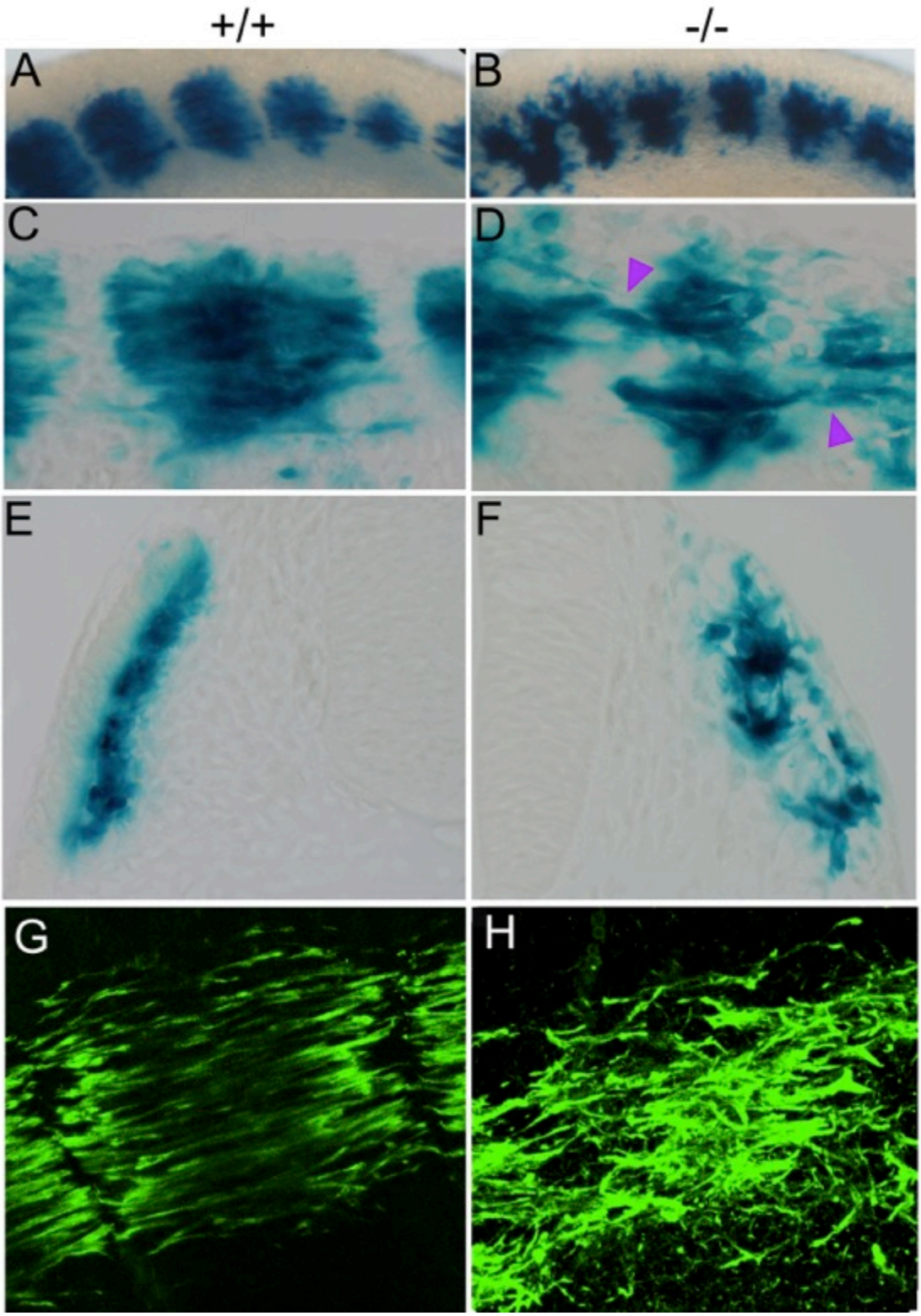
+/+
-/-
A
B
C
D
E
F
G
H

Figure 2. Myocyte orientation and protein localization is disrupted in the *Paraxis*$^{-/-}$ myotome. E9.5 wild type (A, C, E) and *Paraxis*$^{-/-}$ (B, D, F) embryos carrying a -1565Myogenin-LacZ transgene were stained for β-galactosidase activity. Whole mount embryos (A and B) display disorganized myotomes in the absence of *Paraxis*. Sagittal sections (C and D) through anterior somites reveal a general lack of myocyte elongation, with occasional myocyte extension beyond somite borders (purple arrowheads) in *Paraxis*$^{-/-}$ embryos. Transverse sections (E and F) through anterior somites demonstrate a medial-lateral extension of the myotome in *Paraxis*$^{-/-}$ embryos. Immunofluorescent staining for DESMIN in wild type (G) and *Paraxis*$^{-/-}$ (H) embryos reveals mislocalization of the intermediate filament protein from the tips of elongating myocytes in mutant embryos.

to the ECM within the myotendinous junctions that form between somites (Towler, 2004; Wang et al., 2013). DESMIN was located throughout the elongated myocyte in wild type embryos, however, it was most highly concentrated at the anterior and posterior tips of the myocytes (Figure 2G). In embryos lacking *Paraxis*, DESMIN was distributed evenly throughout the disorganized myocytes, and did not appear to be concentrated at the tips (Figure 2H).This result suggests that the proper distribution of anchoring proteins at the ends of myocytes is altered in the absence of *Paraxis* expression, and that this may contribute to the misalignment of myocytes in the *Paraxis*$^{-/-}$ myotome. This observation also raises the possibility that *Paraxis*$^{-/-}$ myofibers have a functional defect, as DESMIN localization is important for mechanical integrity and contractility (Li, 1997).

The integrin α4 subunit is another protein expressed in elongating myocytes within the myotome, and thought to be involved in the extension and anchoring of myocytes to the fibronectin-rich borders of somites. In whole mount *in situ* hybridization (WISH) of E10.5 wild type embryos, Itga4 expression was noted in both the epaxial and hypaxial myotome regions (Figure 3A). Using qPCR, we observed that Itga4 transcription was reduced 5-fold in *Paraxis*$^{-/-}$ myotomes (Figure 3C). WISH revealed that the loss of Itga4 was localized to the epaxial myotome in the dorsal half of the somite, while the hypaxial myotome expression appeared largely unchanged in the E10.5 *Paraxis*$^{-/-}$ embryos (Figure 3B). These data demonstrate that PARAXIS activity is required for the expression of proteins involved in myocyte-ECM interactions in the myotome, and that the disruption of these interactions may cause a lack of myocyte extension and anchorage.

Muscle lineage specification in the dermomyotome is disrupted in Paraxis$^{-/-}$ *embryos.*

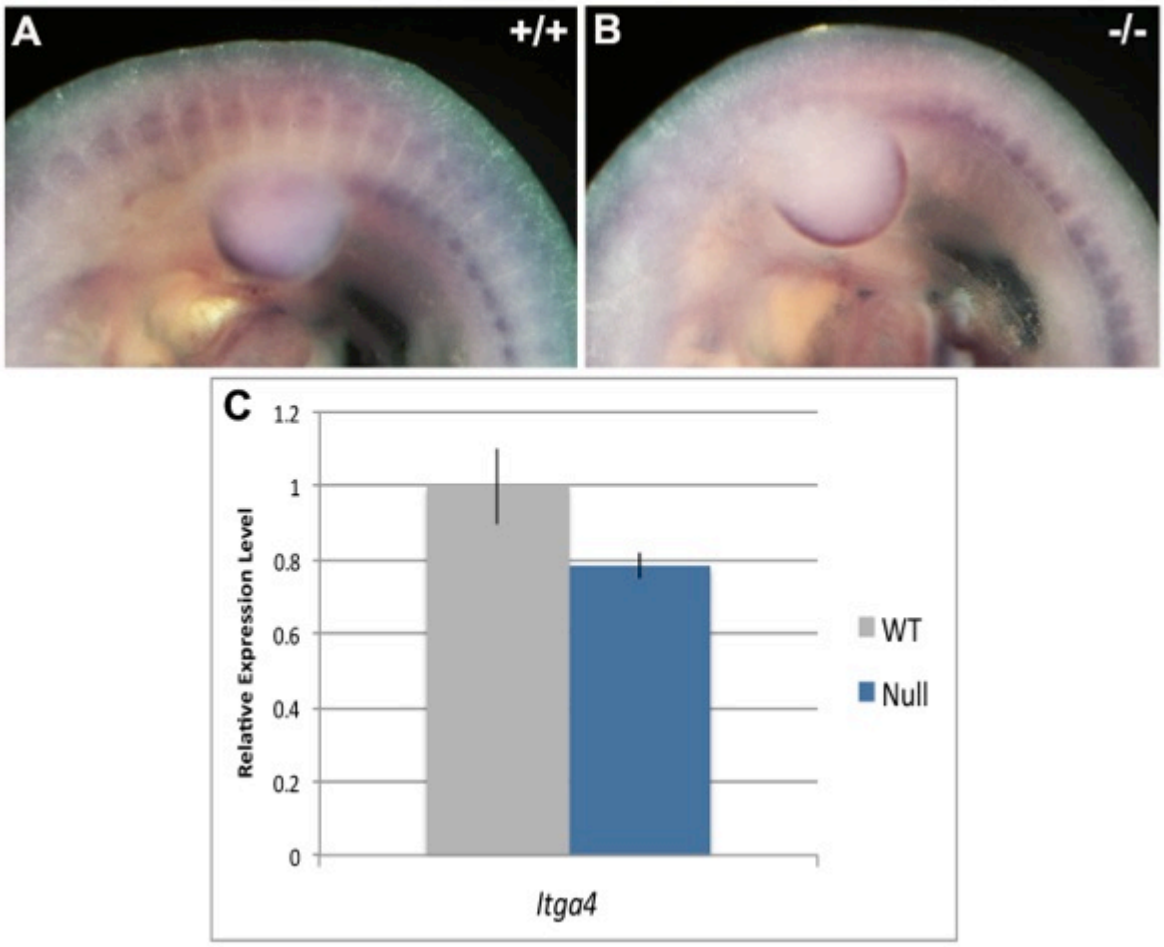

Figure 3. *Itga4* expression is downregulated in the epaxial myotome of *Paraxis*$^{-/-}$ embryos. Whole mount *in situ* hybridization (WISH) was performed on E10.5 wild type (A) and *Paraxis*$^{-/-}$ (B) embryos with a probe specific for *Itga4* mRNA. Staining in the epaxial myotome of forelimb-level somites is not visible in the absence of *Paraxis*. Quantification of the downregulation in mutant embryos by qPCR revealed a 20% reduction in expression level, relative to wild type embryos.

The disorganization of myocytes and structural proteins in the myotomes of *Paraxis*$^{-/-}$ embryos may be due to the disruption of the somitic compartment from which they are derived: the dermomyotome. It has been known for some time that *Paraxis*$^{-/-}$ embryos do not possess epithelial dermomyotomes (Burgess et al., 1996), but the specification of these cells has not been examined in depth. To address this, we used indirect immunofluorescence to assess the expression levels of PAX7 and PAX3, which are concentrated in different regions of the dermomyotome of E10.5 embryos. PAX7 was distributed throughout the central dermomyotome of wild type embryos (Figure 4A). Cells in the region of the dermomyotome of *Paraxis*$^{-/-}$ embryos expressed PAX7 at a level that appeared similar to wild type embryos, though the cells were dispersed over a wider area (Figure 4B). Expression of PAX3, on the other hand, which is predominantly localized to the DML and VLL in wild type embryos (Figure 4C), was significantly reduced in mutant embryo dermomyotomes (Figure 4D and G), supporting the previous finding of a decrease in *Pax3* transcription in embryos lacking *Paraxis* (Wilson-Rawls et al., 1999). Small patches and individual cells stained positive for PAX3 in the region of the *Paraxis*$^{-/-}$ dermomyotome, but the staining was not as robust or as concentrated as in wild type embryos. These results indicate that the PAX3^{+ve} myogenic cells of the DML and VLL are improperly specified in the *Paraxis*$^{-/-}$ dermomyotome region, but that the PAX7^{+ve} MPCs of the central dermomyotome are specified and may compensate for a lack of PAX3 in the developing trunk muscles.

MEOX2 directs epaxial dermomyotome myogenic specification via the regulation of Pax3 expression. In order to determine if the decrease in PAX3 expression in *Paraxis*$^{-/-}$ embryos was due to misregulation of this pathway, we performed WISH with a probe specific for *Meox*2. Wild type E10.5 embryos express *Meox*2 in the DML of the forelimb-level dermomyotome (Figures 4E and 8A), while *Meox*2 expression is nearly abolished in

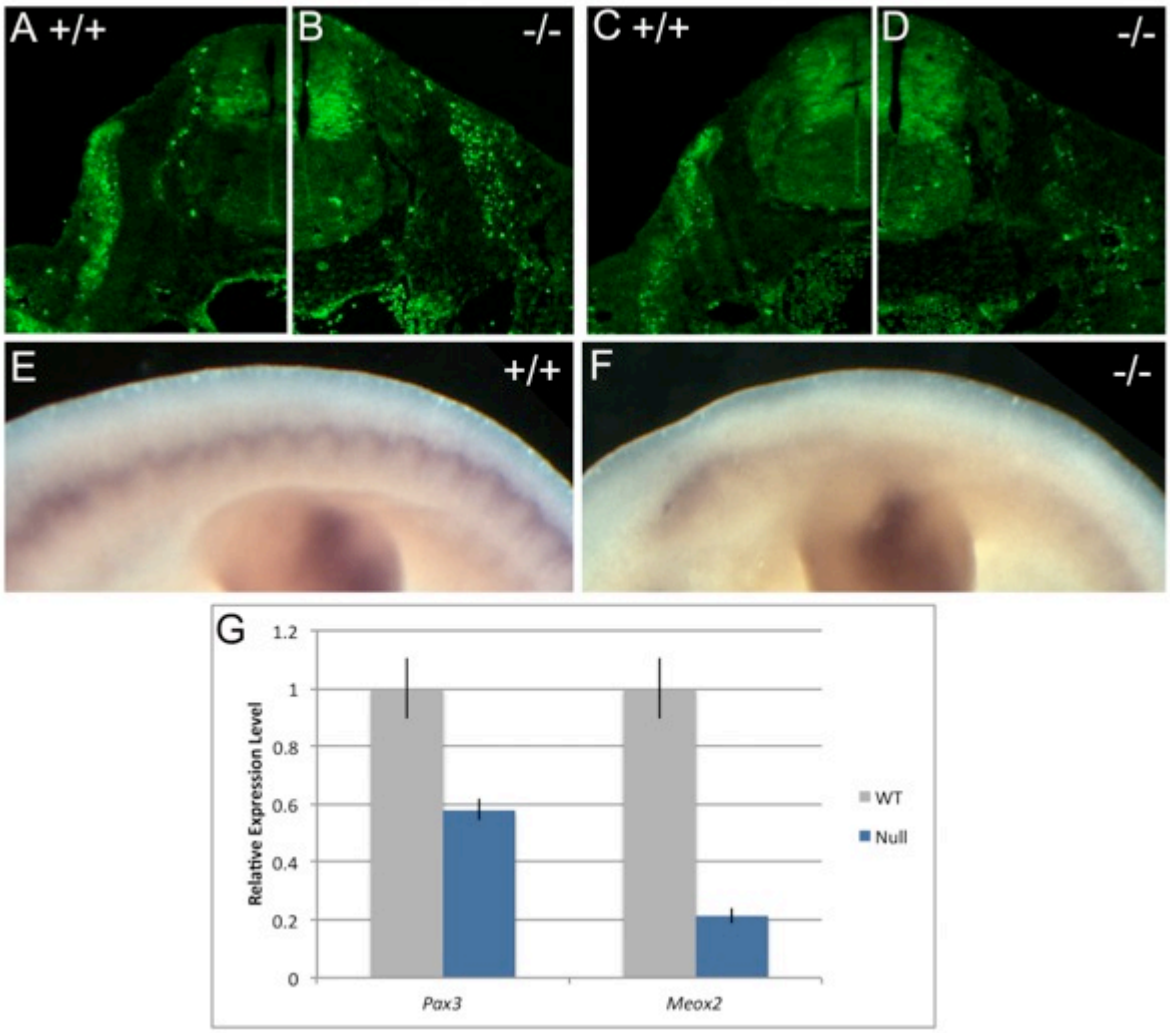

Figure 4. Dermomyotome specification is partially disrupted in *Paraxis*$^{-/-}$ embryos. Section immunofluorescence for PAX7 (A and B) and PAX3 (C and D) reveal similar levels of PAX7 expression in E10.5 wild type (A) and *Paraxis*$^{-/-}$ (B) dermomyotomes. However, there is a dramatic decrease in the number of PAX3-positive cells in the dermomyotomes of mutant embryos (D), compared to wild type embryos (C). WISH with a probe specific for *Meox2* (E and F) reveals a nearly complete ablation of *Meox2* expression in E10.5 forelimb-level dermomyotomes lacking *Paraxis* expression. Quantification of *Pax3* and *Meox2* transcription levels (G) shows them significantly decreased in *Paraxis*$^{-/-}$ embryos. Image magnification in A-D is 100x.

the absence of *Paraxis* (Figures 4F and 8B). Quantification of *Meox2* transcription levels revealed that expression is more than 80% reduced in *Paraxis*$^{-/-}$ dermomyotomes (Figure 4G). This raises the possibility that PARAXIS may regulate PAX3 expression in the epaxial dermomyotome indirectly through MEOX2.

The myotomal basal lamina does not form in the absence of Paraxis *expression.*

During initial myotome formation, PAX3 directly activates the expression of the transcription factor DMRT2 in the dermomyotome. DMRT2 is involved both in laminin production and, indirectly, in the myoblast expression of integrin α6β1, which binds laminin and organizes it into a myotomal basement membrane (Bajanca, 2006; Sato et al., 2010; Seo et al., 2006). PARAXIS activates *Dmrt2* expression in the newly formed somite, where it organizes the basement membrane surrounding the somites (Rowton et al., 2013). To determine whether PARAXIS also regulates *Dmrt2* expression in the dermomyotome, we performed WISH on E9.5 embryos. *Dmrt2* transcripts were detected throughout the dermomyotomes of wild type embryos (Figure 5A), yet appeared completely absent from *Paraxis*$^{-/-}$ embryos (Figure 5B). Immunofluorescent detection of laminin demonstrated that *Paraxis*$^{-/-}$ embryos produce laminin protein in the mature somite, but that it is not organized into a basal lamina separating the myotome from the sclerotome compartments (Figure 5D), as it is in wild type embryos (green arrowheads in Figure 5C). These results suggest that the disruption in myotomal basal lamina formation in *Paraxis*$^{-/-}$ embryos is associated with a dramatic downregulation of *Dmrt2* expression, but that it is not due to a lack of laminin production.

To examine whether basal lamina disruption is due, instead, to the misregulation of integrin α6β1 in the *Paraxis*$^{-/-}$ myotome, we performed WISH with a probe specific for Itga6. Indeed, E10.5 wild type embryos expressed Itga6 strongly in the myotome (Figure

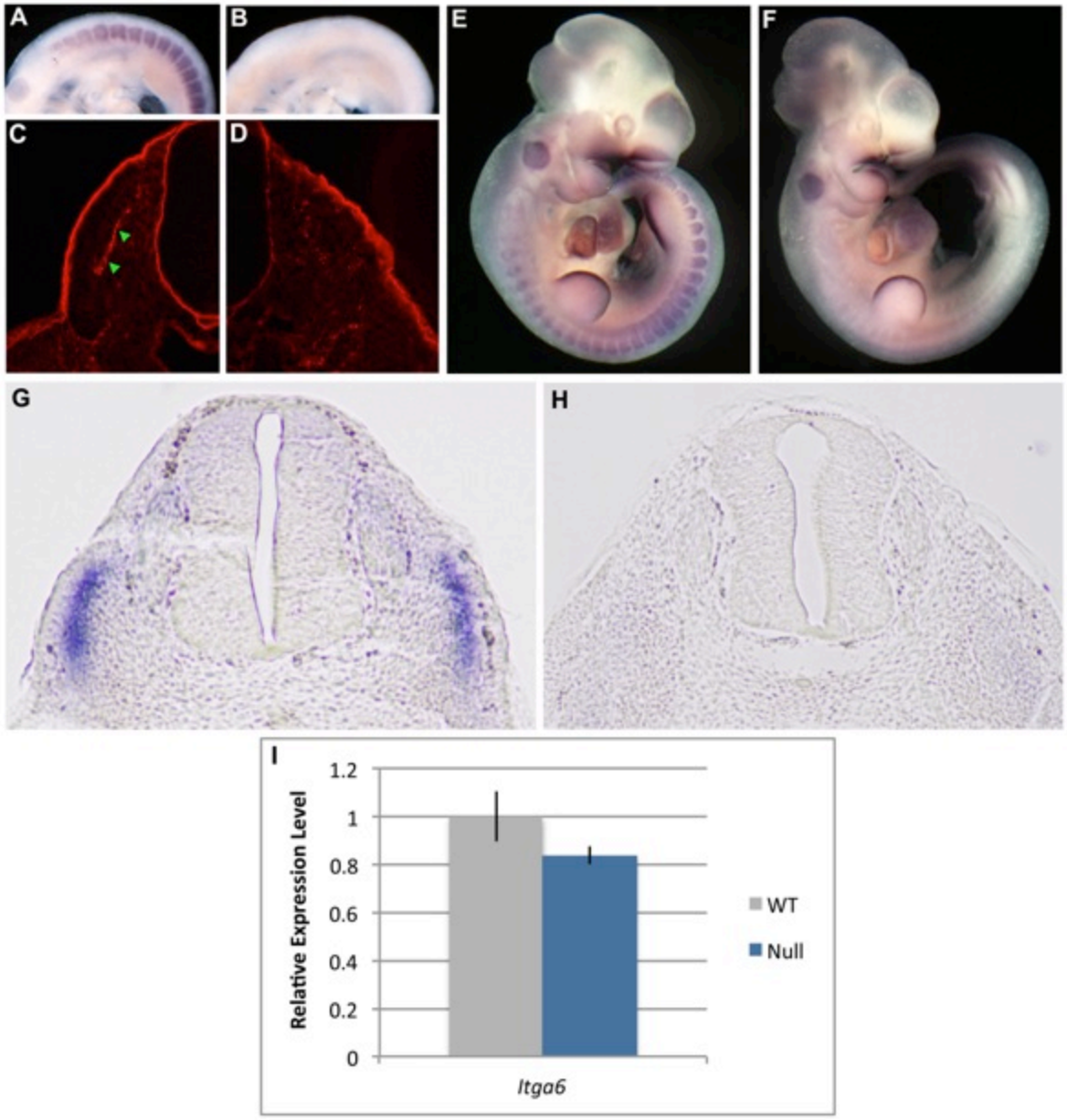

Figure 5. Myotomal basal lamina formation is disrupted in the absence of *Paraxis* expression. *Dmrt2* expression is severely downregulated in E10.5 mutant embryos (B), as compared to wild type embryos (A) and detected by WISH. Immunofluorescence reveals that laminin is present, but disorganized, and does not form a basal lamina (arrowheads in C) in mutant embryos (D). *Itga6* expression is decreased in the myotomes of *Paraxis*$^{-/-}$ embryos (F and H), compared to wild type embryos (E and G). *Itga6* expression in E10.5 myotomes was reduced by 20% in *Paraxis*$^{-/-}$ embryos, relative to wild type levels (I).

5E, G), while *Paraxis*$^{-/-}$ embryos did not (Figure 5F, H). This downregulation was quantified as a nearly 20% reduction by qPCR (Figure 5I). The downregulation of Dmrt2 and Itga6 in embryos lacking *Paraxis* indicates that PARAXIS controls myotome basal lamina formation through the activation of a *Pax3/Dmrt2/integrin α6β1* pathway. Together, observations of *Paraxis*$^{-/-}$ myotome formation suggest that PARAXIS directs epaxial myotome organization through the PAX3-dependent expression of myoblast cell-surface receptors that bind to, and shape, the surrounding ECM.

Forelimb musculature is absent or hypoplastic in Paraxis$^{-/-}$ *neonates.*

It has been demonstrated that *Paraxis*$^{-/-}$ embryos display an approximately 2 day delay in hypaxial myotome formation that is thought to then be compensated for by MYF5-positive myocytes of epaxial origin, resulting in normal neonatal limb musculature (Wilson-Rawls et al., 1999). Given the dramatic disorganization of the myotome in E10.5 *Paraxis*$^{-/-}$ embryos, we hypothesized that PARAXIS may be required for the normal migration of MPCs to the limbs. To test this, we examined the musculature of E18.5 wild type and *Paraxis*$^{-/-}$ limbs in H&E-stained sections. Muscles of the *Paraxis*$^{-/-}$ forelimb displayed varied malformations. Dorsal and ventral muscles of the forelimb zeugopod were unidentifiable in *Paraxis*$^{-/-}$ neonates (Figure 6B), as compared to wild type neonates (Figure 6A). The presence of small myofibers was evident (green arrowhead in Figure 6B inset), but larger fasciculi and intact muscle groups were absent. Furthermore, a large number of adipocytes were present within the area normally occupied by muscle groups in mutant limbs (yellow arrowhead in Figure 6B inset).

Unlike the forelimb zeugopod, all of the muscles of the proximal forelimb were present in *Paraxis*$^{-/-}$ neonates. However, the muscles of the dorsal triceps muscle group

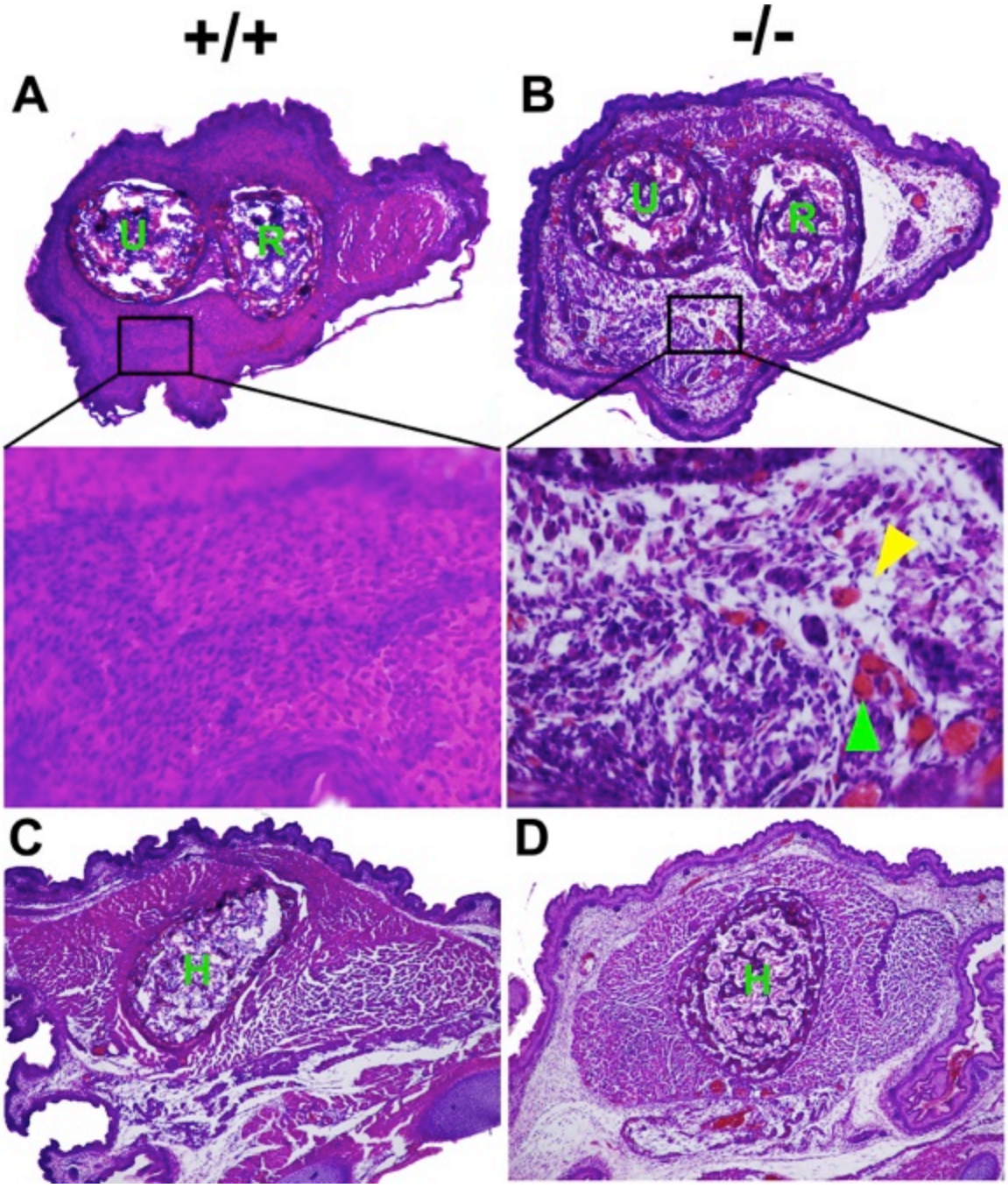

Figure 6. Select forelimb musculature is absent or hypoplastic in *Paraxis*$^{-/-}$ neonates. H&E staining of distal forelimb sections of wild type (A) and mutant (B) neonate forelimbs reveals very few myofibers in *Paraxis*$^{-/-}$ neonates (green arrowhead), and an increase in adipocyte abundance (yellow arrowhead). Sections through proximal forelimbs demonstrate hypoplastic triceps muscles (to the right of the humerus) in mutant embryos. Images in A-D are taken at 40x magnification, except for the insets, which are at 100x.

were hypoplastic (Figure 6C and D), The ventrally-located biceps and brachialis muscles appeared similar in size to wild type muscles, suggesting that the muscle defect was specific to those on the dorsal aspect of the limb. The muscles of the *Paraxis*$^{-/-}$ forelimb stylopod were also surrounded by an overabundance of adipocytes not present in wild type limbs. Muscles of the hindlimb zeugopod and stylopod of neonates lacking PARAXIS were indistinguishable from wild type muscles, with no obvious defects in myogenesis or patterning (data not shown). Together, the defects observed in the distal and proximal forelimb of *Paraxis*$^{-/-}$ neonates indicate varied effects of PARAXIS activity that are specific to the different limb regions, and are essential for proper appendicular muscle development.

A reduced number of myogenic progenitor cells populate the developing limbs of Paraxis$^{-/-}$ *embryos.*

To identify the origin of the myogenesis defects seen in the forelimbs of neonates lacking *Paraxis*, we evaluated the progress of myogenesis in the developing limbs of E12.5 wild type and *Paraxis*$^{-/-}$ embryos. Sagittal sections through the developing limbs of E12.5 *Paraxis*$^{-/-}$ embryos carrying the -1565 Myogenin-LacZ transgene indicate that limb myogenesis is disrupted as early as E12.5. Robust muscle masses are present in both the dorsal and ventral aspects of the developing forelimb and hindlimb of wild type embryos, surrounding the condensing cartilage primordia at the center of the limbs (Figure 7A, C). Mutant embryos, on the other hand, possess fewer differentiating myocytes in the dorsal and ventral muscle masses of both limbs (Figure 7B, D). Indeed, MYOGENIN-positive cells are nearly absent from *Paraxis*$^{-/-}$ hindlimb sections at E12.5 (Figure 7D).

Quantification of the total number of MYOGENIN-positive cells in the limb reveals a deficit of approximately 60% in the forelimb and 80% in the hindlimb of

embryos lacking *Paraxis*, relative to wild type limbs (Figure 7E). Further, when they are considered separately, the dorsal and ventral muscle masses of *Paraxis*$^{-/-}$ embryos reveal an interesting difference. While both the dorsal and ventral muscle masses of mutant embryo forelimbs and hindlimbs possess fewer differentiating myocytes than their wild type counterparts, a greater deficit is seen in the dorsal muscle mass of the E12.5 forelimb than in the ventral muscle mass (Figure 7F). This is consistent with the hypoplasia of the dorsal musculature in *Paraxis*$^{-/-}$ forelimb stylopods. This dorsal/ventral difference is not observed in the developing hindlimb muscle masses, which is also consistent with neonatal results. These results indicate that PARAXIS activity has an effect on the proper number of differentiating myocytes in the developing forelimb and hindlimb, and that this effect is especially pronounced in the dorsal muscle mass of the E12.5 forelimb.

Proliferation of MPCs and ECM organization in Paraxis$^{-/-}$ *limbs is not disrupted.*

PAX3 activity is required for all of the stages of limb myogenesis prior to differentiation. Because *Pax3* limb expression is downregulated in the absence of *Paraxis*, a deficit in the number of MYOGENIN^{+ve} myocytes in the developing limbs of *Paraxis*$^{-/-}$ embryos could derive from one of these PAX3-dependent stages, including MPC proliferation within the limb, migration into the limb bud or delamination from the VLL of the hypaxial dermomyotome. In order to address the possibility of an MPC proliferation defect in embryos lacking *Paraxis*, we performed WISH on E10.5 wild type and *Paraxis*$^{-/-}$ embryos with a probe specific for *Meox*2, which is expressed in proliferating limb MPCs. E10.5 wild type embryos express *Meox*2 strongly in the forming dorsal muscle mass and, to a lesser extent, the ventral muscle mass (Figure 8A). While *Paraxis*$^{-/-}$ embryos lack *Meox*2 expression in the dermomyotome, expression of the

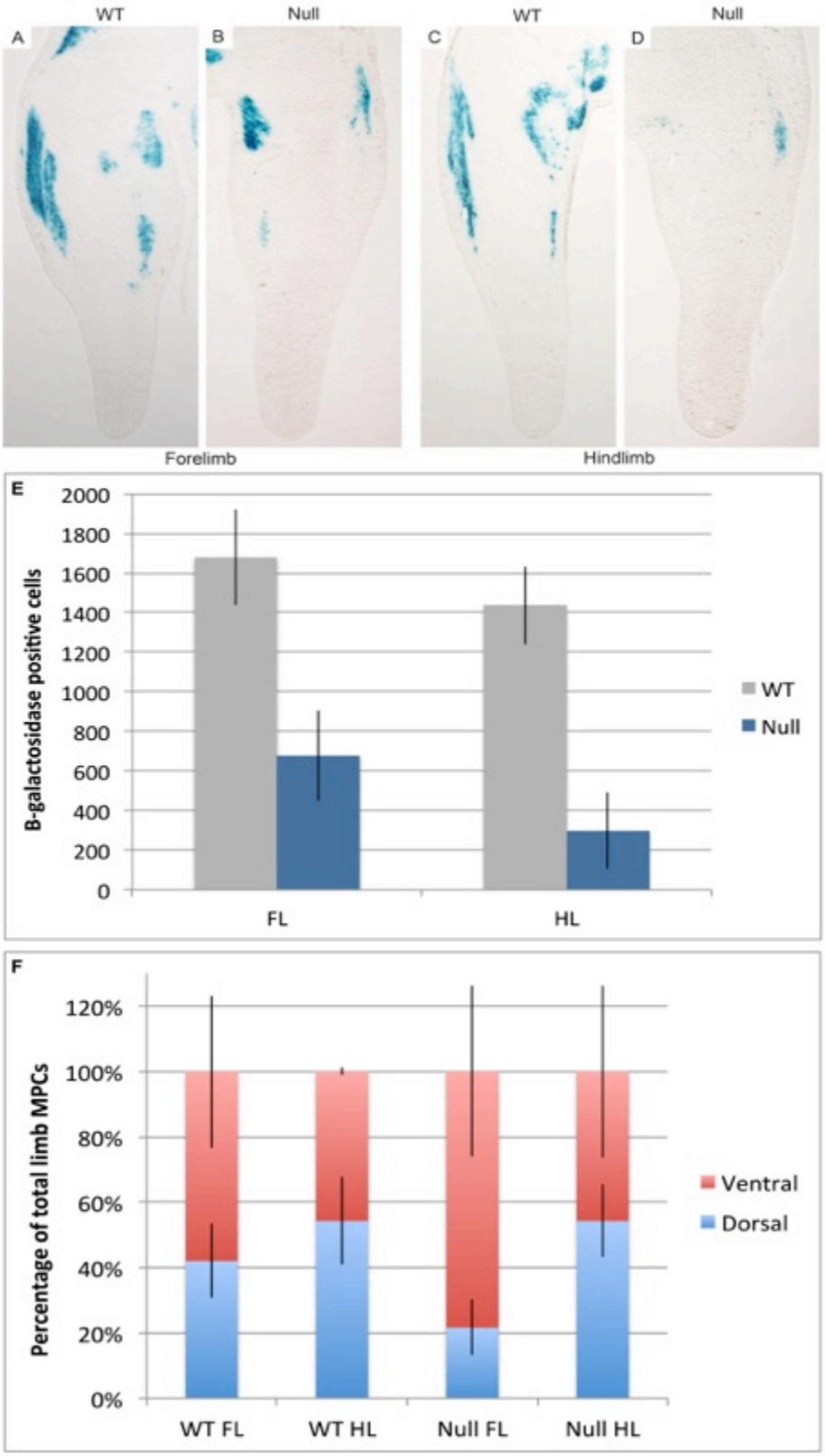
WT
Null
WT
Null
A
B
C
D
Forelimb
Hindlimb
E
B-galactosidase positive cells
2000
1800
1600
1400
1200
1000
800
600
400
200
0
FL
HL
WT
Null
F
Percentage of total limb MPCs
120%
100%
80%
60%
40%
20%
0%
WT FL
WT HL
Null FL
Null HL
Ventral
Dorsal

Figure 7. Myocyte number is reduced in the limbs of embryos lacking *Paraxis* at E12.5. β-galactosidase staining of E12.5 embryo limbs (A-D) demonstrates a reduced number of differentiating myocytes in *Paraxis*$^{-/-}$ forelimbs (B) and hindlimbs (D), as compared to wild type forelimbs (A) and hindlimbs (C). Quantification of MYOGENIN-positive cells (E) reveals a significant decrease in MPC number in mutant forelimbs (T-test: $t_{4.0}$ = 1003.8, P = 0.007) and hindlimbs (T-test: $t_{4.0}$ = 1137.6, P = 0.005). The percentage of dorsal MPCs in the *Paraxis*$^{-/-}$ forelimb is reduced to a greater extent than other limb regions (F).

transcription factor in the E10.5 limb is not reduced (Figure 8B). In fact, a quantitative analysis of *Meox*2 expression levels in the limb indicates that it is slightly upregulated in the absence of *Paraxis* (Figure 8C), raising the possibility that *Meox*2 is upregulated in response to the decrease in MPC number. The maintenance of *Meox*2 expression in the developing limb of *Paraxis*$^{-/-}$ embryos suggests that the deficit in differentiatingmyocytes observed in E12.5 limbs is not due to a defect in MPC proliferation.

Next, we sought to determine if *Paraxis*$^{-/-}$ limb MPCs had a reduced migratory ability. MPC colonization of the limb is dependent upon the proper production and organization of fibronectin and laminin into a scaffold along which integrin-expressing MPCs can migrate. Because *Paraxis*$^{-/-}$ embryos display compromised receptor-driven ECM organization in the newly forming somites (Rowton et al., 2013) and the epaxial myotome, we hypothesized that migratory MPCs also failed to properly shape the ECM in mutant embryo limbs. Fibronectin is expressed throughout the developing limb buds of both wild type (Figure 9A) and *Paraxis*$^{-/-}$ (Figure 9B) E10.5 embryos, as assessed by immunofluorescence. Laminin expression surrounding the surface ectoderm and blood vessels of the *Paraxis*$^{-/-}$ limb (Figure 9D) also appears identical to that of wild type embryos (Figure 9C). Normal localization of fibronectin and laminin in the developing limb mesenchyme of embryos lacking *Paraxis* suggests that MPC migration into the limbs of these embryos is not inhibited by a defect in receptor-driven organization of fibronectin and laminin, and may instead be mediated by another form of cell-environment interaction.

PAX3/MET/LBX1-*dependent hypaxial EMT and migration do not occur in Paraxis*$^{-/-}$ *embryos*.

Migratory limb MPCs require the expression of the PAX3-dependent

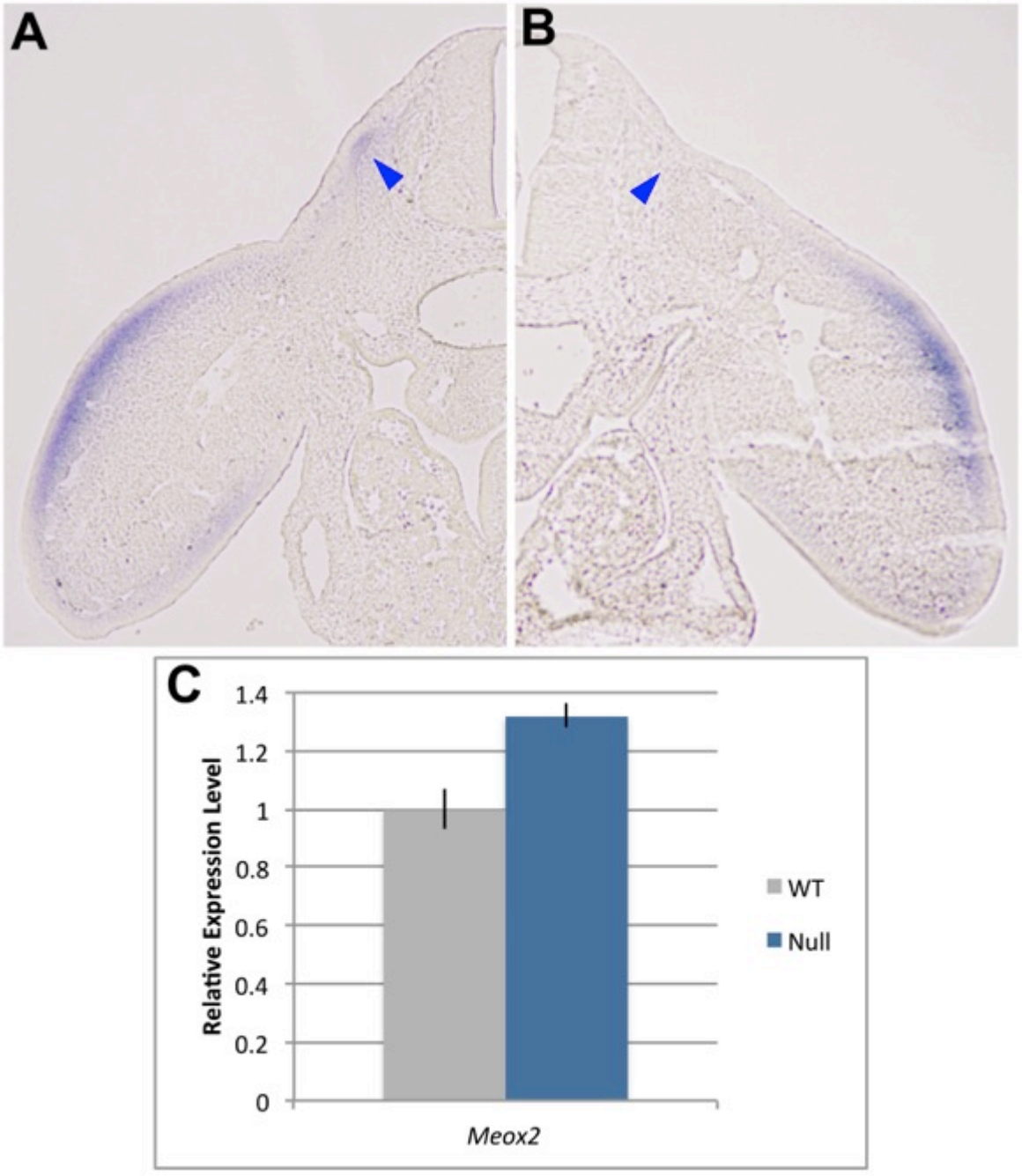

Figure 8. *Meox2* is expressed in the limbs of *Paraxis*$^{-/-}$ embryos. WISH performed on E10.5 wild type (A) and *Paraxis*$^{-/-}$ (B) embryos demonstrates that *Meox2* expression is present in the limbs of mutants, while it is absent from the DML of the dermomyotome (blue arrowheads). *Meox2* transcripts are also present in E12.5 *Paraxis*$^{-/-}$ limb tissue, as measured by qPCR (C).

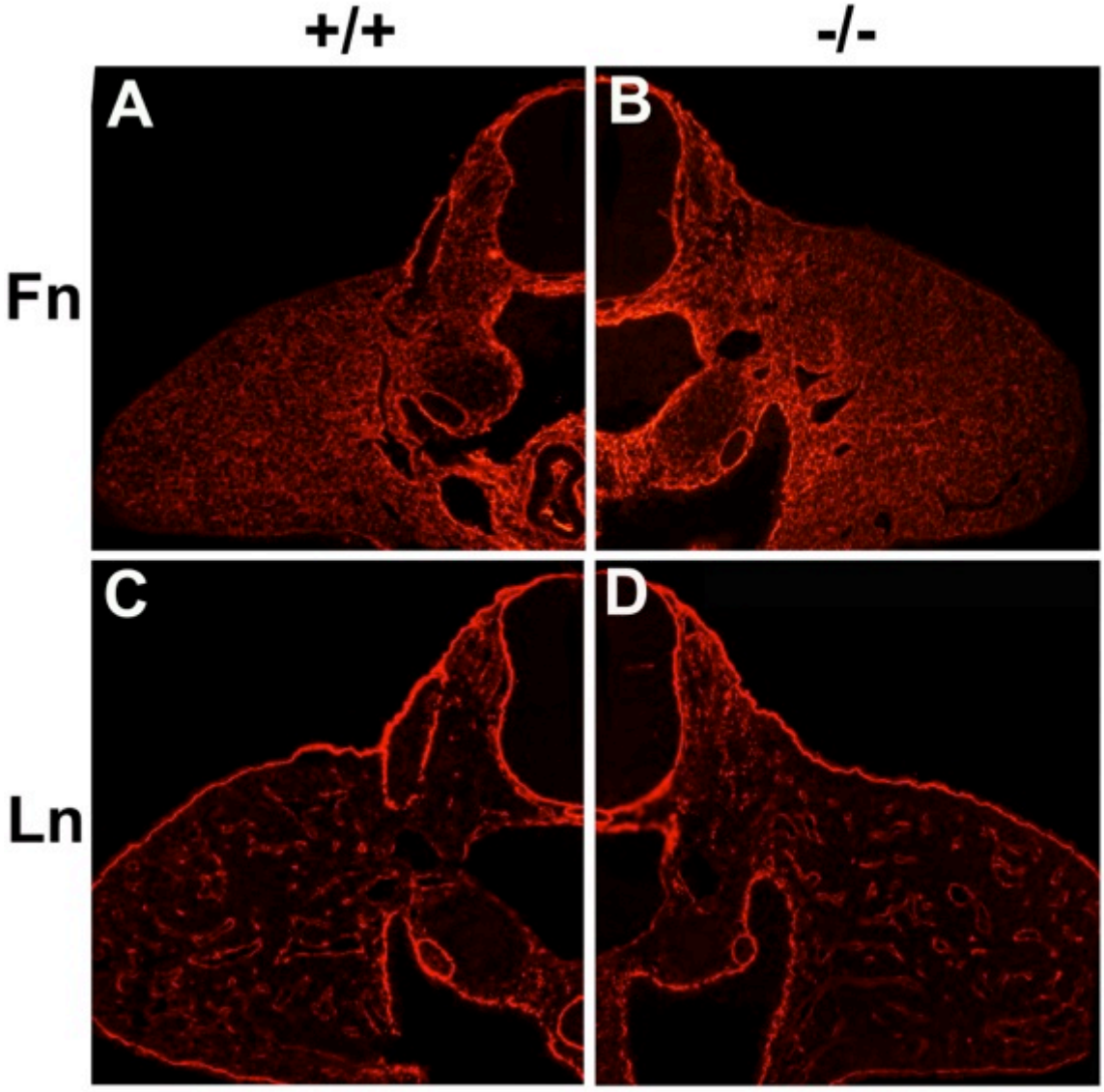

Figure 9. Fibronectin and laminin are normally localized in the limbs of *Paraxis*$^{-/-}$ embryos. Fibronectin (A and B) staining appears normally distributed in the limb buds of E10.5 *Paraxis*$^{-/-}$ embryos (B), as compared to wild type embryos (A). Laminin is localized to the surface ectoderm and blood vessels within the limb buds of both wild type (C) and *Paraxis*$^{-/-}$ (D) embryos. Image magnification is 100x.

transcription factor LBX1 in order to migrate away from the hypaxial dermomyotome and towards the limb (Brohmann et al., 2000; Gross et al., 2000). LBX1^{+ve} cells express the cytokine receptor CXCR4, whose ligand, SDF1, is expressed in the limb mesenchyme and attracts MPCs into the limb (Vasyutina, 2005). To assess the involvement of LBX1 activity in the *Paraxis*$^{-/-}$ limb muscle defect, we examined the expression of *Lbx1* in the mutant embryo. *Lbx1* is expressed in MPCs migrating towards the neck, heart, diaphragm and both limb buds in wild type embryos (Figure 10A, C and E). We observed a nearly complete ablation of *Lbx1* expression in the *Paraxis*$^{-/-}$ embryo (Figure 10B, D and F) using WISH. When measured quantitatively, *Lbx1* expression is reduced by 40% in the E10.5 hypaxial dermomyotome and 70% E12.5 limb (Figure 10M and N).

The migration of limb MPCs is dependent upon their earlier delamination from the epithelial VLL of the dermomyotome. This EMT requires the activation of the MET receptor in MPCs by its ligand HGF/SF, which is expressed by the limb bud mesenchyme. *Met* expression is known to require activation by PAX3 in hypaxial MPCs (Yang et al., 1996), so we evaluated the expression domain and level of *Met* in *Paraxis*$^{-/-}$ embryos. *Met* transcripts were noted in the DML and VLL of the wild type dermomyotome, as well as the forelimb and hindlimb buds at E10.5 (Figure 10G, I, K). In the absence of *Paraxis*, *Met* expression was undetectable in all of these regions, as assessed by WISH (Figure 10H, J, L). Quantification of this reduction confirmed that *Met* transcript levels were reduced by approximately 30% in E10.5 hypaxial dermomyotomes and that the 30% reduction was maintained in E12.5 limbs (Figure 10M, N). We confirmed that HGF/SF is expressed normally in the *Paraxis*$^{-/-}$ limb (data not shown), indicating that any defect in delamination from the VLL would be caused by the misregulation of the MET receptor, rather than its ligand, rendering the cells unresponsive to proper HGF signaling.

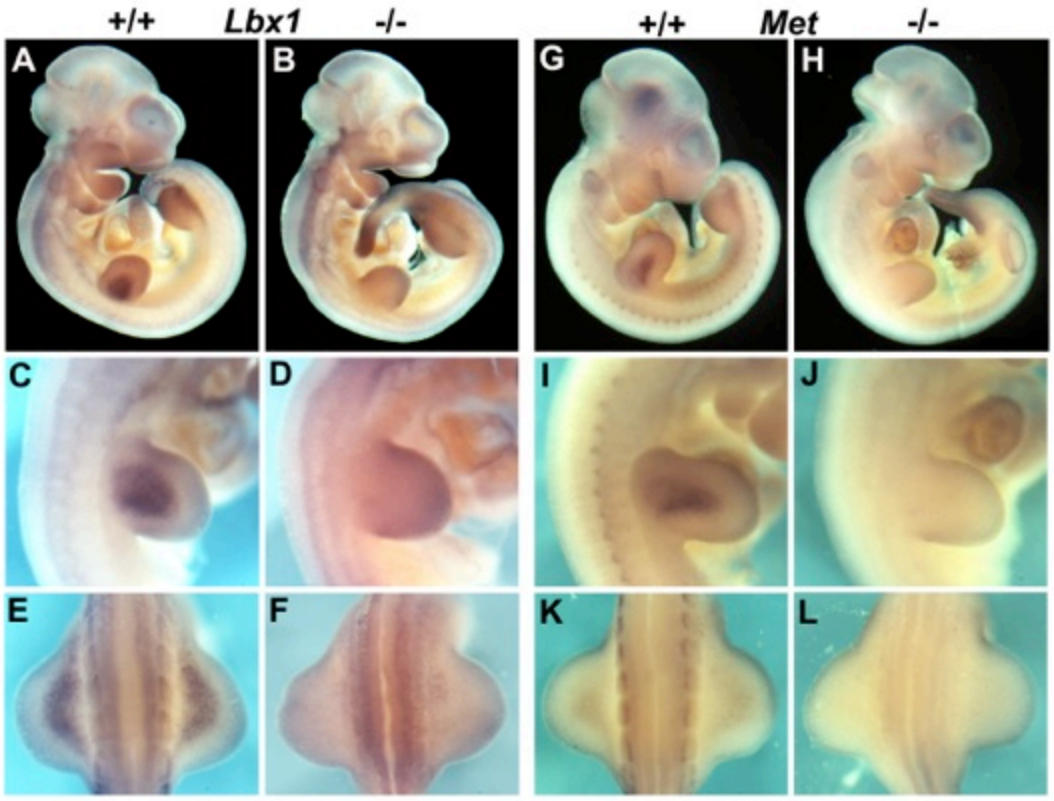
+/+
Lbx1
-/-
+/+
Met
-/-
A
B
G
H
C
D
I
J
E
F
K
L

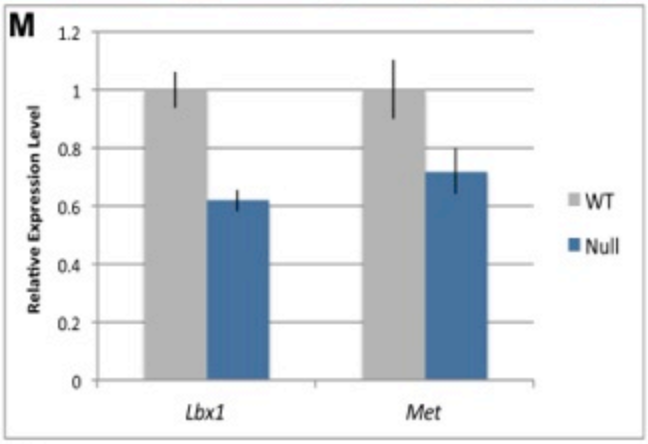
M
Relative Expression Level
1.2
1
0.8
0.6
0.4
0.2
0
Lbx1
Met
WT
Null

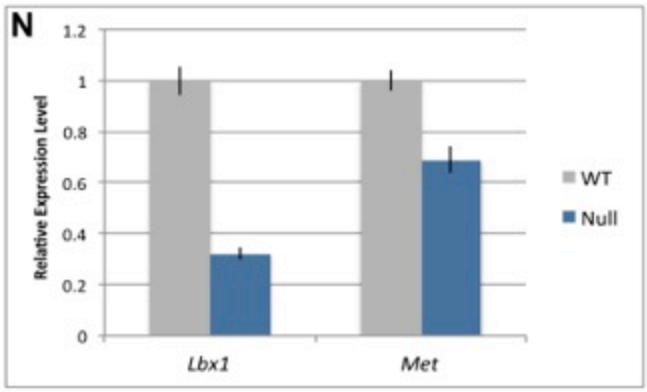
N
Relative Expression Level
1.2
1
0.8
0.6
0.4
0.2
0
Lbx1
Met
WT
Null

Figure 10. The expression of *Lbx1* and *Met* are reduced in embryos lacking *Paraxis*. *Lbx1* expression (A-F) is severely reduced in the forelimb (C and D) and hindlimb (E and F) buds of E10.5 *Paraxis*$^{-/-}$ embryos, as compared to wild type. *Met* expression is similarly reduced (G-L). Quantification of *Lbx1* and *Met* in E10.5 somite (M) and E12.5 limb (N) tissue reveals that the decrease in expression is significant, and that it does not recover by E12.5.

To confirm that migratory MPCs of the *Paraxis*$^{-/-}$ dermomyotome exhibit a delamination defect caused by a lack of *Pax3* expression, we examined the number of delaminating MPCs expressing PAX3 in cells near the VLL. Immunofluorescence revealed that many PAX3-expressing MPCs undergo EMT in the hypaxial dermomyotome (blue arrowhead) and migrate to colonize the limb bud (red arrowheads in Figure 11A). In mutant embryos that lack an epithelial dermomyotome, however, only a few cells express PAX3 in the hypaxial region and the limb bud (Figure 11B). By E12.5, levels of *Pax3* transcription in the *Paraxis*$^{-/-}$ limb are reduced by approximately 50% (Figure 11C). The severe reduction in *Pax3*, *Met* and *Lbx1* expression in *Paraxis*$^{-/-}$ embryos predicts that the appendicular muscle defects seen in the mutant forelimbs are caused by fewer MPCs delaminating from the dermomyotome and migrating into the limb. It is possible that the epithelial morphology of the dermomyotome is necessary for proper MPC gene expression and EMT, and that the lack of an epithelial dermomyotome in the absence of *Paraxis* expression causes MPCs to be incapable of responding to the migration-promoting signals emanating from the limb bud.

PARAXIS regulates the expression of Pax3 in the hypaxial dermomyotome directly, and indirectly through the transcription factors EYA2, SIX1 and SIX4.

Expression of *Pax3* in the hypaxial dermomyotome and migrating MPCs is dependent upon a hypaxial enhancer found within the *Pax3* promoter, -18kb from the transcriptional start site (Brown et al., 2005). Due to the reduction of *Pax3* expression in the hypaxial myoblasts of *Paraxis*$^{-/-}$ embryos, and the presence of four Eboxes within and surrounding the *Pax3* hypaxial enhancer, we tested the possibility that PARAXIS directly controls the expression of *Pax3* from this enhancer. An 816bp promoter region including the enhancer was cloned upstream of the SV40 promoter driving expression of

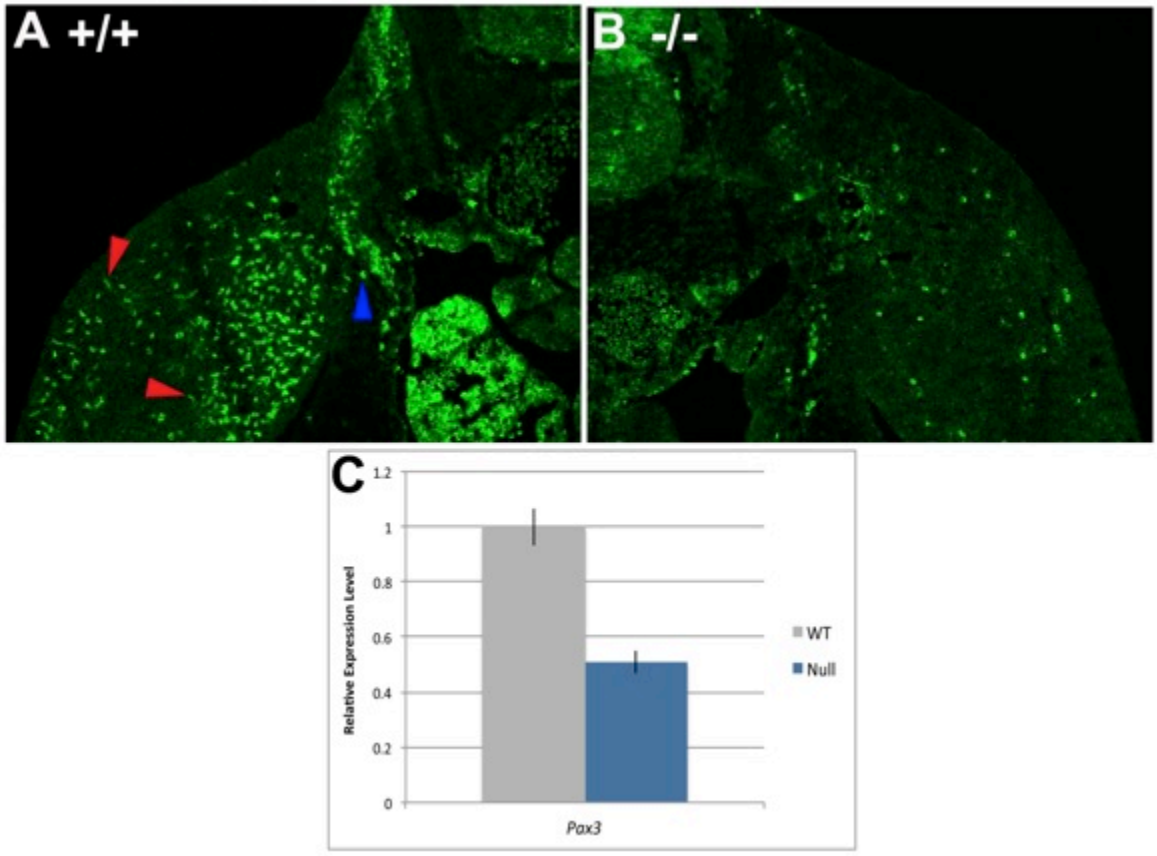

Figure 11. Fewer PAX3-positive cells populate the limb buds of *Paraxis*$^{-/-}$ embryos. Embryos lacking *Paraxis* expression (B) have very few PAX3-positive cells in the regions of the dermomyotome and limb buds, while wild type embryos (A) display several delaminating (blue arrowhead) and migrating (red arrowheads) PAX3-positive MPCs. Image magnification is 100x. Quantification of *Pax3* transcription levels demonstrates a 50% reduction in expression level in the absence of *Paraxis* expression (C).

a luciferase reporter gene, and was transfected into two myogenic cell lines along with expression vectors containing the coding sequence of myc-tagged PARAXIS and its putative binding partner, E12.

In both primary satellite cells and C2C12 myoblasts transfected with an empty pGL3p vector, no combination of transcription factors was able to activate the expression of luciferase (Figure 12A and B). When transfected with pGL3p containing the *Pax3* hypaxial enhancer, however, both E12 and PARAXIS alone were able to activate the transcription of luciferase. In satellite cells, the co-transfection of E12 and PARAXIS, led to the largest fold increase in luciferase activity, though this fold increase was not significantly higher than that caused by the transfection of PARAXIS alone (Figure 12A). In C2C12s, E12 and PARAXIS synergy led to the highest fold-increase of 4.7-fold (Figure 12B), and this increase was greater than those caused by either protein alone. These results suggest that PARAXIS directly activates transcription from the *Pax3* hypaxial enhancer, and that it can do so as a homodimer or heterodimer, depending on its cellular context.

While no other transcription factors have yet been shown to activate *Pax3* transcription from this enhancer, EYA2 and SIX1/4 combine to affect *Pax3* expression in the hypaxial dermomyotome and migrating MPCs. To examine whether PARAXIS may also activate *Pax3* expression indirectly, through the activation of these transcription factors, we used WISH and qPCR to evaluate their expression levels in the absence of *Paraxis*. The expression of Eya2 was weaker in the epaxial and hypaxial lips of the dermomyotomes of *Paraxis*$^{-/-}$ E10.5 embryos (Figure 13B), relative to wild type embryos (Figure 13A). The downregulation of Eya2 was also reflected in the lack of Eya2-expressing MPCs migrating into the limb buds of mutant embryos (Figure 13A and B), and was confirmed by qPCR, where it was suppressed by more than 50% (Figure 13E).

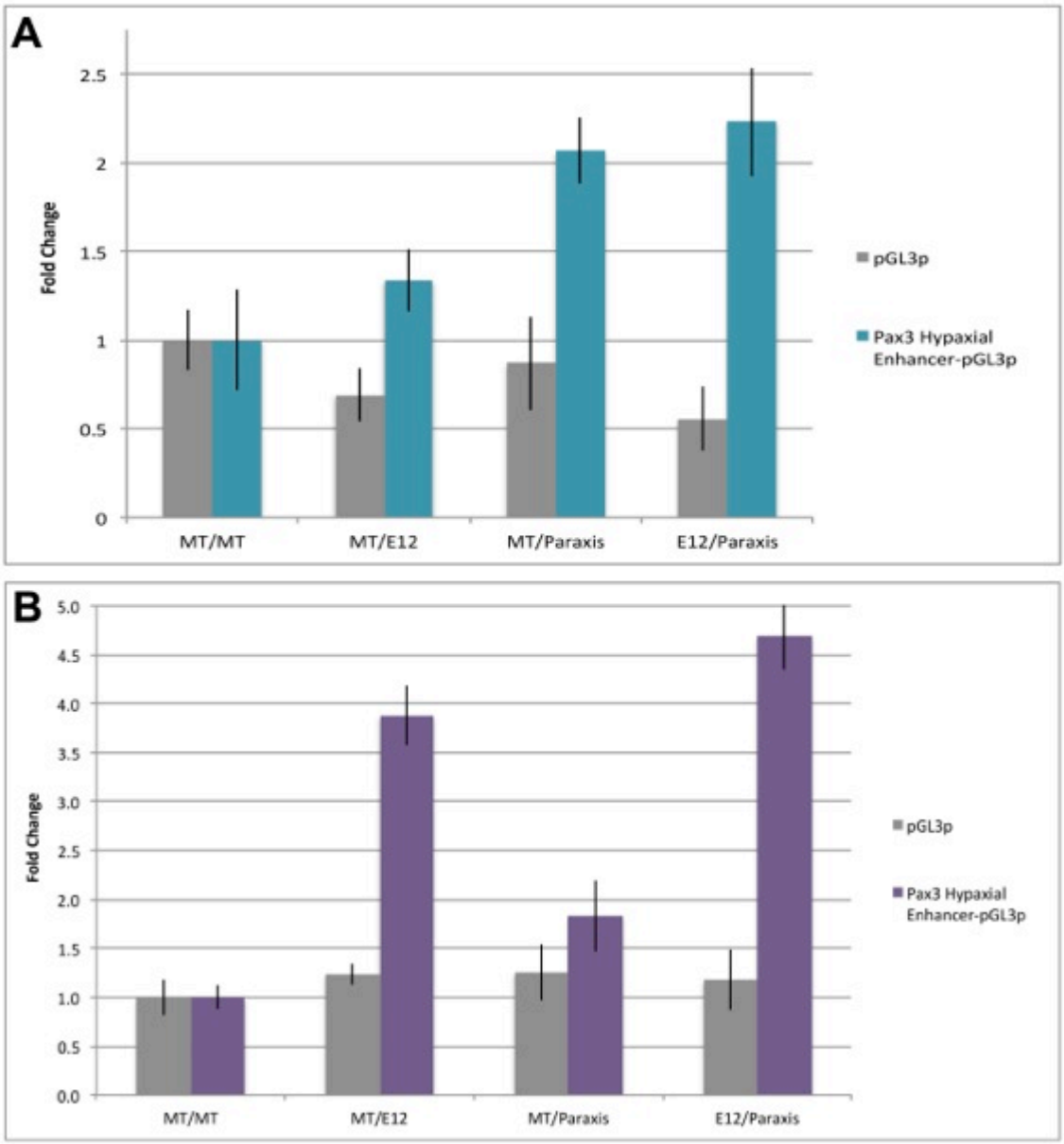

Figure 12. PARAXIS can activate transcription from the *Pax3* hypaxial enhancer in myogenic cell lines. Mouse satellite cells (A) were co-transfected with a plasmid containing the *Pax3* hypaxial enhancer and plasmids encoding a 6x myc-tag (MT), E12 and PARAXIS in different combinations. Cells transfected with PARAXIS and PARAXIS/E12 displayed a 2-fold increase in luciferase activity. C2C12 myoblasts (B) were transfected similarly. C2C12s transfected with E12 and PARAXIS/E12 displayed a 3.8 and 4.7-fold increase in luciferase activity, respectively.

*Six*1 expression in the dermomyotome was similarly downregulated in E10.5 embryos lacking *Paraxis* (Figure 13C and D). Limb bud expression of *Six*1 did not only seem to reflect the presence of migratory MPCs, but was also expressed in a more posterior domain of the developing limb (Figure 13C). In *Paraxis*$^{-/-}$ embryos, *Six*1 expression in this posterior domain was maintained, while the MPC domain was not, probably due to a lack of migratory MPCs (Figure 13D). Both *Six*1 and *Six*4 were downregulated by 30% in *Paraxis*$^{-/-}$ myotomes (Figure 13E). These results demonstrate that PARAXIS is required for proper expression of the *Pax3* regulators EYA2 and SIX1/4, suggesting that PARAXIS may indirectly control *Pax3* expression in the hypaxial dermomyotome through the activation of intermediate regulators.

PARAXIS expression is excluded from myoblasts during early events in embryogenesis, however, its activity is required for the proper development of epaxial and hypaxial skeletal muscle. Epaxial myoblasts in mutant embryos colonize the myotome in a disorganized manner, while hypaxial myotome formation and MPC migration is delayed (Wilson-Rawls et al., 1999). Here, we have sought to determine the mechanism by which PARAXIS regulates muscle development. Previous studies predicted that downregulation of PAX3 in the absence of PARAXIS could participate in these processes. Here we performed a more in depth study of the ECM, ECM receptors and transcription factors associated with early myogenesis. We found that, in fact, many downstream targets of PAX3 are also downregulated in *Paraxis*$^{-/-}$ embryos, strongly supporting the importance of PAX3 regulation in the *Paraxis*$^{-/-}$ phenotype. However, there are some distinctions between PAX3 regulation in the myotome and the limb buds that raise the possibility of a complex regulatory network in which PARAXIS induces the transcription of PAX3 through varied mechanisms.

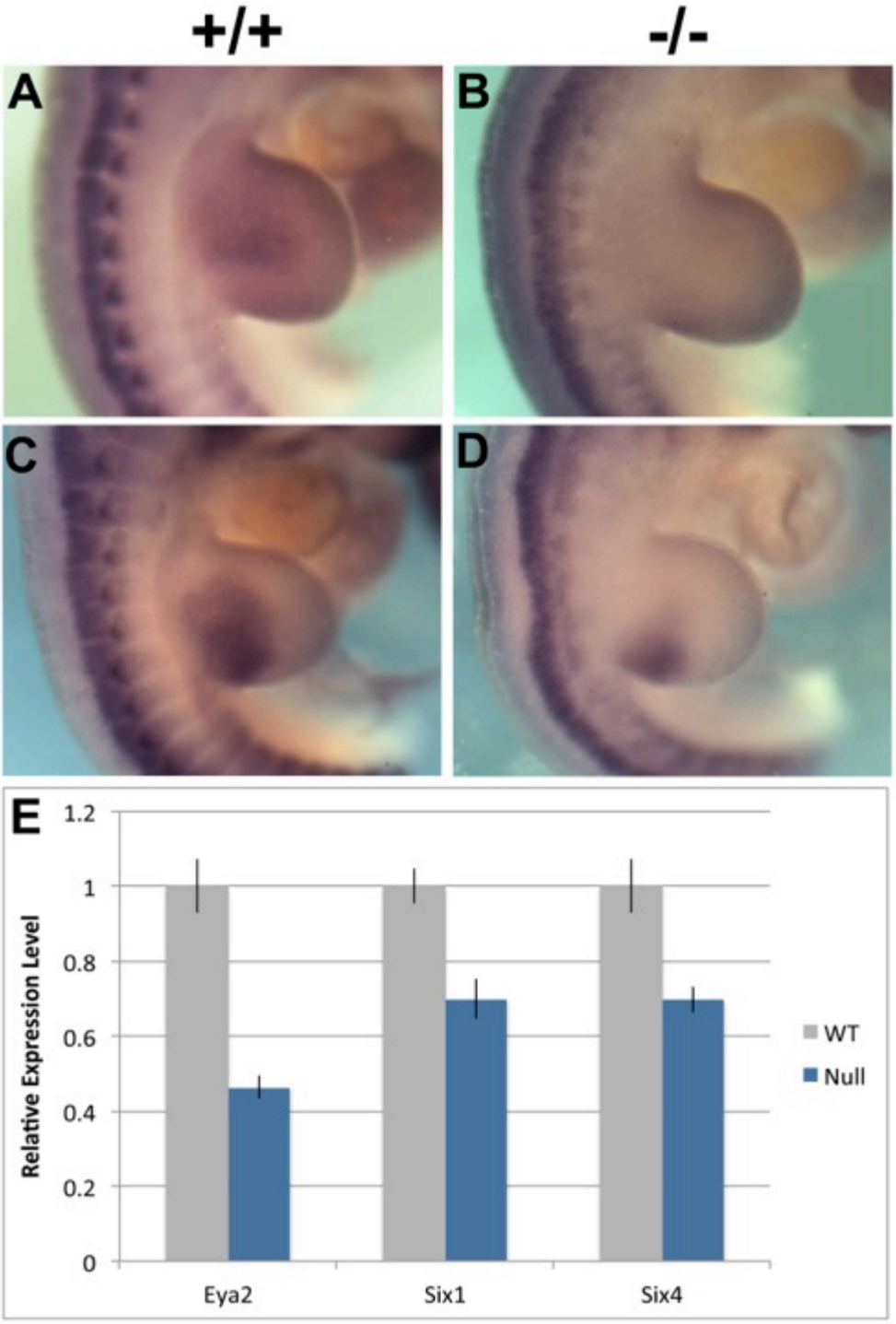

Figure 13. *Eya2* and *Six1* expression is decreased in *Paraxis*$^{-/-}$ embryos. WISH reveals lower levels of *Eya2* (A and B) and *Six1* (C and D) expression in the limb buds of E10.5 mutant embryos, compared to wild type embryos. Quantification of expression level in E10.5 somite tissue confirms the downregulation of *Eya2*, *Six1* and *Six4* in the absence of *Paraxis* (E).

Discussion

PARAXIS regulates the expression of ECM receptors during initial myotome formation

The formation of the myotomal basal lamina is critical to myotome organization, as it provides a scaffold for myocytes extending from anterior to posterior in a parallel fashion with central nuclei (Anderson et al., 2009; Seo et al., 2006; Tajbakhsh et al., 1996). *Paraxis*$^{-/-}$ myotomes are disorganized, with myocytes that fail to extend to the full somite width, cross and expand medially as a group to invade the sclerotome compartment. Based on our understanding of myotome formation, the *Paraxis*$^{-/-}$ phenotype is consistent with defective basal lamina formation or the inability of myocytes to bind to the extracellular matrix proteins of the basal lamina. We present evidence suggesting that both deficits may be occurring in the *Paraxis*$^{-/-}$ somites, including the reduction of *Dmrt2* expression required for laminin expression, disruption to the organization of the existing laminin, and reduction of *Itga6* expression. ITGA6 is a component of the integrin α6β1, which is the only laminin-specific receptor expressed in the early myotome (Bajanca et al., 2004). Inactivation of *Itga6* leads to the medial spreading of myocytes (Bajanca, 2006), similar to what was observed in the *Paraxis*$^{-/-}$ somites. The α4 subunit of the integrin α4β1 is also downregulated in the *Paraxis* mutants. Integrin α4β1 is normally expressed on elongating myocyte tips where it binds fibronectin in the basal lamina (Wayner et al., 1989; Bajanca et al., 2004), and the inhibition of fibronectin between somites leads to a disruption in myofiber organization in zebrafish embryos (Snow et al., 2008). Overall, these studies predict that PARAXIS participates in establishing the morphology of the early myotome through the regulation of the laminin scaffold and the production of integrin receptors that mediate myocyte binding.

PARAXIS regulates the expression of receptors and transcription factors required for MPC EMT and migration into the limb bud

Paraxis$^{-/-}$ embryos exhibit a delay in MYOD-regulated hypaxial myogenesis and MPC migration into the limb bud. However, it has been suggested that this defect is compensated by MYF5+ myoblasts of epaxial origin by E12.5 (Wilson-Rawls et al., 1999). Here, we have shown that, while certain aspects of appendicular myogenesis are rescued in *Paraxis*$^{-/-}$ embryos, not all of the effects of delayed hypaxial myogenesis are overcome. Specifically, *Paraxis*$^{-/-}$ neonates are born with hypoplastic dorsal forelimb stylopod muscles and an absence of forelimb zeugopod muscles, and these defects are reflected in a reduction in MPC number within the limb at E12.5. The specificity of the musculature defects seen in *Paraxis*$^{-/-}$ neonates is reminiscent of *Lbx1* and *Met* mutants, which also display defects only in certain muscle groups (Gross et al., 2000; Schafer and Braun, 1999). Similar to *Paraxis*$^{-/-}$ neonates, the dorsal limb muscles, rather than the ventral muscles, of *Lbx1*$^{-/-}$ mice are especially affected (Gross et al., 2000; Schafer and Braun, 1999). Furthermore, partially compromising MET receptor function in mouse embryos results in defects in particular forelimb muscles at E15.5 (Maina et al., 2001). The similarities between the specificity of LBX1, MET and PARAXIS activity suggest that these transcription factors participate in the same genetic pathway to regulate appendicular muscle development. This was supported by the observation that *Lbx1* and *Met* expression are dramatically downregulated in the absence of *Paraxis*. The misregulation of both genes points to a role for PARAXIS in two distinct processes: the delamination of MPCs from the VLL of the dermomyotome, and the migration of MPCs away from the somite and into the limb bud.

Our expression studies reveal the importance of PARAXIS in the activation of a PAX3-dependent pathway controlling myotome and limb muscle development. This is

occurring, at least in part, through the regulation of *Pax3* transcription by PARAXIS. However, it is interesting to note that other critical regulators of PAX3 are also misregulated in the *Paraxis*$^{-/-}$ embryos. More specifically, MEOX2, which regulates *Pax3* expression in the dermomyotome and migrating MPCs is expressed in the dermomyotome, but not the limb buds of *Paraxis*$^{-/-}$ embryos. This suggests that PARAXIS may regulate epaxial *Pax3* expression indirectly through a MEOX2-dependent pathway. Further, *Eya2* and *Six1/Six4*, encoding known regulators of *Pax3* expression, are also downregulated in *Paraxis*$^{-/-}$ embryos. Evidence for the ability of SIX1 to bind the *Pax3* hypaxial enhancer (Grifone et al., 2007) indicates that, in vivo, PARAXIS and SIX1 may both bind the enhancer and activate it cooperatively. Collectively, this reveals the potential for a complex feedback loop between PARAXIS and PAX3 in the regulation of early myogenesis.

Chapter 4

Conclusions

The transcription factor PARAXIS has been shown to be essential for the development of the vertebrate musculoskeletal system. Previous studies have implicated the gene in MET and the proliferation and specification of the MPCs that migrate into the limb buds. This work has sought to elucidate the genetic hierarchies within which PARAXIS functions during somitogenesis and muscle development. We have found that PARAXIS regulates the expression of genes important for interactions between cells and their environment. PARAXIS directs epithelialization during somitogenesis by activating receptors that organize the ECM surrounding forming somites. Through participation in PAX3-dependent pathways, PARAXIS regulates the expression of similar receptors during muscle development, in addition to receptors that bind diffusible morphogens. The identification of PARAXIS targets enables us to better understand the mechanisms by which transcription factors control the morphogenesis of the mesodermal lineages. Advances in this field can ultimately be used in the pursuit of treatments and preventions for congenital diseases of the musculoskeletal system.

Paraxis *is a vertebrate-specific transcription factor.*

The evolutionary history of *Paraxis* can provide additional clues as to its present-day function in vertebrates. *Paraxis* and its sister gene, *Scleraxis*, only exist within the genomes of vertebrates, most likely duplicating and diverging during one of the two vertebrate-specific genome duplications. When comparing the amino acid divergence of mouse PARAXIS, SCLERAXIS and the *Drosophila* PARASCLERAXIS orthologue (Figure 1A), the bHLH domains retain a high degree of homology. A comparison of the bHLH

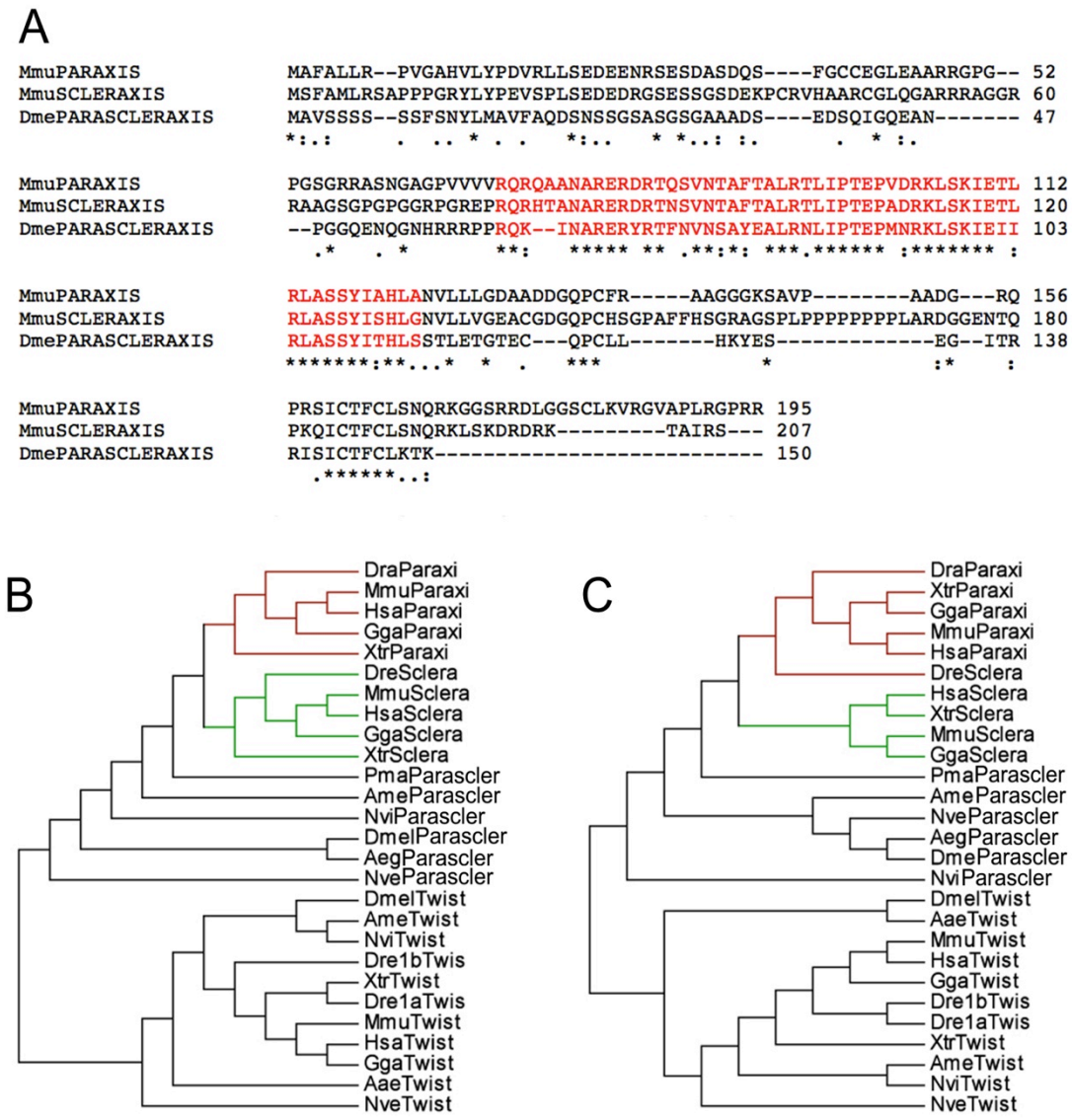

Figure 1. Evolutionary relationships of mouse PARAXIS, SCLERAXIS, *Drosophila* and PARASCLERAXIS proteins. Amino acid sequences for mouse PARAXIS and SCLERAXIS and *Drosophila* PARASCLERAXIS were aligned (A) using ClustalW. Asterisks denote conserved residues, while colons and periods denote semi-conserved residues. The bHLH region is highlighted in red. Evolutionary histories of complete proteins (B) and of bHLH regions (C), including TWIST, were inferred using the Maximum Likelihood and Neighbor-Joining methods in PhyML and MEGA4, respectively. A JTT model of amino acid substitution was used, and the rate variation among sites was modeled with a gamma distribution (shape parameter was estimated to be 0.70 for the complete alignment and 0.28 for the bHLH region alignment). Sequence alignment was constructed using the MAFFT software.

domain and full-length protein across basal chordates and protostomes revealed that PARASCLERAXIS is more closely related to PARAXIS and SCLERAXIS than to TWIST, their closest family member (Figure 1B and C). This predicts that *Parascleraxis* represents the ancestral *Paraxis/Scleraxis* gene that duplicated in the common ancestor of all vertebrates, sometime after the divergence of the agnathans from the group containing vertebrates and chondrichthyes.

The function of PARASCLERAXIS can be inferred by comparing its expression pattern to those of PARAXIS and SCLERAXIS. *Parascleraxis* expression has only been evaluated in one non-vertebrate chordate, the lamprey *Petromyzon marinus*, where it was found to be expressed in sclerotomal cells migrating into the medial fin from a somitic region surrounding the neural tube (Freitas et al., 2006). The expression of *Parascleraxis* in lamprey overlaps with that of *Scleraxis* in the catshark median fin, suggesting that the ancestral function of PARASCLERAXIS may be more similar to that of vertebrate SCLERAXIS. *Drosophila parascleraxis* (CG33557 / CG12648) is expressed during and after germband extension in 10 cells that were originally identified as midline CNS cells (Peyrefitte et al., 2001). These *parascleraxis*-expressing cells were subsequently re-identified as CNS-affiliated dorsal median (DM) cells of mesodermal origin (Kearney et al., 2004). DM cells are positioned along the ventral midline of the *Drosophila* embryo, at the borders of adjacent mesodermal segments. Upon germband retraction, DM cells extend processes laterally to join the muscle attachment sites in the body wall (Chiang et al., 1994), while expressing high levels of extracellular matrix proteins found in basement membranes, including laminin and collagen (Montell and Goodman, 1989; Lunstrum et al., 1988). Interestingly, DM cells are specified by signals from the midline CNS (Luer et al., 1997) and require *wingless* (WNT) signaling to be properly patterned (Zhou et al., 1997), both of which are also characteristics of

Paraxis/Scleraxis-expressing cells in vertebrate embryos. Together, the expression patterns of *Parascleraxis* in lamprey and *Drosophila* suggest a conserved role for the transcription factor in cells that regulate the extracellular matrix during muscle development.

PARAXIS *regulates the interaction of the paraxial mesoderm with its microenvironment*.

Both invertebrate and vertebrate embryonic studies suggest that the function of PARAXIS/SCLERAXIS/PARASCLERAXIS throughout its evolutionary history has been to control the developmental patterning and integration of distinct mesodermal cell types. In vertebrates however, the function of PARAXIS in the regulation of the morphological state of cells from the paraxial mesoderm appears paradoxical. In the mesenchymal tissue of the anterior PSM, PARAXIS is essential for MET during somitogenesis. During myogenesis, on the other hand, PARAXIS is expressed in the epithelial lips of the dermomyotome, where it appears to participate in EMT as MPCs delaminate and migrate into the limb bud. However, if we also consider the importance of PARAXIS in regulating the morphology of myocytes in the forming myotome, a common theme emerges: the regulation of the expression of genes that mediate cell-cell and cell-ECM interactions, as well as the composition and stability of the ECM, is dependent upon PARAXIS.

It is well established that the cellular microenvironment provides signaling cues that influence cell behavior during development and disease. The composition of the pericellular ECM, and proteolytic remodeling of it, controls the microenvironmental signaling context that influences cell shape, motility, growth, survival and differentiation. The proper aggregation and differentiation of human pluripotent

embryonic stem cells, for example, is dependent upon integrin-mediated interactions with laminin in the ECM (Evseenko et al., 2009). Misregulation of cell–ECM interactions can also contribute to many diseases, including developmental, immune, hemostasis and degenerative and malignant disorders (Lukashev and Werb, 1998). Here we demonstrate that PARAXIS is an important developmental regulator of this process. The set of genes that are either up or down regulated by PARAXIS provides insights that may be applicable to understanding the broader regulation of ECM signaling.

Of particular note, PARAXIS activates the expression of genes encoding receptors for ECM constituents, which must be organized into a basement membrane to provide a scaffold to which the epithelium can adhere during somitogenesis. PARAXIS is required for proper expression of *Fap,* which encodes a transmembrane protein that cooperates with integrins to increase fibronectin organization, and *Itgav,* encoding an integrin subunit that binds fibronectin, itself. Interaction between the ECM and integrins are associated with changes in cell morphology and migration through the activation of Rho GTPases. The Rho GTPase family members, RAC1 and CDC42, have been implicated in the switch between epithelial and mesenchymal states of somitic cells. PARAXIS does not directly regulate Rho GTPase transcription, but may indirectly regulate their activity through its control of several integrins. The interaction of PSM cells with their microenvironment is known to be critical for the patterning of the somitic lineages (Rifes and Thorsteinsdottir, 2012), and PARAXIS functions to modulate this interaction.

During epaxial myogenesis, PARAXIS again affects the expression of receptors for ECM molecules, this time in MPCs. *Itga4* and *Itga6,* encoding integrin subunits expressed within the early myotome are downregulated in the absence of *Paraxis*. These integrins bind fibronectin and laminin, respectively, and are essential for myotome basement membrane formation and myocyte elongation. Myocyte-ECM interactions at

myotendinous junctions are also important for defining fiber-type specificity (Snow and Henry, 2009), and future studies will address whether PARAXIS expression is important for musculoskeletal system development after the initial formation of the myotome.

The ECM, itself, is not the only constituent of the pericellular microenvironment. The ECM also harbors signaling molecules released from neighboring cells that can influence cell behavior. PARAXIS promotes hypaxial MPC migration through the activation of genes encoding receptors for morphogens, such as *Met,* and transcription factors that may regulate cytokine receptors, such as *Lbx1*. Taken together, our results point to a role for PARAXIS as a mediator of both MET and EMT. PARAXIS is activated in both morphogenetic contexts, yet performs the same essential function: regulating the cell's ability to interact with proteins in the extracellular environment.

EMT is also required for the metastasis associated with cancer progression, and is therefore a heavily-studied process in the cellular context of the tumor (Thiery, 2002). Here, as in developmental EMT and MET, the control of ECM organization and ECM-cell adhesion is critical to the transition between tissue states. For example, integrin α2β1, a laminin receptor, along with the fibronectin receptors integrins α4β1 and α5β1, direct the ECM remodeling and adhesion that allows melanoma cells to adopt a mesenchymal phenotype and migrate through the ECM surrounding the tumor (Etoh et al., 1992). Matrix metalloproteases, such as MMP9, are also important for pericellular ECM remodeling, as they function to degrade the basement membrane, promoting the invasion and motility potential of colon cancer cells (Lubbe et al., 2006). The upregulation of the MET receptor in hypoxic microenvironment conditions is also associated with breast cancer metastasis (Cooke et al., 2012). PARAXIS regulates the expression of integrins, integrin and ECM regulators, MMP9 and the MET receptor, and

and future studies may address the potential role for PARAXIS in the context of the tumor microenvironment.

Another heavily-studied microenvironment is the muscle satellite cell niche. Satellite cells are muscle-specific stem cells that become activated in response to signals indicating muscle damage. Satellite cells are derived from the dermomyotome (Gros et al., 2005), so the possibility exists that these cells retain *Paraxis* expression during developmental muscle maturation, and into adulthood. Satellite cell-environment interactions are critical to the colonization and maintenance of the satellite cell niche between the basal lamina and sarcolemma during myofiber development (Brohl et al., 2012). Additionally, during adult muscle repair, satellite cells must be competent to respond to pericellular signals within their microenvironment that direct their activation and migration to the site of muscle damage (Yin et al., 2013). Here too, expression of the MET receptor is important, as it binds HGF released from the extracellular matrix and stimulates the activation and proliferation of quiescent satellite cells near damaged muscle (Tatsumi et al., 1998). Due to its regulation of receptors for extracellular signals common to both embryonic and adult muscle, PARAXIS may also prove to be an important regulator of the ability of satellite cells to respond to signaling factors and the ECM within their niche, affecting the efficiency of muscle repair in both normal and disease states.

REFERENCES

Aertgeerts, K. (2005). Structural and Kinetic Analysis of the Substrate Specificity of Human Fibroblast Activation Protein. *Journal of Biological Chemistry* **280**, 19441–19444.

Anderson, C., Thorsteinsdottir, S. and Borycki, A. G. (2009). Sonic hedgehog-dependent synthesis of laminin 1 controls basement membrane assembly in the myotome. *Development* **136**, 3495–3504.

Anderson, D. M., Arredondo, J., Hahn, K., Valente, G., Martin, J. F., Wilson-Rawls, J. and Rawls, A. (2006). Mohawk is a novel homeobox gene expressed in the developing mouse embryo. *Dev. Dyn.* **235**, 792–801.

April DeLaurier, N. B. M. B. R. B. D. D. T. J. M. M. P. L. (2008). The Mouse Limb Anatomy Atlas: An interactive 3D tool for studying embryonic limb patterning. *BMC Developmental Biology* **8**, 83.

Araujo, M. and Nieto, M. A. (1997). The expression of chick EphA7 during segmentation of the central and peripheral nervous system. *Mech. Dev.* **68**, 173–177.

Araujo, M., Piedra, M. E., Herrera, M. T., Ros, M. A. and Nieto, M. A. The expression and regulation of chick EphA7 suggests roles in limb patterning and innervation.

Artym, V. V. (2002). Molecular proximity of seprase and the urokinase-type plasminogen activator receptor on malignant melanoma cell membranes: dependence on beta1 integrins and the cytoskeleton. *Carcinogenesis* **23**, 1593–1602.

Atchley, W. R. and Fitch, W. M. (1997). A natural classification of the basic helix-loop-helix class of transcription factors. *Proceedings of the National Academy of Sciences of the United States of America* **94**, 5172–5176.

Atit, R., Sgaier, S. K., Mohamed, O. A., Taketo, M. M., Dufort, D., Joyner, A. L., Niswander, L. and Conlon, R. A. (2006). β-catenin activation is necessary and sufficient to specify the dorsal dermal fate in the mouse. *Developmental Biology* **296**, 164–176.

Aulehla, A., Wehrle, C., Brand-Saberi, B., Kemler, R., Gossler, A., Kanzler, B. and Herrmann, B. G. (2003). Wnt3a Plays a Major Role in the Segmentation Clock Controlling Somitogenesis. *Dev. Cell* **4**, 395–406.

Bajanca, F. (2006). Integrin 6 1-laminin interactions regulate early myotome formation in the mouse embryo. *Development* **133**, 1635–1644.

Bajanca, F. and Thorsteinsdóttir, S. (2002). Integrin expression patterns during early limb muscle development in the mouse. *Mech. Dev.* **119**, S131–S134.

Bajanca, F., Luz, M., Duxson, M. J. and Thorsteinsd ttir, S. L. (2004). Integrins in the mouse myotome: Developmental changes and differences between the epaxial and hypaxial lineage. *Dev. Dyn.* **231**, 402–415.

Barnes, G. L., Alexander, P. G., Hsu, C. W., Mariani, B. D. and Tuan, R. S. (1997). Cloning and Characterization of ChickenParaxis:A Regulator of Paraxial Mesoderm Development and Somite Formation. *Developmental Biology* **189**, 95–111.

Baum, B. and Georgiou, M. (2011). Dynamics of adherens junctions in epithelial establishment, maintenance, and remodeling. *J. Cell Biol.* **192**, 907–917.

Bellairs, R. (1979). The mechanism of somite segmentation in the chick embryo. *J Embryol Exp Morphol* **51**, 227–243.

Belo, J. A., Bouwmeester, T., Leyns, L., Kertesz, N., Gallo, M., Follettie, M. and De Robertis, E. M. (1997). Cerberus-like is a secreted factor with neuralizing activity expressed in the anterior primitive endoderm of the mouse gastrula. *Mech. Dev.* **68**, 45–57.

Ben-Yair, R. (2005). Lineage analysis of the avian dermomyotome sheet reveals the existence of single cells with both dermal and muscle progenitor fates. *Development* **132**, 689–701.

Bessho, Y. (2003). Periodic repression by the bHLH factor Hes7 is an essential mechanism for the somite segmentation clock. *Genes & Development* **17**, 1451–1456.

Bessho, Y., Miyoshi, G., Sakata, R. and Kageyama, R. (2001). Hes7: a bHLH-type repressor gene regulated by Notch and expressed in the presomitic mesoderm. *Genes Cells* **6**, 175–185.

Bladt, F., Riethmacher, D., Isenmann, S., Aguzzi, A. and Birchmeier, C. (1995). Essential role for the c-met receptor in the migration of myogenic precursor cells into the limb bud. *Nature* **376**, 768–771.

Borycki, A. G., Li, J., Jin, F., Emerson, C. P. and Epstein, J. A. (1999). Pax3 functions in cell survival and in pax7 regulation. *Development* **126**, 1665–1674.

Bothe, I., Ahmed, M. U., Winterbottom, F. L., Scheven, von, G. and Dietrich, S. (2007). Extrinsic versus intrinsic cues in avian paraxial mesoderm patterning and differentiation. *Dev. Dyn.* **236**, 2397–2409.

Brand-Saberi, B., Ebensperger, C., Wilting, J., Balling, R. and Christ, B. (1993a). The ventralizing effect of the notochord on somite differentiation in chick embryos. *Anat. Embryol.* **188**, 239–245.

Brand-Saberi, B., Krenn, V., Grim, M. and Christ, B. (1993b). Differences in the fibronectin-dependence of migrating cell populations. *Anat. Embryol.* **187**, 17–26.

Brand-Saberi, B., Müller, T. S., Wilting, J., Christ, B. and Birchmeier, C. (1996a). Scatter Factor/Hepatocyte Growth Factor (SF/HGF) Induces Emigration of Myogenic Cells at Interlimb Levelin Vivo. *Developmental Biology* **179**, 303–308.

Brand-Saberi, B., Wilting, J., Ebensperger, C. and Christ, B. (1996b). The formation of somite compartments in the avian embryo. *Int. J. Dev. Biol.* **40**, 411–

420.

Brent, A. (2002). Developmental regulation of somite derivatives: muscle, cartilage and tendon. *Current Opinion in Genetics & Development* **12**, 548–557.

Brent, A. E., Schweitzer, R. and Tabin, C. J. (2003). A somitic compartment of tendon progenitors. *Cell* **113**, 235–248.

Brohl, D., Vasyutina, E., Czajkowski, M. T., Griger, J., Rassek, C., Rahn, H. P., Purfurst, B., Wende, H. and Birchmeier, C. (2012). Colonization of the satellite cell niche by skeletal muscle progenitor cells depends on Notch signals. *Dev. Cell* **23,** 469-481.

Brohmann, H., Jagla, K. and Birchmeier, C. (2000). The role of Lbx1 in migration of muscle precursor cells. *Development* **127**, 437–445.

Bronner-Fraser, M. and Stern, C. (1991). Effects of mesodermal tissues on avian neural crest cell migration. *Developmental Biology* **143**, 213–217.

Brown, C. B., Engleka, K. A., Wenning, J., Min Lu, M. and Epstein, J. A. (2005). Identification of a hypaxial somite enhancer element regulatingPax3 expression in migrating myoblasts and characterization of hypaxial muscle Cre transgenic mice. *genesis* **41**, 202–209.

Brunelli, S., Relaix, F., Baesso, S., Buckingham, M. and Cossu, G. (2007). Beta catenin-independent activation of MyoD in presomitic mesoderm requires PKC and depends on Pax3 transcriptional activity. *Developmental Biology* **304**, 604–614.

Buckingham, M. (2006). Myogenic progenitor cells and skeletal myogenesis in vertebrates. *Current Opinion in Genetics & Development* **16**, 525–532.

Buckingham, M., Bajard, L., Chang, T., Daubas, P., Hadchouel, J., Meilhac, S., Montarras, D., Rocancourt, D. and Relaix, F. (2003). The formation of skeletal muscle: from somite to limb. **202**, 59–68.

Bulman, M. P., Kusumi, K., Frayling, T. M., McKeown, C., Garrett, C., Lander, E. S., Krumlauf, R., Hattersley, A. T., Ellard, S. and Turnpenny, P. D. (2000). Mutations in the human Delta homologue, DLL3, cause axial skeletal defects in spondylocostal dysostosis. *Nat Genet* **24**, 438–441.

Burgess, R., Cserjesi, P., Ligon, K. L. and Olson, E. N. (1995). Paraxis: a basic helix-loop-helix protein expressed in paraxial mesoderm and developing somites. *Developmental Biology* **168**, 296–306.

Burgess, R., Rawls, A., Brown, D., Bradley, A. and Olson, E. N. (1996). Requirement of the paraxis gene for somite formation and musculoskeletal patterning. *Nature* **384**, 570–573.

Carpio, R., Honor, S. M., Araya, C. and Mayor, R. (2004). Xenopus paraxis homologue shows novel domains of expression. *Dev. Dyn.* **231**, 609–613.

Cheng, T. C., Hanley, T. A., Mudd, J., Merlie, J. P. and Olson, E. N. (1992). Mapping of myogenin transcription during embryogenesis using transgenes linked to the myogenin control region. *J. Cell Biol.* **119**, 1649–1656.

Cheng, T. C., Wallace, M. C., Merlie, J. P. and Olson, E. N. (1993). Separable regulatory elements governing myogenin transcription in mouse embryogenesis. *Science* **261**, 215–218.

Chiang, C., Patel, N., Young, K. E. and Beachy, P. A. (1994). The novel homeodomain gene *buttonless* specifies differentiation and axonal guidance function of *Drosophila* dorsal median cells. *Development* **120,** 3581-3593.

Christ, B. and Ordahl, C. P. (1995). Early stages of chick somite development. *Anat. Embryol.* **191**, 381–396.

Christ, B. and Wilting, J. (1992). From somites to vertebral column. *Ann. Anat.* **174**, 23–32.

Christ, B., Huang, R. and Wilting, J. (2000). The development of the avian vertebral column. *Anat. Embryol.* **202**, 179–194.

Christ, B., Jacob, H. J. and Jacob, M. (1978). On the formation of the myotomes in avian embryos. An experimental and scanning electron microscope study. *Experientia* **34**, 514–516.

Christ, B., Jacob, M. and Jacob, H. J. (1983). On the origin and development of the ventrolateral abdominal muscles in the avian embryo. An experimental and ultrastructural study. *Anat. Embryol.* **166**, 87–101.

Cinnamon, Y. (2006). Differential effects of N-cadherin-mediated adhesion on the development of myotomal waves. *Development* **133**, 1101–1112.

Cinnamon, Y., Kahane, N. and Kalcheim, C. (1999). Characterization of the early development of specific hypaxial muscles from the ventrolateral myotome. *Development* **126**, 4305–4315.

Cooke, J. and Zeeman, E. C. (1976). A clock and wavefront model for control of the number of repeated structures during animal morphogenesis. *Journal of Theoretical Biology* **58**, 455–476.

Cooke, V. G., LeBleu, V. S., Keskin, D., Kahn, Z., O'Connell, J. T., Teng, Y., Duncan, M. B., Xie, L., Maeda, G., Vong, S., Sugimoto, H., Rocha, R. M., Damascena, A., Brentani, R. R. and Kalluri, R. (2012). Pericyte depleteion results in hypoxia-associated epithelial-to-mesenchymal transition and metastasis mediated by met signaling pathway. *Cancer Cell* **21,** 66-81.

Correia, K. M. and Conlon, R. A. (2000). Surface ectoderm is necessary for the morphogenesis of somites. *Mech. Dev.* **91**, 19–30.

Cserjesi, P. and Olson, E. N. (1991). Myogenin induces the myocyte-specific enhancer binding factor MEF-2 independently of other muscle-specific gene

products. *Mol. Cell. Biol.* **11**, 4854–4862.

Cserjesi, P., Brown, D., Ligon, K. L., Lyons, G. E., Copeland, N. G., Gilbert, D. J., Jenkins, N. A. and Olson, E. N. (1995). Scleraxis: a basic helix-loop-helix protein that prefigures skeletal formation during mouse embryogenesis. *Development* **121**, 1099–1110.

Dale, J. K., Maroto, M., Dequeant, M. L., Malapert, P., McGrew, M. and Pourquie, O. (2003). Periodic Notch inhibition by Lunatic Fringe underlies the chick segmentation clock. *Nature* **421**, 275–278.

Danker, K., Hacke, H. and Wedlich, D. (1992). Effects of heat shock on the pattern of fibronectin and laminin during somitogenesis in Xenopus laevis. *Dev. Dyn.* **193**, 136–144.

Davies, O. R., Lin, C.-Y., Radzisheuskaya, A., Zhou, X., Taube, J., Blin, G., Waterhouse, A., Smith, A. J. H. and Lowell, S. (2013). Tcf15 Primes Pluripotent Cells for Differentiation. *Cell Reports* **3**, 472–484.

Dear, T. N. and Boehm, T. (1999). Diverse mRNA expression patterns of the mouse calpain genes Capn5, Capn6 and Capn11 during development. *Mech. Dev.* **89**, 201–209.

Delfini, M. C., Hirsinger, E., Pourquie, O. and Duprez, D. (2000). Delta 1-activated notch inhibits muscle differentiation without affecting Myf5 and Pax3 expression in chick limb myogenesis. *Development* **127**, 5213–5224.

Delfini, M.-C., La Celle, De, M., Gros, J., Serralbo, O., Marics, I., Seux, M., Scaal, M. and Marcelle, C. (2009). The timing of emergence of muscle progenitors is controlled by an FGF/ERK/SNAIL1 pathway. *Developmental Biology* **333**, 229–237.

Denetclaw, W. F., Christ, B. and Ordahl, C. P. (1997). Location and growth of epaxial myotome precursor cells. *Development* **124**, 1601–1610.

Dequeant, M. L., Glynn, E., Gaudenz, K., Wahl, M., Chen, J., Mushegian, A. and Pourquie, O. (2006). A Complex Oscillating Network of Signaling Genes Underlies the Mouse Segmentation Clock. *Science* **314**, 1595–1598.

Dequéant, M.-L. and Pourquié, O. (2008). Segmental patterning of the vertebrate embryonic axis. *Nat Rev Genet* **9**, 370–382.

Deries, M., Schweitzer, R. and Duxson, M. J. (2010). Developmental fate of the mammalian myotome. *Dev. Dyn.* **239**, 2898–2910.

Dickson, G., Azad, A., Morris, G. E., Simon, H., Noursadeghi, M. and Walsh, F. S. (1992). Co-localization and molecular association of dystrophin with laminin at the surface of mouse and human myotubes. *J. Cell. Sci.* **103 (Pt 4)**, 1223–1233.

Dietrich, S., Abou-Rebyeh, F., Brohmann, H., Bladt, F., Sonnenberg-Riethmacher, E., Yamaai, T., Lumsden, A., Brand-Saberi, B. and

Birchmeier, C. (1999). The role of SF/HGF and c-Met in the development of skeletal muscle.

Diez del Corral, R., Olivera-Martinez, I., Goriely, A., Gale, E., Maden, M. and Storey, K. (2003). Opposing FGF and retinoid pathways control ventral neural pattern, neuronal differentiation, and segmentation during body axis extension. *Neuron* **40**, 65–79.

Duband, J. L., Dufour, S., Hatta, K., Takeichi, M., Edelman, G. M. and Thiery, J. P. (1987). Adhesion molecules during somitogenesis in the avian embryo. *J. Cell Biol.* **104**, 1361–1374.

Dubrulle, J., McGrew, M. J. and Pourquié, O. (2001). FGF Signaling Controls Somite Boundary Position and Regulates Segmentation Clock Control of Spatiotemporal Hox Gene Activation. *Cell* **106**, 219–232.

Dunwoodie, S. L., Clements, M., Sparrow, D. B., Sa, X., Conlon, R. A. and Beddington, R. S. (2002). Axial skeletal defects caused by mutation in the spondylocostal dysplasia/pudgy gene Dll3 are associated with disruption of the segmentation clock within the presomitic mesoderm. *Development* **129**, 1795–1806.

Duprez, D., Fournier-Thibault, C. and Le Douarin, N. (1998). Sonic Hedgehog induces proliferation of committed skeletal muscle cells in the chick limb. *Development* **125**, 495–505.

E E Quertermous, H. H. M. A. B. T. Q. (1994). Cloning and characterization of a basic helix-loop-helix protein expressed in early mesoderm and the developing somites. *Proceedings of the National Academy of Sciences of the United States of America* **91**, 7066.

Ebensperger, C., Wilting, J., Brand-Saberi, B., Mizutani, Y., Christ, B., Balling, R. and Koseki, H. (1995). Pax-1, a regulator of sclerotome development is induced by notochord and floor plate signals in avian embryos. *Anat. Embryol.* **191**, 297–310.

Edmondson, D. G., Cheng, T. C., Cserjesi, P., Chakraborty, T. and Olson, E. N. (1992). Analysis of the myogenin promoter reveals an indirect pathway for positive autoregulation mediated by the muscle-specific enhancer factor MEF-2. *Mol. Cell. Biol.* **12**, 3665–3677.

Edmondson, D. G., Lyons, G. E., Martin, J. F. and Olson, E. N. (1994). Mef2 gene expression marks the cardiac and skeletal muscle lineages during mouse embryogenesis. *Development* **120**, 1251–1263.

Epstein, J. A., Shapiro, D. N., Cheng, J., Lam, P. Y. and Maas, R. L. (1996). Pax3 modulates expression of the c-Met receptor during limb muscle development. *Proceedings of the National Academy of Sciences of the United States of America* **93**, 4213–4218.

Ervasti, J. M. and Campbell, K. P. (1993). A role for the dystrophin-glycoprotein complex as a transmembrane linker between laminin and actin. *J. Cell Biol.* **122**,

809–823.

Etoh, T., Byers, H. R. and Mihm, M. C. (1992). Integrin expression in malignant melanoma and their role in cell attachment and migration on extracellular matrix proteins. *J. Dermatol.* **19**, 841-846.

Evans, D. J. R., Valasek, P., Schmidt, C. and Patel, K. (2006). Skeletal muscle translocation in vertebrates. *Brain Struct Funct* **211**, 43–50.

Evseenko, D., Schenke-Layland, K., Dravid, G., Zhu, Y., Hao, Q.L., Scholes, J., Wang, X.C., Maclellan, W.R. and Crooks, G.M. (2009). Identification of the critical extracellular matrix proteins that promote human embryonic stem cell assembly. *Stem Cells Dev*. **18,** 919-928.

Fan, C. M. and Tessier-Lavigne, M. (1994). Patterning of mammalian somites by surface ectoderm and notochord: evidence for sclerotome induction by a hedgehog homolog. *Cell* **79**, 1175–1186.

Forsberg, H., Crozet, F. and Brown, N. A. (1998). Waves of mouse Lunatic fringe expression, in four-hour cycles at two-hour intervals, precede somite boundary formation. *Curr. Biol.* **8**, 1027–1030.

Frayne, J. (2002). Human tMDC III: a sperm protein with a potential role in oocyte recognition. *Molecular Human Reproduction* **8**, 817–822.

Freitas, R., Zhang, G. and Cohn, M. J. (2006). Evidence that mechanisms of fin development evolved in the midline of early vertebrates. *Nature* **442**, 1033–1037.

Fukui, Y., Hashimoto, O., Sanui, T., Oono, T., Koga, H., Abe, M., Inayoshi, A., Noda, M., Oike, M., Shirai, T., et al. (2001). Haematopoietic cell-specific CDM family protein DOCK2 is essential for lymphocyte migration. *Nature* **412**, 826–831.

Gaspera, Della, B., Armand, A.-S., Lecolle, S., Charbonnier, F. and Chanoine, C. (2012). Mef2d Acts Upstream of Muscle Identity Genes and Couples Lateral Myogenesis to Dermomyotome Formation in Xenopus laevis. *PLoS ONE* **7**, e52359.

Geetha-Loganathan, P. (2006). Regulation of ectodermal Wnt6 expression by the neural tube is transduced by dermomyotomal Wnt11: a mechanism of dermomyotomal lip sustainment. *Development* **133**, 2897–2904.

George, E. L., Georges-Labouesse, E. N., Patel-King, R. S., Rayburn, H. and Hynes, R. O. (1993). Defects in mesoderm, neural tube and vascular development in mouse embryos lacking fibronectin. *Development* **119**, 1079–1091.

Girós, A., Grgur, K., Gossler, A. and Costell, M. (2011). α5β1 Integrin-Mediated Adhesion to Fibronectin Is Required for Axis Elongation and Somitogenesis in Mice. *PLoS ONE* **6**, e22002.

Glazier, J. A., Zhang, Y., Swat, M., Zaitlen, B. and Schnell, S. (2008). *Current*

Topics in Developmental Biology. Elsevier.

Godfrey, E. W. and Gradall, K. S. (1998). Basal lamina molecules are concentrated in myogenic regions of the mouse limb bud. *Brain Struct Funct* **198**, 481–486.

Gomez, C., Özbudak, E. M., Wunderlich, J., Baumann, D., Lewis, J. and Pourquié, O. (2008). Control of segment number in vertebrate embryos. *Nature* **454**, 335–339.

Goulding, M., Lumsden, A. and Paquette, A. J. (1994). Regulation of Pax-3 expression in the dermomyotome and its role in muscle development. *Development* **120**, 957–971.

Gray, R. S., Bayly, R. D., Green, S. A., Agarwala, S., Lowe, C. J. and Wallingford, J. B. (2009). Diversification of the expression patterns and developmental functions of the dishevelled gene family during chordate evolution. *Dev. Dyn.* **238**, 2044–2057.

Grifone, R., Demignon, J., Giordani, J., Niro, C., Souil, E., Bertin, F., Laclef, C., Xu, P.-X. and Maire, P. (2007). Eya1 and Eya2 proteins are required for hypaxial somitic myogenesis in the mouse embryo. *Developmental Biology* **302**, 602–616.

Grifone, R., Demignon, J., Houbron, C., Souil, E., Niro, C., Seller, M. J., Hamard, G. and Maire, P. (2005). Six1 and Six4 homeoproteins are required for Pax3 and Mrf expression during myogenesis in the mouse embryo.

Gros, J., Manceau, M., Thomé, V. and Marcelle, C. (2005). A common somitic origin for embryonic muscle progenitors and satellite cells. *Nature* **435**, 954–958.

Gros, J., Scaal, M. and Marcelle, C. (2004). A Two-Step Mechanism for Myotome Formation in Chick. *Dev. Cell* **6**, 875–882.

Gros, J., Serralbo, O. and Marcelle, C. (2008). WNT11 acts as a directional cue to organize the elongation of early muscle fibres. *Nature* **457**, 589–593.

Gross, M. K., Moran-Rivard, L., Velasquez, T., Nakatsu, M. N., Jagla, K. and Goulding, M. (2000). Lbx1 is required for muscle precursor migration along a lateral pathway into the limb. *Development* **127**, 413–424.

Hall, A. (2005). Rho GTPases and the control of cell behaviour. *Biochem. Soc. Trans* **33**, 891.

Haraguchi, M., Okubo, T., Miyashita, Y., Miyamoto, Y., Hayashi, M., Crotti, T. N., McHugh, K. P. and Ozawa, M. (2008). Snail regulates cell-matrix adhesion by regulation of the expression of integrins and basement membrane proteins. *J. Biol. Chem.* **283**, 23514-23523.

Hasty, P., Bradley, A., Morris, J. H., Edmondson, D. G., Venuti, J. M., Olson, E. N. and Klein, W. H. (1993). Muscle deficiency and neonatal death in mice with a targeted mutation in the myogenin gene. *Nature* **364**, 501–506.

Heanue, T. A., Reshef, R., Davis, R. J., Mardon, G., Oliver, G., Tomarev, S., Lassar, A. B. and Tabin, C. J. (1999). Synergistic regulation of vertebrate muscle development by Dach2, Eya2, and Six1, homologs of genes required for Drosophila eye formation. *genesdev.cshlp.org.ezproxy1.lib.asu.edu*.

Helfman, D. M., Kim, E. J., Lukanidin, E. and Grigorian, M. (2005). The metastasis associated protein S100A4: role in tumour progression and metastasis. *Br J Cancer* **92**, 1955–1958.

Heymann, S., Koudrova, M., Arnold, H. H., Köster, M. and Braun, T. (1996). Regulation and Function of SF/HGF during Migration of Limb Muscle Precursor Cells in Chicken. *Developmental Biology* **180**, 566–578.

Hinterberger, T. J., Sassoon, D. A., Rhodes, S. J. and Konieczny, S. F. (1991). Expression of the muscle regulatory factor MRF4 during somite and skeletal myofiber development. *Developmental Biology* **147**, 144–156.

Hoffman, E. P., Brown, R. H. and Kunkel, L. M. (1987). Dystrophin: the protein product of the Duchenne muscular dystrophy locus. *Cell* **51**, 919–928.

Holley, S. A., Geisler, R. and Nüsslein-Volhard, C. Control of her1 expression during zebrafish somitogenesis by a Delta-dependent oscillator and an independent wave-front activity.

Hollway, G. and Currie, P. (2005). Vertebrate myotome development. *Birth Defect Res C* **75**, 172–179.

Holowacz, T., Zeng, L. and Lassar, A. B. (2006). Asymmetric localization of numb in the chick somite and the influence of myogenic signals. *Dev. Dyn.* **235**, 633–645.

Hu, P., Geles, K. G., Paik, J.-H., DePinho, R. A. and Tjian, R. (2008). Codependent activators direct myoblast-specific MyoD transcription. *Dev. Cell* **15**, 534–546.

Huang, R. and Christ, B. (2000). Origin of the epaxial and hypaxial myotome in avian embryos. *Anat. Embryol.* **202**, 369–374.

Huang, R., Zhi, Q., Izpisua-Belmonte, J.-C., Christ, B. and Patel, K. (1999). Origin and development of the avian tongue muscles. *Brain Struct Funct* **200**, 137–152.

Huang, R., Zhi, Q., Patel, K., Wilting, J. and Christ, B. (2000). Dual origin and segmental organisation of the avian scapula. *Development* **127**, 3789–3794.

Inuzuka, H., Redies, C. and Takeichi, M. (1991). Differential expression of R- and N-cadherin in neural and mesodermal tissues during early chicken development. *Development* **113**, 959–967.

Ito, Y., Toriuchi, N., Yoshitaka, T., Ueno-Kudoh, H., Sato, T., Yokoyama, S., Nishida, K., Akimoto, T., Takahashi, M., Miyaki, S., et al. (2010). The Mohawk homeobox gene is a critical regulator of tendon differentiation.

pnas.org.ezproxy1.lib.asu.edu.

Jacob, M., Christ, B., Jacob, H. J. and Poelmann, R. E. (1991). The role of fibronectin and laminin in development and migration of the avian Wolffian duct with reference to somitogenesis. *Anat. Embryol.* **183**, 385–395.

Johnson, J., Rhee, J., Parsons, S. M., Brown, D., Olson, E. N. and Rawls, A. (2001). The anterior/posterior polarity of somites is disrupted in paraxis-deficient mice. *Developmental Biology* **229**, 176–187.

Jones, J., Marian, D., Weich, E., Engl, T., Wedel, S., Relja, B., Jonas, D. and Blaheta, R. A. (2007). CXCR4 chemokine receptor engagement modifies integrin dependent adhesion of renal carcinoma cells. *Experimental Cell Research* **313**, 4051–4065.

Jouve, C., Palmeirim, I., Henrique, D., Beckers, J., Gossler, A., Ish-Horowicz, D. and Pourquie, O. (2000). Notch signalling is required for cyclic expression of the hairy-like gene HES1 in the presomitic mesoderm. *Development* **127**, 1421–1429.

Julich, D., Mould, A. P., Koper, E. and Holley, S. A. (2009). Control of extracellular matrix assembly along tissue boundaries via Integrin and Eph/Ephrin signaling. *Development* **136**, 2913–2921.

Jülich, D., Geisler, R., Holley, S. A.Tübingen 2000 Screen Consortium (2005). Integrinalpha5 and delta/notch signaling have complementary spatiotemporal requirements during zebrafish somitogenesis. *Dev. Cell* **8**, 575–586.

Kablar, B., Krastel, K., Ying, C., Asakura, A., Tapscott, S. J. and Rudnicki, M. A. (1997). MyoD and Myf-5 differentially regulate the development of limb versus trunk skeletal muscle. *Development* **124**, 4729–4738.

Kablar, B., Krastel, K., Ying, C., Tapscott, S. J., Goldhamer, D. J. and Rudnicki, M. A. (1999). Myogenic Determination Occurs Independently in Somites and Limb Buds. *Developmental Biology* **206**, 219–231.

Kahane, N., Cinnamon, Y. and Kalcheim, C. (1998). The origin and fate of pioneer myotomal cells in the avian embryo. *Mech. Dev.* **74**, 59–73.

Kalcheim, C. and Teillet, M. A. (1989). Consequences of somite manipulation on the pattern of dorsal root ganglion development. *Development* **106**, 85–93.

Kardon, G., Campbell, J. K. and Tabin, C. J. (2002). Local Extrinsic Signals Determine Muscle and Endothelial Cell Fate and Patterning in the Vertebrate Limb. *Dev. Cell* **3**, 533–545.

Kassar-Duchossoy, L. (2005). Pax3/Pax7 mark a novel population of primitive myogenic cells during development. *Genes & Development* **19**, 1426–1431.

Kearney, J. B., Wheeler, S. R., Estes, P., Parente, B. and Crews, S.T. (2004). Gene expression profiling of the developing *Drosophila* CNS midline cells.

Developmental Biology **275,** 473-492.

Keynes, R. J. and Stern, C. D. (1984). Segmentation in the vertebrate nervous system. *Nature* **310**, 786–789.

Kikuchi, K., Tsuchiya, K., Otabe, O., Gotoh, T., Tamura, S., Katsumi, Y., Yagyu, S., Tsubai-Shimizu, S., Miyachi, M., Iehara, T., et al. (2008). Effects of PAX3-FKHR on malignant phenotypes in alveolar rhabdomyosarcoma. *Biochem. Biophys. Res. Commun.* **365**, 568–574.

Kimura, Y., Matsunami, H., Inoue, T., Shimamura, K., Uchida, N., Ueno, T., Miyazaki, T. and Takeichi, M. (1995). Cadherin-11 Expressed in Association with Mesenchymal Morphogenesis in the Head, Somite, and Limb Bud of Early Mouse Embryos. *Developmental Biology* **169**, 347–358.

Kosher, R. A., Walker, K. H. and Ledger, P. W. (1982). Temporal and spatial distribution of fibronectin during development of the embryonic chick limb bud. *Cell Differ.* **11**, 217–228.

Koshida, S., Kishimoto, Y., Ustumi, H., Shimizu, T., Furutani-Seiki, M., Kondoh, H. and Takada, S. (2005). Integrinα5-Dependent Fibronectin Accumulation for Maintenance of Somite Boundaries in Zebrafish Embryos. *Dev. Cell* **8**, 587–598.

Lackmann, M. (1998). Distinct Subdomains of the EphA3 Receptor Mediate Ligand Binding and Receptor Dimerization. *Journal of Biological Chemistry* **273**, 20228–20237.

Lash, J. W. (1985). Somitogenesis: investigations on the mechanism of compaction in the presomitic mass and a possible role for fibronectin. *Prog. Clin. Biol. Res.* **171**, 45–60.

Lash, J. W., Seitz, A. W., Cheney, C. M. and Ostrovsky, D. (1984). On the role of fibronectin during the compaction stage of somitogenesis in the chick embryo. *J. Exp. Zool.* **232**, 197–206.

Lassar, A. B., Buskin, J. N., Lockshon, D., Davis, R. L., Apone, S., Hauschka, S. D. and Weintraub, H. (1989). MyoD is a sequence-specific DNA binding protein requiring a region of myc homology to bind to the muscle creatine kinase enhancer. *Cell* **58**, 823–831.

Lee, H. K. and Deneen, B. (2012). Daam2 is required for dorsal patterning via modulation of canonical Wnt signaling in the developing spinal cord. *Dev. Cell* **22**, 183–196.

Lee, H.-O., Mullins, S. R., Franco-Barraza, J., Valianou, M., Cukierman, E. and Cheng, J. D. (2011). FAP-overexpressing fibroblasts produce an extracellular matrix that enhances invasive velocity and directionality of pancreatic cancer cells. *BMC Cancer* **11**, 245.

Leimeister, C., Schumacher, N., Steidl, C. and Gessler, M. (2000). Analysis of

HeyL expression in wild-type and Notch pathway mutant mouse embryos. *Mech. Dev.* **98**, 175–178.

Levy, M. T., McCaughan, G. W., Abbott, C. A., Park, J. E., Cunningham, A. M., M ller, E., Rettig, W. J. and Gorrell, M. D. (1999). Fibroblast activation protein: A cell surface dipeptidyl peptidase and gelatinase expressed by stellate cells at the tissue remodelling interface in human cirrhosis. *Hepatology* **29**, 1768–1778.

Li, Y., Fenger, U., Niehrs, C. and Pollet, N. (2003). Cyclic expression of esr9 gene in Xenopus presomitic mesoderm. *Differentiation* **71**, 83–89.

Li, Z. (1997). Desmin Is Essential for the Tensile Strength and Integrity of Myofibrils but Not for Myogenic Commitment, Differentiation, and Fusion of Skeletal Muscle. *J. Cell Biol.* **139**, 129–144.

Linask, K. K., Ludwig, C., Han, M. D., Liu, X., Radice, G. L. and Knudsen, K. A. (1998). N-cadherin/catenin-mediated morphoregulation of somite formation. *Developmental Biology* **202**, 85–102.

Linker, C. (2005). -Catenin-dependent Wnt signalling controls the epithelial organisation of somites through the activation of paraxis. *Development* **132**, 3895–3905.

Loebel, D. A. F., Tsoi, B., Wong, N. and Tam, P. P. L. (2005). A conserved noncoding intronic transcript at the mouse Dnm3 locus. *Genomics* **85**, 782–789.

Lubbe, W. J., Zhou, Z. Y., Fu, W., Zuzga, D., Schulz, S., Fridman, R., Muschel, R. J., Waldman, S. A. and Pitari, G. M. (2006). Tumor epithelial cell matrix metalloproteinase 9 is a target for antimetastatic therapy in colorectal cancer. *Clin. Cancer Res.* **12**, 1876-1882.

Luer, K., Urban, J., Klambt, C. and Technau, G.M. (1997), Induction of identified mesodermal cells by CNS midline progenitors in *Drosophila*. *Development* **124,** 2681-2690.

Lukashev, M. E. and Werb, Z. (1998). ECM signalling: orchestrating cell behaviour and misbehaviour. *Trends in Cell Biology* **8**, 437-441.

Lunstrum, G. P., Bachinger, H. P., Fessler, L. I., Duncan, K. G., Nelson, R. E. and Fessler, J. H. (1988). *Drosophila* basement membrane procollagen IV. Protein characterization and distribution. *J. Biol. Chem.* **263,** 18318-18327.

Maina, F., Pante, G., Helmbacher, F., Andres, R., Porthin, A., Davies, A.M., Ponzetto, C. and Klein, R. (2001). Coupling Met to specific pathways results in distinct developmental outcomes. *Molecular Cell* 7, 1293-1306.

Mankoo, B. S. (2003). The concerted action of Meox homeobox genes is required upstream of genetic pathways essential for the formation, patterning and differentiation of somites. *Development* **130**, 4655–4664.

Mankoo, B. S., Collins, N. S., Ashby, P., Grigorieva, E., Pevny, L. H., Candia,

A., Wright, C. V., Rigby, P. W. and Pachnis, V. (1999). Mox2 is a component of the genetic hierarchy controlling limb muscle development. *Nature* **400**, 69–73.

Marcelle, C., Wolf, J. and Bronner-Fraser, M. (1995). Thein VivoExpression of the FGF Receptor FREK mRNA in Avian Myoblasts Suggests a Role in Muscle Growth and Differentiation. *Developmental Biology* **172**, 100–114.

Maroto, M., Bone, R. A. and Dale, J. K. (2012). Somitogenesis. *Development* **139**, 2453–2456.

Maroto, M., Reshef, R., Münsterberg, A. E., Koester, S., Goulding, M. and Lassar, A. B. (1997). Ectopic Pax-3 Activates MyoD and Myf-5 Expression in Embryonic Mesoderm and Neural Tissue. *Cell* **89**, 139–148.

Maruhashi, M., Van De Putte, T., Huylebroeck, D., Kondoh, H. and Higashi, Y. (2005). Involvement of SIP1 in positioning of somite boundaries in the mouse embryo. *Dev. Dyn.* **234**, 332–338.

Mascarenhas, J. B., Littlejohn, E. L., Wolsky, R. J., Young, K. P., Nelson, M., Salgia, R. and Lang, D. (2010). PAX3 and SOX10 activate MET receptor expression in melanoma. *Pigment Cell & Melanoma Research* **23**, 225–237.

Mauger, A. (1972). [The role of somitic mesoderm in the development of dorsal plumage in chick embryos. I. Origin, regulative capacity and determination of the plumage-forming mesoderm]. *J Embryol Exp Morphol* **28**, 313–341.

McMahon, J. A., Takada, S., Zimmerman, L. B., Fan, C. M., Harland, R. M. and McMahon, A. P. (1998). Noggin-mediated antagonism of BMP signaling is required for growth and patterning of the neural tube and somite. *Genes & Development* **12**, 1438–1452.

Meier, S. (1984). Somite formation and its relationship to metameric patterning of the mesoderm. *Cell Differ.* **14**, 235–243.

Mennerich, D., Schafer, K. and Braun, T. (1998). Pax-3 is necessary but not sufficient for lbx1 expression in myogenic precursor cells of the limb. *Mech. Dev.* **73**, 147–158.

Mikheeva, S. A., Mikheev, A. M., Petit, A., Beyer, R., Oxford, R. G., Khorasani, L., Maxwell, J.-P., Glackin, C. A., Wakimoto, H., González-Herrero, I., et al. (2010). TWIST1 promotes invasion through mesenchymal change in human glioblastoma. *Molecular Cancer* **9**, 194.

Mizuno, S., Kurosawa, T., Matsumoto, K., Mizuno-Horikawa, Y., Okamoto, M. and Nakamura, T. (1998). Hepatocyte growth factor prevents renal fibrosis and dysfunction in a mouse model of chronic renal disease. *J. Clin. Invest.* **101,** 1827-1834.

Molkentin, J. D. and Olson, E. N. (1996). Defining the regulatory networks for muscle development. *Current Opinion in Genetics & Development* **6**, 445–453.

Montell, D. J. and Goodman, C. S. (1989). *Drosophila* Laminin: sequence of B2 subunit and expression of all three subunits during embryogenesis. *J. Cell Biol.* **109,** 2441-2453.

Morimoto, M., Takahashi, Y., Endo, M. and Saga, Y. (2005). The Mesp2 transcription factor establishes segmental borders by suppressing Notch activity. *Nature* **435**, 354–359.

Mostafavi-Pour, Z., Askari, J. A., Parkinson, S. J., Parker, P. J., Ng, T. T. C. and Humphries, M. J. (2003). Integrin-specific signaling pathways controlling focal adhesion formation and cell migration. *J. Cell Biol.* **161**, 155–167.

Mueller, S. C. (1999). A Novel Protease-docking Function of Integrin at Invadopodia. *Journal of Biological Chemistry* **274**, 24947–24952.

Murre, C., McCaw, P. S., Vaessin, H., Caudy, M., Jan, L. Y., Jan, Y. N., Cabrera, C. V., Buskin, J. N., Hauschka, S. D., Lassar, A. B., et al. (1989). Interactions between heterologous helix-loop-helix proteins generate complexes that bind specifically to a common DNA sequence. *Cell* **58**, 537–544.

Nabeshima, Y., Hanaoka, K., Hayasaka, M., Esumi, E., Li, S., Nonaka, I. and Nabeshima, Y. (1993). Myogenin gene disruption results in perinatal lethality because of severe muscle defect. *Nature* **364**, 532–535.

Nakagawa, O., Nakagawa, M., Richardson, J. A., Olson, E. N. and Srivastava, D. (1999). HRT1, HRT2, and HRT3: A New Subclass of bHLH Transcription Factors Marking Specific Cardiac, Somitic, and Pharyngeal Arch Segments. *Developmental Biology* **216**, 72–84.

Nakajima, Y. (2006). Identification of Epha4 enhancer required for segmental expression and the regulation by Mesp2. *Development* **133**, 2517–2525.

Nakaya, M.-A., Habas, R., Biris, K., Dunty, W. C., Jr., Kato, Y., He, X. and Yamaguchi, T. P. (2004). Identification and comparative expression analyses of Daam genes in mouse and Xenopus. *Gene Expression Patterns* **5**, 97–105.

Niedermeyer, J., Garin-Chesa, P., Kriz, M., Hilberg, F., Mueller, E., Bamberger, U., Rettig, W. J. and Schnapp, A. (2001). Expression of the fibroblast activation protein during mouse embryo development. *Int. J. Dev. Biol.* **45**, 445–447.

Nieto, M. A. The Ins and Outs of the Epithelial to Mesenchymal Transition in Health and Disease. *http://dx.doi.org/10.1146/annurev-cellbio-092910-154036*.

Noden, D. M. (1983). The embryonic origins of avian cephalic and cervical muscles and associated connective tissues. *Am. J. Anat.* **168**, 257–276.

Noren, N. K. and Pasquale, E. B. (2004). Eph receptor–ephrin bidirectional signals that target Ras and Rho proteins. *Cell* **16**, 655–666.

Oginuma, M., Niwa, Y., Chapman, D. L. and Saga, Y. (2008). Mesp2 and Tbx6

cooperatively create periodic patterns coupled with the clock machinery during mouse somitogenesis. *Development* **135**, 2555–2562.

Olson, E. N. (1990). MyoD family: a paradigm for development? *Genes & Development* **4**, 1454–1461.

Olson, E. N. and Klein, W. H. (1994). bHLH factors in muscle development: dead lines and commitments, what to leave in and what to leave out. *Genes & Development* **8**, 1–8.

Ordahl, C. P. and Le Douarin, N. M. (1992). Two myogenic lineages within the developing somite. *Development* **114**, 339–353.

Ott, M. O., Bober, E., Lyons, G., Arnold, H. and Buckingham, M. (1991). Early expression of the myogenic regulatory gene, myf-5, in precursor cells of skeletal muscle in the mouse embryo. *Development* **111**, 1097–1107.

Palmeirim, I., Henrique, D., Ish-Horowicz, D. and Pourquié, O. (1997). Avian hairy Gene Expression Identifies a Molecular Clock Linked to Vertebrate Segmentation and Somitogenesis. *Cell* **91**, 639–648.

Pardanaud, L., Luton, D., Prigent, M., Bourcheix, L. M., Catala, M. and Dieterlen-Lievre, F. (1996). Two distinct endothelial lineages in ontogeny, one of them related to hemopoiesis. *Development* **122**, 1363–1371.

Peyrefitte, S., Kahn, D. and Haenlin, M. (2001). New members of the *Drosophila* Myc transcription factor subfamily revealed by a genome-wide examination for basic helix-loop-helix genes. *Mech. Dev.* **104,** 99-104.

Poliakov, A., Cotrina, M. and Wilkinson, D. G. (2004). Diverse Roles of Eph Receptors and Ephrins in the Regulation of Cell Migration and Tissue Assembly. *Cell* **7**, 465–480.

Radice, G. L., Rayburn, H., Matsunami, H., Knudsen, K. A., Takeichi, M. and Hynes, R. O. (1997). Developmental Defects in Mouse Embryos Lacking N-Cadherin. *Developmental Biology* **181**, 64–78.

Raz, E. and Mahabaleshwar, H. (2009). Chemokine signaling in embryonic cell migration: a fisheye view. *Development* **136**, 1223–1229.

Relaix, F. E. D. E. R., Rocancourt, D., Mansouri, A. and Buckingham, M. (2005). A Pax3/Pax7-dependent population of skeletal muscle progenitor cells. *Nature* **435**, 948–953.

Rhee, J., Takahashi, Y., Saga, Y., Wilson-Rawls, J. and Rawls, A. (2003). The protocadherin papc is involved in the organization of the epithelium along the segmental border during mouse somitogenesis. *Developmental Biology* **254**, 248–261.

Rifes, P. and Thorsteinsdóttir, S. (2012). Extracellular matrix assembly and 3D organization during paraxial mesoderm development in the chick embryo.

Developmental Biology **368**, 370–381.

Rifes, P., Carvalho, L., Lopes, C., Andrade, R. P., Rodrigues, G., Palmeirim, I. and Thorsteinsdottir, S. (2007). Redefining the role of ectoderm in somitogenesis: a player in the formation of the fibronectin matrix of presomitic mesoderm. *Development* **134**, 3155–3165.

Rowton, M., Ramos, P., Anderson, D. M., Rhee, J. M., Cunliffe, H. E. and Rawls, A. (2013). Regulation of mesenchymal-to-epithelial transition by PARAXIS during somitogenesis. *Dev. Dyn.* **242**, 1332–1344.

Rozen, S. and Skaletsky, H. (1999). *Primer3 on the WWW of General Users and for Biologist Programmers*. New Jersey: Humana Press.

Saga, Y. (2012). The mechanism of somite formation in mice. *Current Opinion in Genetics & Development* **22**, 331–338.

Saga, Y., Hata, N., Koseki, H. and Taketo, M. M. (1997). Mesp2: a novel mouse gene expressed in the presegmented mesoderm and essential for segmentation initiation. *Genes & Development* **11**, 1827–1839.

Saleem, M., Kweon, M. H., Johnson, J. J., Adhami, V. M., Elcheva, I., Khan, N., Bin Hafeez, B., Bhat, K. M. R., Sarfaraz, S., Reagan-Shaw, S., et al. (2006). S100A4 accelerates tumorigenesis and invasion of human prostate cancer through the transcriptional regulation of matrix metalloproteinase 9. *Proceedings of the National Academy of Sciences* **103**, 14825–14830.

Sanz-Rodriguez, F. (2001). Chemokine stromal cell-derived factor-1alpha modulates VLA-4 integrin-mediated multiple myeloma cell adhesion to CS-1/fibronectin and VCAM-1. *Blood* **97**, 346–351.

Sassoon, D., Lyons, G., Wright, W. E., Lin, V., Lassar, A., Weintraub, H. and Buckingham, M. (1989). Expression of two myogenic regulatory factors myogenin and MyoDl during mouse embryogenesis. *Nature* **341**, 303–307.

Sato, T., Rocancourt, D., Marques, L., Thorsteinsdóttir, S. and Buckingham, M. (2010). A Pax3/Dmrt2/Myf5 Regulatory Cascade Functions at the Onset of Myogenesis. *PLoS Genet* **6**, e1000897.

Savagner, P., Kusewitt, D. F., Carver, E. A., Magnino, F., Choi, C., Gridley, T. and Hudson, L.G. (2005). Developmental transcription factor slug is required for effective re-epithelialization by adult keratinocytes. *J. Cell Physiol.* **202**, 858-866.

Sawada, A., Shinya, M., Jiang, Y. J., Kawakami, A., Kuroiwa, A. and Takeda, H. (2001). Fgf/MAPK signalling is a crucial positional cue in somite boundary formation. *Development* **128**, 4873–4880.

Scaal, M. and Christ, B. (2004). Formation and differentiation of the avian dermomyotome. *Brain Struct Funct* **208**, 411–424.

Schafer, K. and Braun, T. (1999). Early specification of limb muscle precursor cells

by the homeobox gene

Lbx1h. *Nat Genet* **23**, 213–216.

Schmidt, C., Bladt, F., Goedecke, S., Brinkmann, V., Zschiesche, W., Sharpe, M., Gherardi, E. and Birchmeler, C. (1995). Scatter factor/hepatocyte growth factor is essential for liver development. *Nature* **373**, 699–702.

Schmidt, C., Stoeckelhuber, M., McKinnell, I., Putz, R., Christ, B. and Patel, K. (2004). Wnt 6 regulates the epithelialisation process of the segmental plate mesoderm leading to somite formation. *Developmental Biology* **271**, 198–209.

Schmidt-Hansen, B. (2004). Functional Significance of Metastasis-inducing S100A4(Mts1) in Tumor-Stroma Interplay. *Journal of Biological Chemistry* **279**, 24498–24504.

Schneider, C. A., Rasband, W. S. and Eliceiri, K. W. (2012). NIH Image to ImageJ: 25 years of image analysis. *Nat Meth* **9**, 671–675.

Schneider, M., Hansen, J. L. and Sheikh, S. P. (2008). S100A4: a common mediator of epithelial–mesenchymal transition, fibrosis and regeneration in diseases? *J Mol Med* **86**, 507–522.

Schweitzer, R., Chyung, J. H., Murtaugh, L. C., Brent, A. E., Rosen, V., Olson, E. N., Lassar, A. and Tabin, C. J. (2001). Analysis of the tendon cell fate using Scleraxis, a specific marker for tendons and ligaments.

Seo, K. W., Wang, Y., Kokubo, H., Kettlewell, J. R., Zarkower, D. A. and Johnson, R. L. (2006). Targeted disruption of the DM domain containing transcription factor Dmrt2 reveals an essential role in somite patterning. *Developmental Biology* **290**, 200–210.

Shanmugalingam, S. and Wilson, S. W. (1998). Isolation, expression and regulation of a zebrafish paraxis homologue. *Mech. Dev.* **78**, 85–89.

Shinohara, H. (1999). The musculature of the mouse tail is characterized by metameric arrangements of bicipital muscles. *Okajimas Folia Anat Jpn* **76**, 157-169.

Shukunami, C., Takimoto, A., Oro, M. and Hiraki, Y. (2006). Scleraxis positively regulates the expression of tenomodulin, a differentiation marker of tenocytes. *Developmental Biology* **298**, 234–247.

Smith, J. J., Kuraku, S., Holt, C., Sauka-Spengler, T., Jiang, N., Campbell, M. S., Yandell, M. D., Manousaki, T., Meyer, A., Bloom, O. E., et al. (2013). Sequencing of the sea lamprey (Petromyzon marinus) genome provides insights into vertebrate evolution. *Nat Genet* **45**, 415–421.

Snow, C. J. and Henry, C. A. (2009). Dynamic formation of microenvironments at the myotendinous junction correlates with muscle fiber morphogenesis in zebrafish. *Gene Expr. Patterns* **9,** 37-42.

Snow, C. J., Peterson, M. T., Khalil, A. and Henry, C. A. (2008). Muscle development is disrupted in zebrafish embryos deficient for fibronectin. *Dev. Dyn.* **237**, 2542–2553.

Stern, C. D. and Keynes, R. J. (1987). Interactions between somite cells: the formation and maintenance of segment boundaries in the chick embryo. *Development* **99**, 261–272.

Svensson, L. (1999). Fibromodulin-null Mice Have Abnormal Collagen Fibrils, Tissue Organization, and Altered Lumican Deposition in Tendon. *Journal of Biological Chemistry* **274**, 9636–9647.

Šošić, D., Brand-Saberi, B., Schmidt, C., Christ, B. and Olson, E. N. (1997). Regulation ofparaxisExpression and Somite Formation by Ectoderm- and Neural Tube-Derived Signals. *Developmental Biology* **185**, 229–243.

Tajbakhsh, S. and Buckingham, M. (2000). The Birth of Muscle Progenitor Cells in the Mouse: Spatiotemporal Considerations. In *Current Topics in Developmental Biology*, pp. 225–268. Elsevier.

Tajbakhsh, S. and Buckingham, M. E. (1994). Mouse limb muscle is determined in the absence of the earliest myogenic factor myf-5. *Proceedings of the National Academy of Sciences of the United States of America* **91**, 747–751.

Tajbakhsh, S., Rocancourt, D. and Buckingham, M. (1996). Muscle progenitor cells failing to respond to positional cues adopt non-myogenic fates in myf-5 null mice. *Nature* **384**, 266–270.

Tajbakhsh, S., Rocancourt, D., Cossu, G. and Buckingham, M. (1997). Redefining the Genetic Hierarchies Controlling Skeletal Myogenesis: Pax-3 and Myf-5 Act Upstream of MyoD. *Cell* **89**, 127–138.

Takahashi, Y., Sato, Y., Suetsugu, R. and Nakaya, Y. (2005). Mesenchymal-to-epithelial transition during somitic segmentation: a novel approach to studying the roles of Rho family GTPases in morphogenesis. *Cells Tissues Organs* **179**, 36–42.

Takahashi, Y., Takagi, A., Hiraoka, S., Koseki, H., Kanno, J., Rawls, A. and Saga, Y. (2007). Transcription factors Mesp2 and Paraxis have critical roles in axial musculoskeletal formation. *Dev. Dyn.* **236**, 1484–1494.

Tan, M. L., Choong, P. F. M. and Dass, C. R. (2010). Direct anti-metastatic efficacy by the DNA enzyme Dz13 and downregulated MMP-2, MMP-9 and MT1-MMP in tumours. *Cancer Cell Int.* **10**, 9.

Tatsumi, R., Anderson, J. E., Nevoret, C. J., Halevy, O. and Allen, R. E. (1998). HGF/SF is present in normal adult skeletal muscle and is capable of activating satellite cells. *Dev. Biol.* **194,** 114-28.

Teillet, M.-A., Kalcheim, C. and Le Douarin, N. M. (1987). Formation of the dorsal root ganglia in the avian embryo: Segmental origin and migratory behavior of neural crest progenitor cells. *Developmental Biology* **120**, 329–347.

Thiery, J. P. (2002). Epithelial-mesenchymal transitions in tumor progression. *Nature Reviews Cancer* **2**, 442-454.

Thiery, J. P. and Sleeman, J. P. (2006). Complex networks orchestrate epithelial|[ndash]|mesenchymal transitions. *Nature Reviews Molecular Cell Biology* **7**, 131–142.

Thorsteinsdóttir, S., Deries, M., Cachaço, A. S. and Bajanca, F. (2011). The extracellular matrix dimension of skeletal muscle development. *Developmental Biology* **354**, 191–207.

Tonami, K., Kurihara, Y., Arima, S., Nishiyama, K., Uchijima, Y., Asano, T., Sorimachi, H. and Kurihara, H. Calpain-6, a microtubule-stabilizing protein, regulates Rac1 activity and cell motility through interaction with GEF-H1.

Towler, M. C. (2004). Clathrin Isoform CHC22, a Component of Neuromuscular and Myotendinous Junctions, Binds Sorting Nexin 5 and Has Increased Expression during Myogenesis and Muscle Regeneration. *Mol. Biol. Cell* **15**, 3181–3195.

Tsang, M., Lijam, N., Yang, Y., Beier, D. R., Wynshaw-Boris, A. and Sussman, D. J. (1996). Isolation and characterization of mouseDishevelled-3. *Dev. Dyn.* **207**, 253–262.

Tseng, H.-T. and Jamrich, M. (2004). Identification and developmental expression of Xenopus paraxis. *Int. J. Dev. Biol.* **48**, 1155–1158.

Van Aelst, L. (2002). Role of Rho family GTPases in epithelial morphogenesis. *Genes & Development* **16**, 1032–1054.

Vasyutina, E. (2005). CXCR4 and Gab1 cooperate to control the development of migrating muscle progenitor cells. *Genes & Development* **19**, 2187–2198.

Venters, S. J. and Ordahl, C. P. (2002). Persistent myogenic capacity of the dermomyotome dorsomedial lip and restriction of myogenic competence. *Development* **129**, 3873–3885.

Venters, S. J. and Ordahl, C. P. (2005). Asymmetric cell divisions are concentrated in the dermomyotome dorsomedial lip during epaxial primary myotome morphogenesis. *Brain Struct Funct* **209**, 449–460.

Wang, Z., Cui, J., Wong, W. M., Li, X., Xue, W., Lin, R., Wang, J., Wang, P., Tanner, J. A., Cheah, K. S. E., et al. (2013). Kif5b controls the localization of myofibril components for their assembly and linkage to the myotendinous junctions. *dev.biologists.org.ezproxy1.lib.asu.edu*.

Watanabe, T., Saito, D., Tanabe, K., Suetsugu, R., Nakaya, Y., Nakagawa, S. and Takahashi, Y. (2007). Tet-on inducible system combined with in ovo electroporation dissects multiple roles of genes in somitogenesis of chicken embryos. *Developmental Biology* **305**, 625–636.

Watanabe, T., Sato, Y., Saito, D., Tadokoro, R. and Takahashi, Y. (2009).

EphrinB2 coordinates the formation of a morphological boundary and cell epithelialization during somite segmentation.

Watkins, J. (2009). *Structure and Function of the Musculoskeletal System* (2nd ed.). Champaign, Il: Human Kinetics Publishers.

Wayner, E. A., Garcia-Pardo, A., Humphries, M. J., McDonald, J. A. and Carter, W. G. (1989). Identification and characterization of the T lymphocyte adhesion receptor for an alternative cell attachment domain (CS-1) in plasma fibronectin. *J. Cell Biol.* **109**, 1321–1330.

Weber, S. and Saftig, P. (2012). Ectodomain shedding and ADAMs in development. *Development* **139**, 3693–3709.

Wehrle-Haller, B. (2012). Structure and function of focal adhesions. *Current Opinion in Cell Biology* **24**, 116–124.

Wiggan, O., Fadel, M. P. and Hamel, P. A. (2002). Pax3 induces cell aggregation and regulates phenotypic mesenchymal-epithelial interconversion. *J. Cell. Sci.* **115**, 517–529.

WIGGAN, O., SHAW, A. and BAMBURG, J. (2006). Essential requirement for Rho family GTPase signaling in Pax3 induced mesenchymal–epithelial transition. *Cellular Signalling* **18**, 1501–1514.

Williams, B. A. and Ordahl, C. P. (1994). Pax-3 expression in segmental mesoderm marks early stages in myogenic cell specification. *Development* **120**, 785–796.

Wilson-Rawls, J. (2004). Paraxis Is a Basic Helix-Loop-Helix Protein That Positively Regulates Transcription through Binding to Specific E-box Elements. *Journal of Biological Chemistry* **279**, 37685–37692.

Wilson-Rawls, J., Hurt, C. R., Parsons, S. M. and Rawls, A. (1999). Differential regulation of epaxial and hypaxial muscle development by paraxis. *Development* **126**, 5217–5229.

Wilting, J., Brand-Saberi, B., Huang, R., Zhi, Q., Köntges, G., Ordahl, C. P. and Christ, B. (1995). Angiogenic potential of the avian somite. *Dev. Dyn.* **202**, 165–171.

Woods, A. and Couchman, J. R. (2001). Syndecan-4 and focal adhesion function. *Current Opinion in Cell Biology* **13**, 578–583.

Yang, J. and Weinberg, R. A. (2008). Epithelial-mesenchymal transition: at the crossroads of development and tumor metastasis. *Dev. Cell* **14**, 818–829.

Yang, J. T., Bader, B. L., Kreidberg, J. A., Ullman-Culleré, M., Trevithick, J. E. and Hynes, R. O. (1999). Overlapping and Independent Functions of Fibronectin Receptor Integrins in Early Mesodermal Development. *Developmental Biology* **215**, 264–277.

Yang, J. T., Rayburn, H. and Hynes, R. O. (1993). Embryonic mesodermal defects in alpha 5 integrin-deficient mice. *Development* **119**, 1093–1105.

Yang, X. M., Vogan, K., Gros, P. and Park, M. (1996). Expression of the met receptor tyrosine kinase in muscle progenitor cells in somites and limbs is absent in Splotch mice. *Development* **122**, 2163–2171.

Yasuhiko, Y. (2006). Tbx6-mediated Notch signaling controls somite-specific Mesp2 expression. *Proceedings of the National Academy of Sciences* **103**, 3651–3656.

Yin, H., Price, F. and Rudnicki, M. A. (2013). Satellite cells and the muscle stem cell niche. *Physiol. Rev.* **93,** 23-67.

Zhang, W., Behringer, R. R. and Olson, E. N. (1995). Inactivation of the myogenic bHLH gene MRF4 results in up-regulation of myogenin and rib anomalies. *Genes & Development* **9**, 1388–1399.

Zhou, L., Xiao, H. and Nambu, J. R. (1997). CNS midlline to mesoderm signaling in *Drosophila*. *Mech. Dev.* **67,** 59-68.